CORROSION MONITORING IN RC BEAMS USING ACOUSTIC EMISSION AND ULTRASONIC GUIDED WAVES

A Dissertation submitted

In partial Fulfillment of the Requirements for

For the degree of

MASTERS OF ENGINEERING

IN

CIVIL (STRUCTURES) ENGINEERING

Submitted by

VIPIN SHARMA

(ROLL NO. 801222022)

UNDER THE GUIDANCE OF

Dr. SHRUTI SHARMA

Assistant Professor

Civil Engineering Department

Thapar University Patiala

CIVIL ENGINEERING DEPARTMENT

THAPAR UNIVERSITY, PATIALA 147004

CERTIFICATE

Certified that the thesis **"Corrosion Monitoring in RC beams using Acoustic Emission and Ultrasonic Guided wave"** which is submitted by **Mr. Vipin Sharma**, in partial fulfillment of the requirements for the award of the degree of Master of Engineering in the **Department of Civil Engineering (CED)**, Thapar University, Patiala, is a record of the candidate's own independent and original research work carried out by him under her supervision and guidance. The matter embodied in this thesis has not been submitted in part or full to any other University or Institute for the award of any degree.

VIPIN SHARMA
(801222022)

Date: 17/07/2014

(Dr. SHRUTI SHARMA)
Assistant Professor
CED, Thapar University
Patiala-147004

Countersigned by:

(Dr. NaveenKwatra)
Head,CED
Thapar University
Patiala-147004

(Dr. S.K.Mohapatra)
Dean, Academic Affairs
Thapar University
Patiala-147004

ACKNOWLEDGEMENT

Time has provided me the cherished opportunity to express my heartfelt gratitude to my guide Dr. Shruti Sharma, Assistant Professor, CED, Thapar University, Patiala, who permitted me to carry out thesis work under her able guidance. I shall ever remain indebted to her for her meticulous guidance, constructive criticism, clear thinking, keen interest, constant encouragement and forbearance right from the beginning of this thesis to its completion.

I wish to express my sincere thanks to Dr. Naveen Kwatra, Associate Professor and Head, CED, Thapar University, Patiala, who has been a constant source of inspiration for me throughout this thesis work.

The cheerful support of my friends and colleagues is sincerely appreciated. Special words of appreciation go to Sh. Ram Simran and other laboratory colleagues, who helped me in my experimental work.

I am also thankful to all the staff members of Civil Engineering Department for their full cooperation and help.

I would like also to extend my love and thanks to my friends. Finally, I would like to express my deepest gratitude and love to my parents, without whom I am nothing, for providing me great opportunities, everlasting support, big encouragement and lots of love.

Vipin Sharma

ABSTRACT

Non-destructive testing is needed for localizing and characterizing the growing damage in existing structures and also for the quality control of new structures. Visual inspection is a commonly used method; however it is not very suitable for early detection of damage and is very much dependent on the experience of the inspector. Ultrasonic guided wave monitoring and acoustic emission technique are the methods that can be used effectively for the structural health diagnosis.

In the present study, a RC beam, of dimensions 150mm×150mm×700mm with an embedded steel bar of dia. 25 mm and 1000mm in length, is subjected to accelerated induced corrosion. Ultrasonic guided wave monitoring is done periodically after every 24 hours for 30 days. A mode with minimum attenuation and mode shape that is sensitive to particular type of damage due to corrosion is chosen from dispersion curves. For this purpose, Pulse-transmission investigation is used using peizo-electric transducers. Also, AE sensors detecting acoustic emission signals are mounted on the RC beam specimen before it is subjected to accelerated corrosion. AE set up simultaneously records the events and hits continuously for 30 days relating to crack initiation and progression due to corrosion in RC beams as the exposure to corrosion increases. It is observed that corrosion of reinforcing bars in concrete is discernible using ultrasonic guided wave and acoustic emission technique.

Ultrasonic guided wave monitoring is done using surface seeking mode and core seeking mode for detecting corrosion. These modes are able to explain the delamination as well as the pitting of the rebar in the RC beam due to corrosion. From acoustic emission monitoring it is observed that there is an immediate increase in cumulative hits and events which corresponds to the development of cracks in the RC beam due to corrosion. Comparing the results from both ultrasonic monitoring and acoustic emission monitoring it is observed that acoustic emission is very effective in detecting the initiation of the corrosion during the initial stages whereas ultrasonic guided waves monitoring gives very clear data during the later age of corrosion propagation.

CONTENTS

LIST OF FIGURES

LIST OF TABLES

CHAPTER 1

INTRODUCTION

1.1 MOTIVATION AND BACKGROUND

Corrosion of reinforcement in concrete has been identified as being one of the most predominant factors responsible for the deterioration of the reinforced concrete structures. The serviceability and the durability of the concrete structures can be seriously affected by the corrosion of reinforcements. Therefore, control and monitoring of reinforcement corrosion assume a significant practical importance to prevent the premature failure of the reinforced concrete structures. Hence, assessment of structural behaviour of corrosion affected is an important issue; which would help in making certain decisions pertaining to the inspection, repair, strengthening, replacement and demolition of such structures.

Various corrosion monitoring techniques have been used by a research group at Thapar University for corrosion monitoring in RC structures. Half-cell potential technique and ultrasonic guided waves have been successfully used for corrosion monitoring. Half-cell potential measurements are simple, inexpensive and virtually non-destructive techniques to assess the corrosion risks of steels in concrete. Due to its simplicity and easy handling, it has been used widely. But it suffers from the drawbacks of measurement of corrosion on concrete which gives variable results under various conditions. Another technique being used these days for corrosion is ultrasonic guided waves monitoring. This technique is very useful in assessing the condition of rebar in the RC structures. Its limitations are that it needs accessibility of the reinforcement and it does not give any information about the effect of corrosion in concrete. This thesis brings out the limitation of Guided waves and suggests that its limitations are overcome by Acoustic emission technique or by the combination of both these techniques for monitoring the corrosion in RC Structures. The Acoustic Emission technique has gained popularity since past few years in the field of structural health monitoring. This technique involves the use of sensors for detecting any acoustic energy released during the formation or propagation of the crack.

1.2 GENERAL

Concrete is a very versatile material with its very own special properties and is the most widely used man-made material. Being a composite material which is very weak in tension and possessing low ductility it is reinforced with steel or any other material of relatively higher tensile strength and ductility. Steel Reinforced concrete (RC) is an extremely popular construction material. It is a composite construction material which is based on the principal that concrete is an ideal environment for the steel. It has been used for decades as the construction material of choice and has proven to be successful in terms of both structural performance and durability. It is economical, versatile and can be moulded to a variety of shapes and finishes. Because of the nature and role of concrete in the creation, rehabilitation and regeneration of the infrastructure system of any country, RC plays a very important part in a nation's economic development. Lack of durability of RC structures has thus not only massive economic implications to a nation's well-being, but it is also one of the greatest threats to sustainable growth of concrete and construction industries.

Corrosion of the reinforcements is recognized as the major problem affecting the durability of the concrete structures as it degrades the bond between the concrete and steel bar. It was previously believed that cover could protect the embedded steel reinforcement from corrosion, and as a consequence, reinforced concrete structures were considered to be highly resistant to corrosion. However, practically, reinforced concrete structures do not perform so well, and their service life is much shorter than what they are designed for. The steel in concrete is always prone to corrosion attack. It has been found that 40% failure of structures is on account of corrosion of embedded steel in concrete (**Sethy, 2005**). Therefore corrosion control of steel reinforcement is a subject of paramount importance. Corrosion is a form of damage which is often insidious and hidden until striking at the worst moment of a system operation.

It has become a serious problem, mainly when the rebar in the concrete is exposed to the chlorides either contributed from the concrete ingredients or penetrated from the surrounding chloride-bearing environment. Salt induced corrosion in reinforcement has undoubtedly become considerable economic burden for various users. Since the iron in the steel has a natural tendency to revert eventually to its most

stable oxide state, this problem, unfortunately, will still be with us, but to a much lesser degree due to the use of various corrosion protection strategies used in the construction process.

The adoption of corrosion protection measures in new construction, such as the use of good design and construction practices, adequate concrete cover depth, low-permeability concrete, corrosion inhibitors, and coated reinforcing steel, is significantly reducing the occurrence of reinforcing steel corrosion in various structures. Carbonation of concrete or penetration of acidic gases into the concrete, are the other causes of reinforcement corrosion. Besides these there are few more factors, some related to the concrete quality, such as w/c ratio, cement content, impurities in the concrete ingredients, presence of surface cracks, etc. and others related to the external environment, such as moisture, oxygen, humidity, temperature, bacterial attack, stray currents, etc., which affect reinforcement corrosion.

Maintenance and repair of reinforced concrete structures mainly due to corrosion damage is presently one of the most significant challenges facing the concrete industry. While there are many ways to try and prevent such damage, the optimum control method relies on an early diagnosis of the problems. Reinforcing steel in good quality concrete does not corrode even if sufficient moisture and oxygen are available. This is due to the spontaneous formation of a thin protective oxide film (passive film) on the steel surface in the highly alkaline pore solution of the concrete. When sufficient chloride ions (from de-icing salts or from sea water) have penetrated to the reinforcement or when the pH of the pore solution drops to low values due to carbonation, the protective film is destroyed and the reinforcing steel is depassivated.

Although corrosion of steel may not immediately affect the integrity and the ultimate load carrying capacity of a RC structural member, it is the most complex, insidious and destructive form of damage. Once it starts, it is almost impossible to stop the process until eventually the safety, stability and design service life are all drastically reduced with time. Hence, to build environmentally sustainable structures, it is clear that modern construction should be driven by considerations of the durability rather than the strength. Durability of RC indispensable and needs to be ensured in future works from both an economic and environmental viewpoint.

1.3 MECHANISM OF CORROSION

Durability can be related to the transport properties and the chemical composition of the concrete. Transport facilities are a function of concrete permeability and cracking. Penetrability can be defined as the ease with which an ion molecule or fluid may move through concrete. It is a function of interconnection between the pores, the pore size distribution, and its tortousity. It is a major factor responsible for the degree of protection of steel reinforcement provided by the concrete cover. It is affected by several parameters such as the water/ binder ratio and the hydration of cement. The penetration of species that cause corrosion in RC such as chloride ions, oxygen, carbon dioxide and moisture into the concrete is governed by the quality and the condition of cover concrete. The presence of cracks in the concrete cover may therefore aggravate the problem of corrosion in RC structures. Once crack occur, they may influence the reinforcement corrosion process by accelerating the ingress of detrimental species (chloride, sulphates and carbon dioxide) and result in further cracking. In other words, we can say that these cracks create preferential path for the penetration of various types of potentially aggressive agents. This can result in substantial reduction in service life owing to the rapid initiation and propagation of steel corrosion. Hence, the reduction of the penetrability and the elimination of cracking or minimization of the crack width increase the durability of concrete.

Corrosion with rusting of reinforcement in concrete comprises two stages. In a first stage (or step), the aggressive elements, such as chloride or carbon dioxide (CO_2) (Cl^-), present in the surrounding environment, penetrate in the concrete. This is an initiation stage. This stage involves the transfers of aggressive agents (mainly carbon oxide and water) of water and of oxygen, including the corrosion initiation (depassivation of reinforcement). The second stage is the propagation which starts, when these aggregates bodies are in rather high concentrations at the reinforcement's level. This corresponds to the rust growth, which can lead to the formation of cracks and can break the concrete cover. This is a stage of corrosion growth, leading to concrete damage, to spalling, cracks, etc. This stage starts when the contents of aggressive agents are high enough closed to reinforcing steel.

So, to describe steel corrosion, it is advisable to define, on the one hand, the penetration of the aggressive events through concrete and, on the other hand, the

conditions of depassivation of reinforcement, then the dissolution rate of metal and rust growth.

Corrosion of steel embedded in concrete is an electrochemical process. The corrosion process is stated to be similar to the action, which takes place in a flash battery. The surface of the corroding steel functions as a mixed electrode that is a composite of anodes and cathodes electrically connected through the body of steel itself, upon which coupled anodic and cathodic reactions take place. Concrete pore water functions as an aqueous medium, i.e., a complex electrolyte. Therefore, a reinforcement corrosion cell is formed, as shown in

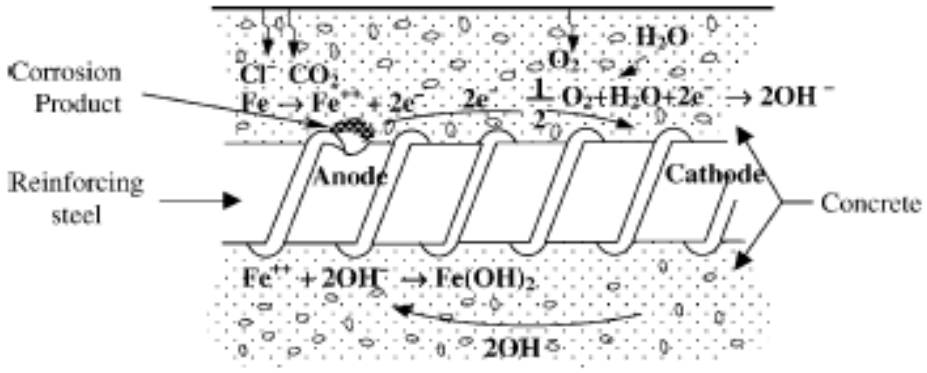

Fig.1.1: Corrosion of reinforcement steel in concrete as an electrochemical process (Ahmed, 2003)

1.3.1 Anodic and Cathodic Reactions

Reactions at the anodes and cathodes are broadly referred to as half cell reactions. The anodic reaction is the oxidation process, which results in dissolution or loss of metal whilst the cathodic reaction is the reduction process which results in reduction of dissolved oxygen forming hydroxyl ions. For steel embedded in concrete, following are the possible anodic reactions depending on the pH of interstitial electrolyte, presence of aggressive anions, and the existence of an appropriate electrochemical potential at the steel surface:

$$3Fe + 4H_20 \rightarrow Fe_30_4 + 8H^+ + 8e^- \quad \text{.....(1.1)}$$

$$2Fe + 3H_20 \rightarrow Fe_20_3 + 6H^+ + 6e^- \text{.....(1.2)}$$

$$2Fe + 3H_20 \rightarrow Hfe0_2^- + 3H^+ + 2e^- \text{..... (1.3)}$$

$$Fe \rightarrow Fe_2^{+} + 2e^{-} \quad \text{.....(1.4)}$$

The possible cathodic reactions depend upon the availability of oxygen and on the pH in the vicinity of the steel surface. The most likely reactions are as follows:

$$3H_20 + 0_2 + 4e^{-} \rightarrow 40H^{-} \quad \text{.....(1.5)}$$

OR

$$2H^{+} + 2e^{-} \rightarrow H_2 \quad \text{.....(1.6)}$$

The phenomenological model of reinforcement corrosion in sea environments presented by li et.al showed that a typical corrosion loss (loss of mass) during the corrosion process can be divided into four phases as shown in the following figure

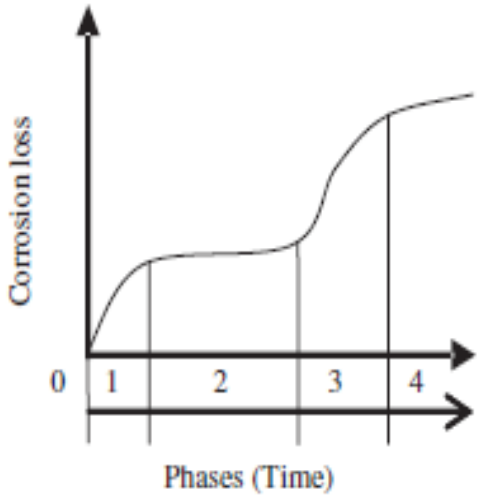

Fig.1.2: Evaluation of corrosion loss in steel under sea water immersion. (Kawasaki et al., 2010)

At phase 1, the onset of corrosion is initiated. The activity of the process is dominated by the rate of penetration of oxygen and water. Then a corrosion loss decreases at phase 2, because the flow of oxygen is eventually inhibited by the rust on the surface of the rebar. The mass loss due to corrosion increases again at phase 3, because the corrosion penetrates inside and the expansion of corrosion products occurs. Eventually, the corrosion progresses at an almost constant speed at phase 4. Thus the phenomenological model is characterized by two transition phases of the onset of corrosion and the growth of corrosion products.

1.4 FACTORS AFFECTING THE CORROSION OF STEEL IN CONCRETE

The factors affecting the corrosion may be classified into two major categories, as follows:

(a) Internal Factors
(b) External Factors

1.4.1 Internal Factors affecting corrosion of steel in concrete

They include mostly the environmental parameters, as follows:

- **Availability of oxygen and moisture at rebar level**

  Presence of oxygen and moisture supports the corrosion. Moisture fulfils the electrolytic requirement of the corrosion cell, and moisture and oxygen together help in the formation of OH^- thereby producing more rust component. Oxygen also affects the progress of cathodic reactions. In the absence of enough oxygen, even in the situation of depassivation, corrosion will not progress due to cathodic polarization.

- **Relative Humidity and Temperature**

  The relative humidity mainly affects the carbonation of concrete. Within 50-100% RH, the increase of environmental relative humidity decreases the carbonation of concrete. Within 50-30% RH, a decrease in environmental RH may not cause a decrease in the carbonation of the concrete especially in the normal concentration of $C0_2$ even after long period of exposure.

  A rise in temperature may result in a twofold effect:

  (a) The electrode reaction rates are generally increased.
  (b) The oxygen solubility is decreased resulting in the reduction in the rate of corrosion.

- **Carbonation and entry of acidic gaseous pollutants to the rebar level**

  The effect of carbonation and other acidic gases, such as $S0_2$ and $N0_2$, is due to their tendency to reduce the pH of concrete. The fall in the pH to certain levels may cause commencement of reinforcement corrosion, loss of passivity of concrete against reinforcement corrosion and catastrophic reinforcement corrosion, as shown in the **Table 1.1**.

Table 1.1: State of reinforcement at various pH levels (Ahmed, 2003)

PH of Concrete	State of Reinforcement Corrosion
Below 9.5	Commencement of steel corrosion
At 8.0	Passive film on the steel surface disappears
Above 9.5	Catastrophic corrosion occurs

- **Aggressive anions, mostly chloride ions, reaching to the rebar level, either through the concrete ingredients or from the external source.**

  Chloride in the concrete may be present in the following form:

  (a) Acid soluble concrete which is equal to the total amount of concrete present in the concrete or that is soluble in nitric acid.

  (b) Bound chloride which is the sum of chemically bound chloride with hydration products of the cement, such as C_3A(tri calcium aluminates) or C_4AF(tetra calcium alumina ferrate) phases, and loosely bound chloride with C-S-H gel.

  (c) Free or water soluble chloride which is concentration of free chloride ions within the pore solution of concrete, and is extractable in water under defined conditions.

It is generally recognized that only the free chloride ions influence the corrosion process. It is reported that the resistivity decreases and the corrosion rate increases with an increase in the chloride content. However, change in pH is found to be insignificant due to change in the chloride content of concrete. The risk of reinforcement corrosion associated with levels of chloride content in both carbonated and uncarbonated concrete is presented in the **Table 1.2.**

Table 1.2: Corrosion risk in concrete containing chloride (Ahmed, 2003)

Total chloride (wt.% of cement)	Condition of concrete adjacent to reinforcement	Corrosion Risk
Less than 0.4%	Carbonated	High
	Uncarbonated made with cement containing less than 8% C_3A.	Moderate
	Uncarbonated, made with cement containing 8% or more C_3A.	Low
0.4-1.0%	As above	High
	As above	High
	As above	Moderate
More than 1%	All Cases	High

Table 1.3 shows the recommended chloride content limits for various codes.

Table 1.3: Chloride Content limits as recommended by some code of practice (Ahmed,2003)

Country	Recommended limits of chloride content (% by mass of cement)
U.S.A	0.15% for chloride exposure and 0.3% for Chloride free exposure
U.K	0.30%

India	0.15%

1.4.2 External Factors affecting Corrosion of reinforcement

- **Cement Composition**: The cement in concrete provides protection to the reinforcing steel against corrosion in the following ways:

  (a) By maintaining a high pH of the order of the 12.5-13 owing to the presence of $Ca(0H)_2$ and other alkaline materials in the hydration product of cement,

  (b) By binding a significant amount of total chlorides as a result of chemical reaction between C_3A and C_4AF content of cement in concrete. Thus the threshold chloride value shifts to higher side with an increase in C_3A content.

- **Impurities in Aggregates**: Aggregates containing chloride salts cause serious corrosion problems, particularly those associated with sea water and those whose natural sites in ground water containing high concentration of chloride ions.

- **Impurities in Mixing and Curing Water**: Mixing and curing water, either contaminated with sufficient quantity of chloride or being highly acidic due to any undesirable substance present in the water, may prove to be detrimental as far as corrosion of reinforcement is concerned.

- **Admixtures**: Addition of calcium chloride in concrete, as a common admixture for accelerating the hydration of the cement is perhaps a most significant reason for the presence of chloride in concrete in the RC structures exposed to the normal weather conditions.

- **(W/C) Ratio:** Water cement ratio, known to control principally the strength, durability and impermeability of concrete, does not itself control the rate of corrosion of reinforcements. When RC structures are immersed in some aggressive solution, it is the permeability of the concrete, which is the function

of (w/c) ratio, affects the corrosion of rebar. The depth of penetration of chloride threshold level increases with an increase in the w/c ratio. The carbonation depth has been found to be linearly increasing with an increase in the w/c ratio. The oxygen diffusion coefficient is also found to be increasing with an increase in w/c ratio.

1.5 Corrosion Monitoring in R.C Structures

This section gives an overview of the need of corrosion monitoring and various techniques by which it can be done.

1.5.1 Need of corrosion monitoring

Reinforced concrete structures are expected to be durable because of high tensile strength and high stiffness of reinforced concrete. However, this expectation is not met in practice and the failure of RC structures occurs when they are exposed to adverse environmental conditions over a period of time. This leads to short service lives and high maintenance and repair costs. Hence, it becomes necessary to monitor the development of corrosion problems in a new or existing RC structure before it is repaired or rehabilitated. Civil engineers need to inspect any possible durability problem before it causes serious damage and therefore, they require such monitoring techniques that give information about how much damage has been caused in the structure due to corrosion and how rapidly the damage will grow with time. Corrosion monitoring techniques are the corrosion measurement methods that give a complete picture of change in the condition of structure in time as well as in all three dimensions of the structure. The corrosion monitoring techniques give an idea about the internal as well as external damage caused, thus enabling the engineer to provide suitable protection measures to the concrete structures.

Repair of corrosion affected structures is often difficult, expensive, hazardous and disruptive to the operations of the building and structures. This repair is required when the structure has lost its load carrying capacity. This process takes lot of time and if proper action is taken well in advance, then the costly repairs can be avoided. This is possible if the structures are monitored regularly. Therefore, there is a critical need for monitoring of R.C Structures by the use of new and emerging materials and

technologies that will facilitate the functionality and efficiency, along with increasing the overall durability and life span of the structures.

Corrosion monitoring gives a complete picture of the changing condition of a structure with time and there are several methods of monitoring the corrosion of steel reinforcement in concrete. In the last few decades, a number of damage detection techniques such as Destructive and Non-Destructive techniques have been developed to analyse changes in structure due to corrosion. Destructive techniques result in accurate measurements and gives specific characteristics of materials by destroying the specimen. Non-destructive techniques, on the other hand, monitor the material quality without destroying the specimen. The inspection ability of these systems is very limited and extremely costly. Therefore, in many areas of modern engineering, non-destructive evaluation (NDE) techniques have provided valuable and often critical information for the safe operation of the most complex systems. Such usefulness has recently been greatly enhanced by the tremendous advances in computer and communication tools.

The various non-destructive techniques to monitor corrosion in reinforced concrete structures are given below:

- Half Cell Potential Method.
- Linear Polarization Resistance Method.
- Ultrasonic Pulse Velocity Method.
- Open Circuit Potential Measurements.
- Surface Potential Measurements.
- Electrochemical Impedance Spectroscopy.
- Acoustic Emission.
- Impact Echo method.
- Infrared Thermography.

In this study we will mainly be dealing with two non destructive tests for monitoring the corrosion

- Ultrasonic pulse velocity method
- Acoustic Emission

1.6 ULTRASONIC PULSE VELOCITY METHOD

Ultrasonic refers to sound energy above the audible frequency of 20 kHz. UPV is a non-destructive technique that can be used to predict material strength and detect internal damage in the structure such as cracking, decay, voids, honeycomb, etc. This technique is readily applied to the concrete structures and is very efficient in finding out the areas of weak concrete in a generally sound RC structure. In this method, electrical energy is converted into pulses of longitudinal, elastic stress waves by a transducer that is in direct contact with the concrete surface to be tested. A good contact between the transducer and concrete surface is made by using a coupling gel. The acoustic pulses generated by the transducer traverse through the concrete and after reflection, the pulses are received by transducer and converted back to electrical energy. The time taken by the wave to travel through the structure and reflect back is measured by electronic means and this is used to calculate the parameter "pulse velocity".

$$\text{Pulse velocity} = L/T \quad \text{.....(1.7)}$$

The value of pulse velocity determines the quality of concrete.

As mentioned earlier, the ultrasonic approach refers to the study of sound waves having frequencies higher than the human audible range i.e., above 20 kHz. Upper range of these waves can be as high as 15-30 GHz. However, for most SHM applications, the upper bound of frequency rarely exceeds 20MHz. Ultrasonic monitoring is based on the ability of ultrasonic waves to "see through" solid/opaque material and detect surface or internal flaws without affecting the material adversely. It is noteworthy that there are no changes in the dimensions of the structure that is examined by ultrasonic test. This can be achieved only when the maximum applied stress does not exceed the elastic limit so that the resultant strain is proportional to the applied stress. Hence, it is necessary that the ultrasonic intensity is sufficiently low for the elastic limit not to be exceeded. It involves introducing a very low energy level, high frequency stress pulse or „wave packet" into a material and observing the subsequent propagation and reflection of this energy. The means for introducing and detecting the stress waves are based generally on the piezoelectric effect. The ultrasonic waves are sensitive to the location, extent and character of defects in a structure and, the wave characteristics change accordingly. By studying the propagation, reflection, and attenuation of these waves, it is possible to determine the

fundamental properties of the materials such as elastic constants and damping characteristics and employ them for damage diagnosis. Thus, non-destructive ultrasonic technique can be used as a means for monitoring the soundness/ health of structures by the propagation of acoustic waves through structures.

1.6.1 Ultrasonic Guided Waves

Elastic waves in all frequency ranges- ultrasonic, sonic and subsonic- can be classified into two groups; Body waves or bulk waves and, surface waves or guided waves (fig.).

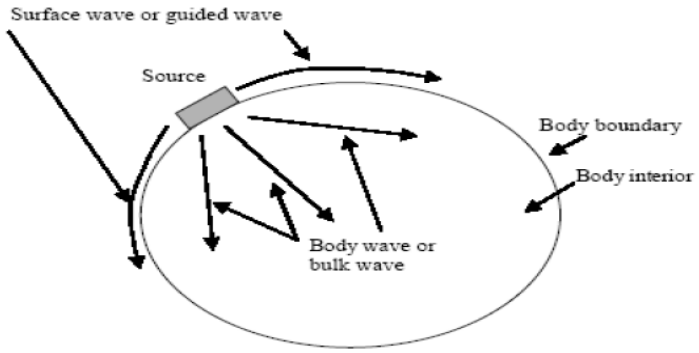

Fig. 1.3: Body waves and Surface waves generated by an ultrasonic source (Kundu, 2004)

Body waves travel through the bulk material while surface waves propagate along the surface. Sound waves travel as a bulk wave in any elastic material where the sound does not interact with the edges of material therefore acting as infinite extent of material. The velocity of sound in material varies with its elastic properties which can be calculated by measuring the time of flight between the two points.

Velocity can be related to a variety of different material properties and conditions and is often used as a test of concrete uniformity, where velocity is usually displayed on a contour map. Large cracks and voids can be detected by an increase in travel time. However, when ultrasonic wave is constrained within the boundaries and is guided by the geometry of the structure, it becomes a guided wave, that has the ability to travel long distances with minimum loss of energy. The structure that guides the wave is termed as „waveguide". Surface waves are often called guided waves because of the geometry of the boundary which guides them. The basic requirement for an ultrasonic wave to be a guided wave is that the thickness of the waveguide must be comparable to the operating wavelength (**Fig1.4**). However, if the thickness of the

material is much greater than the operating wavelength, then bulk waves and surface waves exist (**Fig1.5**).

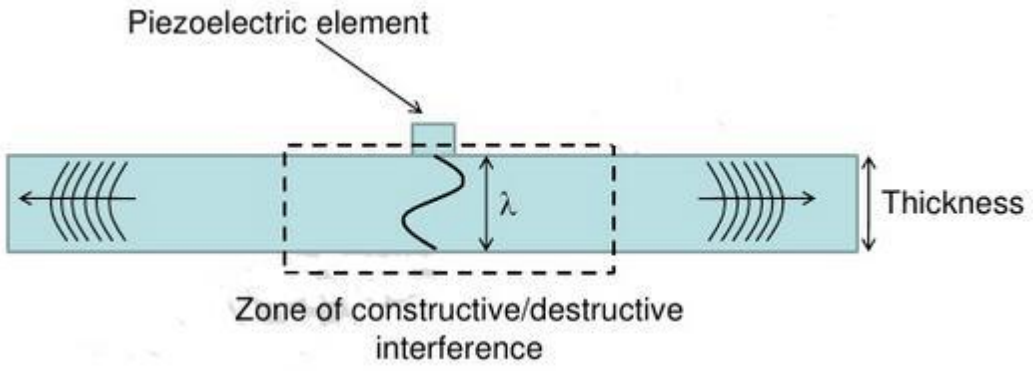

Fig.1.4: Propagation of guided waves through a structure (Kundu, 2004)

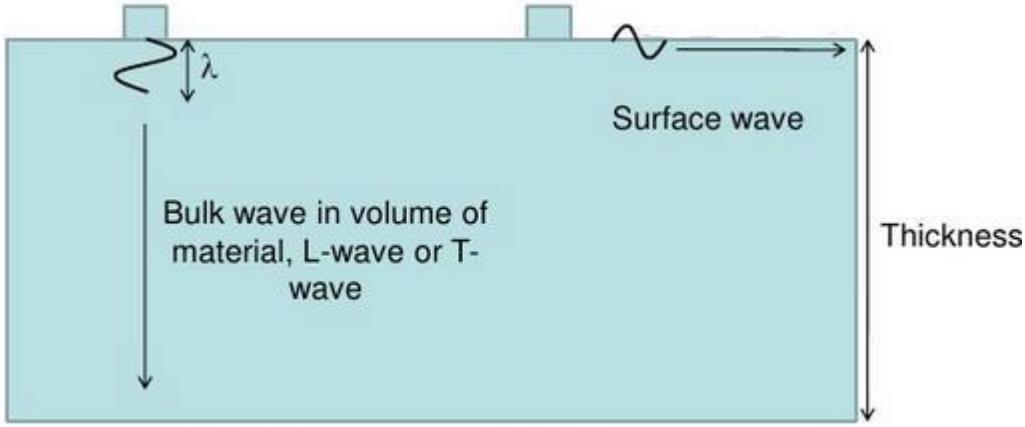

Fig.1.5: Wave Propagation when thickness of material >> wavelength (*www.wins-ndt.com*)

Major advantages of guided waves include quickness, low cost and often improved sensitivity to a variety of defects. For a well-conditioned rebar, guided wave can propagate at least 300 feet and have the whole rebar tested in seconds based on the received time-domain signals.

Another advantage of the guided wave is that it only needs access to a small area of the specimen for source loading, such as rebar end or some small area of the structure. Moreover, guided waves can propagate in the structure as a whole, and therefore, have the potential to inspect the entire structure from a single point. Thus, a guided wave excited at the exposed end of a rebar would be reflected from any defect in the bar, allowing defects to be accurately located. Guided Wave testing (GWT) is

one of the latest methods in the field of non-destructive ultrasonic monitoring for flaw detection. There are numerous advantages of ultrasonic guided wave testing such as:

- High sensitivity, enabling the detection of small flaws
- High penetrating power, enabling the detection of flaws that are deep inside the structure
- Testing is possible through the accessibility of only one surface
- Capability of testing over long distances
- Some capability of estimating the size, orientation, shape and nature of defects
- Greater accuracy than other NDT techniques
- Easily portable
- Non-hazardous to the surrounding materials

Moreover, with this technique, frequency and mode tuning can be done to evaluate different types of deterioration or damage in the structures.

1.6.1.1 Types of guided waves

There are different types of guided waves based on the geometry of the structure (wave guide) through which guided wave travels.

- Plate Wave or Lamb wave.
- Bar Wave.
- Rod Wave.
- Cylindrical Guided Wave
- Rayleigh Wave.
- Generalized Rayleigh-Lamb Wave.

They are as shown in the **Fig.1.6**

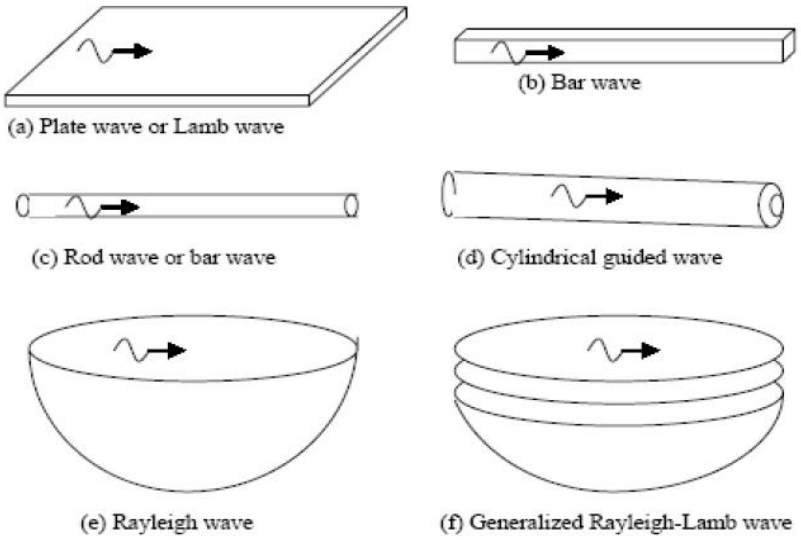

Fig1.6: Different types of guided waves (kundu, 2004)

If the structure of the waveguide is a homogenous half space, then the guided wave propagating along the surface of the half space is called Rayleigh wave, named after its inventor. Waves propagating through a plate like structure with two parallel stress free boundaries are known as Lamb waves. Elastic waves propagating through a hollow cylindrical or pipe structure are called cylindrical guided waves. When the guided waves propagate through a solid rod or bar, they are known as bar waves.

1.6.1.2 Modes of Propagation of ultrasonic guided waves

Ultrasonic waves propagate in the reinforced steel bars in the form of guided waves. The waves are directed in the bar by the geometry of the structure, as discussed in the previous section. The current research uses cylindrical guided waves as the test specimens are cylindrical RC structures. There are three types of propagating waves, or modes in a cylindrical waveguide:

- **Longitudinal Mode(L)**
- **Torsional Mode(T)**
- **Flexural Mode(F)**

Longitudinal modes have radial and axial displacements, torsional modes have angular displacements and flexural modes have axial, radial and angular displacements. These modes are represented by the notation L(m,n), T(m,n) and

F(m,n) respectively. In this notation, ‘m’ represents the circumferential displacement and is a function of cos(mθ) , and ‘n’ represents the sequential order of mode. For longitudinal modes, the variable ‘m’ is zero as they are axially symmetric. For flexural modes, the variable ‘m’ varies as cos(mθ) around the circumference of the steel bar. For e.g., L(0,1) is the notation for first longitudinal mode.

1.6.1.3 Methods for ultrasonic testing

Most commonly used method for ultrasonic testing are:

- Pulse Transmission Method
- Pulse Echo Method

➢ **Pulse Transmission Method**

In the pulse-transmission method, an ultrasonic transmitter is used on one side of the material while a detector is placed on the opposite side. One unit acts as transmitter and the other unit as receiver. The beam from the transmitter T travels through the material to its opposite surface where the receiving transducer R is placed. It is shown in **Fig.1.7.**

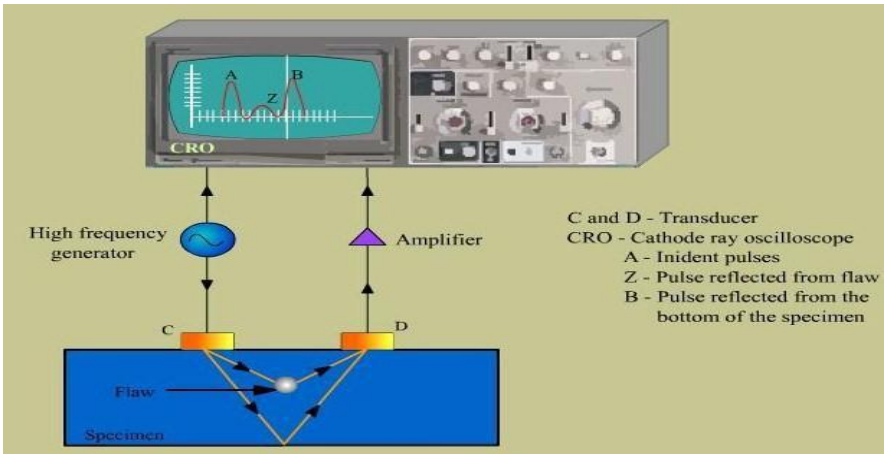

Fig.1.7: Pulse transmission method of testing(www.msheiksirajudden.blogspot.in)

Scanning of the material using this method will result in the location of defects, flaws, and inclusions in the X-Y plane. By measuring the relative change of the amplitudes of the input and the received signals, the relative severity of the flaw is assessed.

- **Pulse Echo Method**

In the pulse-echo method, a piezoelectric transducer with its longitudinal axis located perpendicular to and mounted on or near the surface of the test material is used to transmit and receive ultrasonic energy.

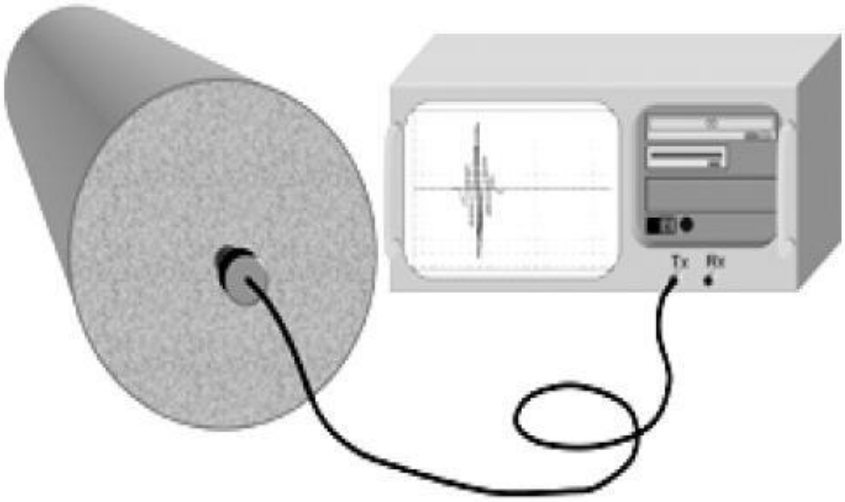

Fig.1.8: Set-up for pulse echo method (He, 2006)

1.7 Acoustic Emission

Acoustic emission (A.E) is one of the most promising methods of monitoring of the structure at different stages of deterioration. AE technique can be adopted to forewarn the maintenance team and to carryout repair work in a timely manner , thus saving the cost of repair and in prolonging the life of structures.

Acoustic emissions are the waves that are generated as energy from elastic or plastic deformations occuring in the material . ASTM E 1316 (2006) defines acoustic emission as " the class of phenomena whereby transient elastic waves are generated by rapid release of energy from localized sources withun the material, or the transient elastic waves so generated ". AE waves can be generated as a result of various sources dislocations, microcracking and other changes due to increase in strain. The method is very senstive which enables it to detect damage long before its visible. AE sensors record the vibrations created by waves when they reach the materials surface. The peizoelectric crystal the detected wave to electric signal, amplify it(internally or using the external pre-amplifier), and send it to the data acquisition system. The passive ability of AE, external excitation or stimulus for data collection once sensors are placed, makes it a suitable candidate for real time monotoring and structural health monitoring of in-service structures.

The method has also shown promise in assessment of damage during load tests of different structures and material including fibre reinforced polymer(FRP), steel, reinforced concrete(RC) and prestressed concrete(PC).

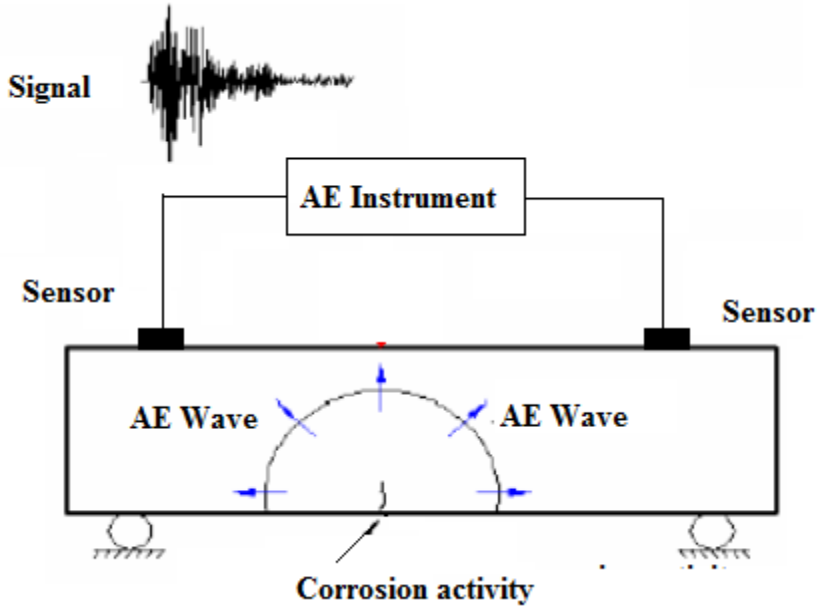

Fig.1.9: Schematic representation of AE Monitoring Process

As indicated earlier, AE waves are generated from a sudden release of energy. The strength of AE signals depends on a number of factors such as distance and orientation of the source with respect to the sensor as well as nature of transferring material. Detected AE signals are usually referred to as ‗hit'. A more detailed analysis can be conducted on the waveform of each signal to calculate a number of parameters such as amplitude, rise time, duration, signal strength, energy, counts, etc. (ASTM E1316). Figure 2.2 shows an AE waveform schematic with some of the parameters described. The definitions of some commonly used AE parameters are described here:

- **Hit**

  Hit is the process of detection and measurement of an AE signal on an individual sensor cannel (ASTM E1316).

- **Event**

  Event is the rise of AE activity that will cause multiple hits on different sensors (ASTM E1316). A single event can be detected on multiple sensors.

- **Amplitude**

  Amplitude (also known as signal amplitude) is the largest voltage peak in the AE signal waveform; customarily expressed in decibels (dB) relative to 1 μV at the preamplifier input (dB) assuming a 40 dB pre-amplification. Decibels is the unit of measurement for AE signal amplitude A, defined by A (dB) = 20 log Vp; where Vp is the peak signal voltage in μV referred to the preamplifier input (ASTM E1316).

- **Duration**

  Duration is defined as the time from the first threshold crossing to the end of the last threshold crossing of the AE signal from the AE threshold (ASTM E1316).

- **Rise time**

  Rise time is the time from an AE signal‘s first threshold crossing to its peak (ASTM E1316).

- **Counts**

  Counts are the number of times the AE signal crosses the detection threshold (ASTM E1316).

- **Signal Strength**

  Signal strength is defined as he measured area of the rectified AE signal with units proportional to volt seconds (the proportionality constant is specified by the AE instrument manufacturer) (ASTM E1316).

$$\frac{1}{2}\int_{t1}^{t2} f_{+}(t)dt \quad + \frac{1}{2}\left|\int_{t1}^{t2} f_{-}(t)dt\right|$$

  where: is the signal strength, is the positive signal envelope function, is the negative signal envelope function, t1 is the time at first threshold crossing, and t2 is the time at last threshold crossing.

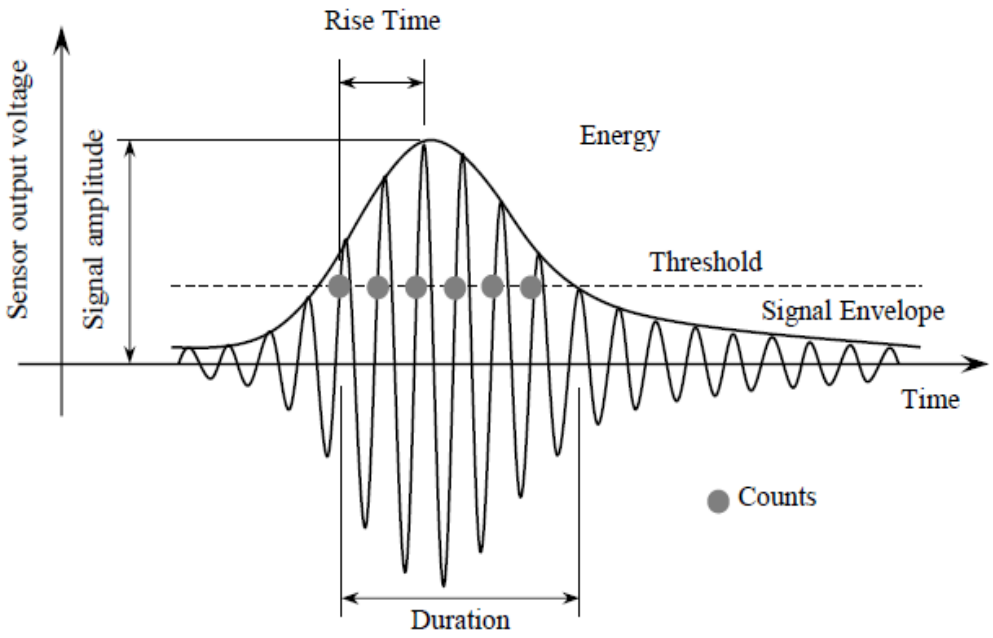

Fig.1.10: Schematic showing some parameters of an AE waveform (Behnia et al.,2014)

- **Average Frequency**

  Average Frequency is the ratio between number of counts and the duration of the AE signal.

- **Peak Frequency**

  Peak frequency is the point in the power spectrum at which the peak magnitude occurs. The peak frequency is a 2 byte value reported in kHz.

- **RMS**

  The root mean square (*RMS*) is a measure of continuous varying AE voltage. It is defined as the rectified time averaged AE signal measured on a linear scale and reported in volts.

- **RA value**

  RA value is the ratio between rise time and maximum amplitude in Volts from an AE signal.

1.7.1 ACOUSTIC EMISSION SOURCE LOCATION

AE has the ability to locate the source of emitted waves. This technique is very similar to that used in seismology to locate the epicentre of earthquakes (**Ono, 2010**). If the speed of AE wave in the tested material is known, source location can be performed using the arrival times of AE signals at different sensor locations. Since it requires more than one sensor, only AE events are detectable using this technique. The algorithms that perform source location are well established and usually embedded in the data acquisition software. AE source locations can be done in a linear or planar or three-dimensional space based on the number of sensors used. AE source location is challenging since the nature of the material, presence of existing cracks in the source-to-sensor path, and the dimensions of the tested member might lead to false events as a result of wave reflections. Previous research showed that AE source location is feasible in RC or PC structures if proper filters were used (**Xu 2008; El Batanouny et al. 2012**).

1.7.2 ADVANTAGES OF USING ACOUSTIC EMISSION TECHNIQUE

There are numerous advantages of using the Acoustic Emission Technique (**AE**) over the conventional NDT methods. Some of them are listed below:

- High sensitivity
- Early and rapid detection of defects, flaws, cracks etc.
- Real time monitoring
- Cost reduction especially maintenance cost.
- Defective area location
- It does not require access to whole area.

Hence, Acoustic Emission (**AE**) technique is a powerful aid to material testing and the study of deformation, fracture and corrosion. It gives an immediate indication of the Response and behaviour of a material under stress intimately connected with strength, damage and failure.

1.8 CLOSING REMARKS

This chapter deals with corrosion mechanism in RC structures, factors affecting the corrosion process, need of corrosion monitoring in RC structures and various Non-

destructive techniques used for corrosion monitoring in the structures. There is no denying from the fact that the NDT techniques can be used effectively for the investigation and evaluation of the actual condition of the structures. However, in this study we chose ultrasonic guided waves and acoustic emission technique for monitoring corrosion because of their advantages over other conventional NDT techniques. In the following chapter, work done by various researchers by using both these techniques will be discussed in detail.

CHAPTER 2

REVIEW OF LITERATURE

Various researchers have worked on the corrosion monitoring of RC structures using ultrasonic and acoustic emission technique. A brief review of work carried out in these subject areas of research has been explained in this section.

2.1 USE OF ULTRASONIC GUIDED WAVES IN R.C STRUCTURES

Pavlakovic et al. (2001) investigated the behaviour of ultrasonic guided modes that show minimum attenuation while propagating along the waveguide formed by the steel bar embedded in lower impedance grout, in order to maximise the inspection range of tendons. Two test specimens were constructed, comprising of a mild steel bar at the center of a plastic pipe filled with grout. For the first specimen, bar was undamaged, and for the second specimen, notches were cut approximately 500 mm from each end of the bar. Both pulse-through and pulse-echo tests were carried out. It was found that the dispersion curves of circular steel bar imbedded in lower impedance medium show a series of modes having attenuation minima at higher frequencies. These attenuation minima occurred at the same frequencies where the energy velocity maxima occurred (**Fig.2.1**).

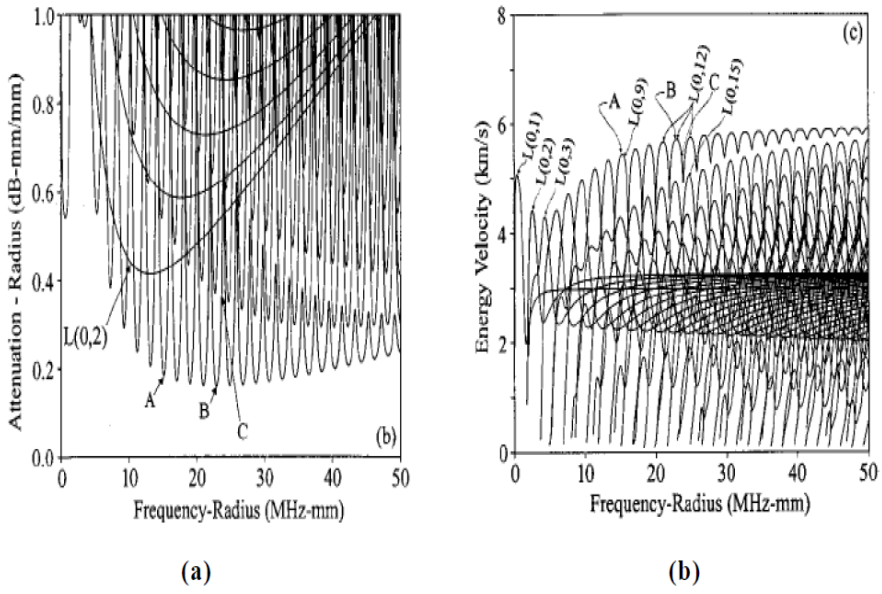

Fig.2.1: Dispersion curves of axis symmetric L (0,n) modes of steel bar imbedded in grout (a) attenuation; (b) energy velocity(Pavlakovic et al., 2003)

The attenuation minima and energy velocity maxima correspond to points where leakage of energy into the imbedding medium is minimized. It can be seen from the figure that the value of attenuation minima decreases with an increase in frequency, up to a frequency- radius of 23 MHz-mm. beyond this point, the material attenuation in the bar becomes a significant factor and attenuation at the minima increases. The experimental investigations also illustrate that the non-leaky mode that exists in a flat plate imbedded in cement grout does not exist in a circular bar imbedded in grout.

Na et al. (2002) investigated the feasibility of detecting and quantifying de lamination at the steel-concrete interface using ultrasonic guided waves. The experiments were performed on three sets of specimens. Specimen sets 1 and 2 comprised of four cylindrical structures each with different amounts of separation (0, 25, 50, 75 % of concrete steel interface). Specimen set 3 comprised of three concrete beam structures- specimen with different amounts of separation without stirrups, specimen with different amount of separation with stirrups and, specimen with same amount of separation at different positions with stirrups. Ultrasonic testing was conducted in through transmission mode. Two experimental set ups were devised for both relatively high and low frequency transducers and four Transmitter/ Receiver arrangements (TRA1, TRA2, TRA3, TRA4) were designed to generate, propagate and receive guided waves through steel bars and concrete (**Fig. 2.2**).

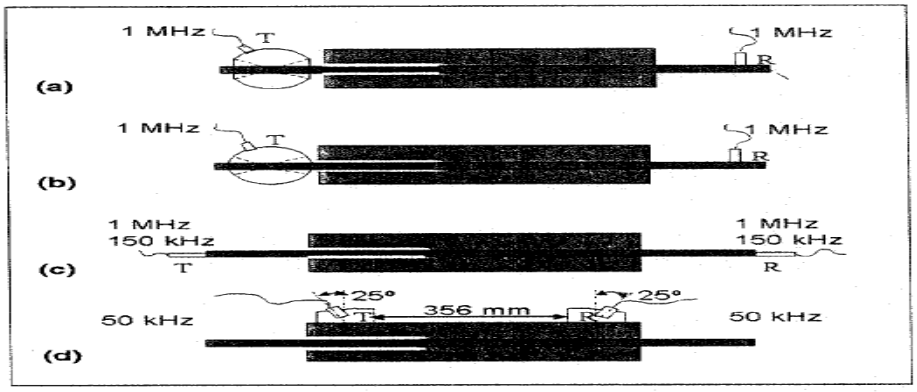

Fig.2.2: Different transmitter/receiver arrangements for experimental investigation: (a and b) spherical solid coupler transducer holders; (c)transmitter and receiver in direct contact at the ends; (d) solid coupler transducer holder on concrete with 25 degree incident and reception angles(Na et al.,2002)

Two annular solid couplers of different dimensions were used to launch flexural cylindrical guided wave modes along the steel bar, and an angular solid

coupler holder was used to launch lamb waves in concrete beams when steel bar was not accessible. Petroleum jelly was used as a couplant. Experiments were conducted 4- 8 times with every arrangement to investigate the consistency of results. Based on the experiments, V(f) curves were obtained

For specimen sets 1 and 2, it was observed that TRA1 is most efficient in predicting or quantifying the degree of separation. The sensitivity was affected by the selection of transducer frequency in TRA3. In case of TRA4, the detection sensitivity was affected by the distance between concrete surface and separation region. For specimen set 3, it was observed that in addition to the above conclusions, the amplitude of V(f) curves of specimens without stirrups were stronger than the specimen with stirrups. The results obtained with TRA1 and TRA2 were considerable if proper transmitter angles were used. The experimental investigation showed that the efficiency of annular shaped holders used for exciting flexural cylindrical guided wave modes was comparatively more than other holders. It was observed that though signals generated by relatively larger angles of incidence were more sensitive to discontinuities, however the propagating signal strength for a large incident angle was not always higher than the signals generated by smaller incident angles. It was concluded that the guided wave technique can be applied to predict or quantify the degree of separation or de lamination using pulse through transmission mode. However, other techniques such as pulse-echo method are required to predict the exact location of separation.

Beard et al. (2003) proposed a method using guided ultrasonic waves to inspect grouted steel tendons, anchors and rock bolts for corrosion and fracture. Two types of reinforcing tendons were constructed- single wire (5 or 7 mm in diameter) and 15 mm seven wire strands. A pulse-echo technique was carried out from the free end of the structure to measure the attenuation experienced by the wave in short lengths of grouted tendons. The amount of attenuation that the wave experienced because of leakage into the embedding material and material losses, was used to evaluate the reflection coefficient of the modes from different geometry breaks. The measurements of attenuation and reflection coefficients were used to determine the maximum length of tendon that can be inspected using this method. The experimental results illustrated that the inspection range for a complete break was limited to about 1.2 and 0.8 m for 7mm and 5 mm dia. wires respectively. For 15 mm stranded

tendons, the inspection range was limited to about 1.5 m for the center wire and about 0.5 m for the six outer wires. This indicate that the use of guided waves for the inspection of small diameter tendons would be limited to provide confirmation of defects in localized areas, due to high level of attenuation and poor reflection of modes. However, it was seen that with an increase in tendon diameter (25-30 mm), the attenuation reduces considerably. The rebars and grouted bolts with a large steel diameter generally have flat ends which are good reflectors of low-leakage modes. And, it was found that the inspection range of such structures could be as much as 5 m.

He et al. (2006) investigated the use of ultrasonic guided waves in a two-layered structure (composed of solid steel and semi-infinite layer of concrete) to measure the length of steel rod embedded in concrete and to estimate the amount of delamination between a steel rock bolt and concrete. A Semi-Analytical Finite Element Method (SAFEM) model was used to calculate the high frequency theoretical wave structures for a rod embedded in concrete. The ultrasonic testing was conducted on six specimens with different amounts of de lamination (0, 25, 33, 50, 75 and 100% of the entire rod length) using pulse-echo technique. (**Fig.2.3**)

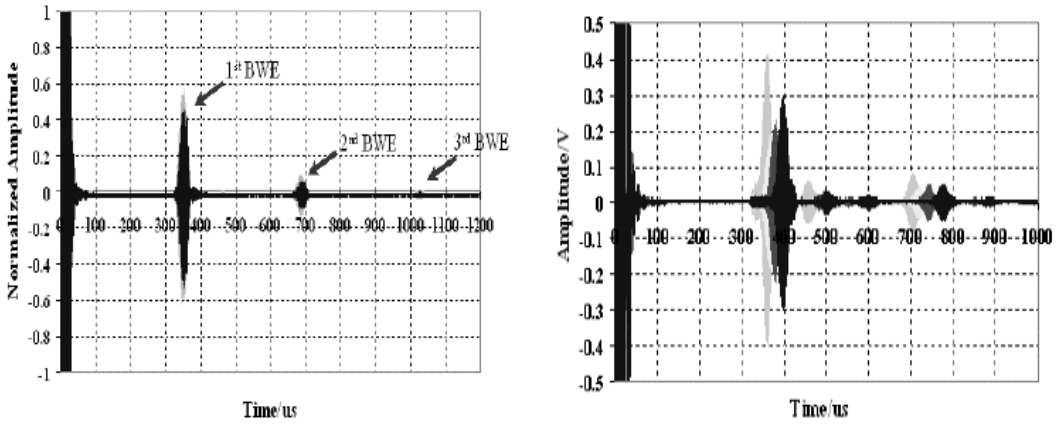

(a) 2MHz transducer (b) 1MHz transducer

Fig.2.3: Several experimental results obtained using pulse-echo measurements at different frequencies. (a) Waveform at 1.8MHz, grey for no de lamination, black for 1/3 de lamination (b) Echoes at 1.58, 1.38, 1.18 and 0.98MHz from left to right.(He et al., 2006)

The experimental results illustrate that, in order to determine the length of an embedded rod, one must use guided wave modes at higher frequencies. A transducer with a centre frequency of 1 MHz or higher was found to be suitable for length

determination. For most frequencies above 1 MHz, there was a little amplitude difference between a completely bonded interface and a 33% de laminated specimen, as seen in **Fig 2.3**.

The lower frequency guided wave modes showed better results while estimating de lamination at the steel-concrete interface. It was concluded that any transducer with a centre frequency larger than 2 MHz is not suitable for de lamination estimation.

Fig.2.4 shows that higher frequency modes at excitation frequency of 2.6 MHz and 2.8 MHz are insensitive to the presence of de lamination, as there is a little change in signal amplitude.

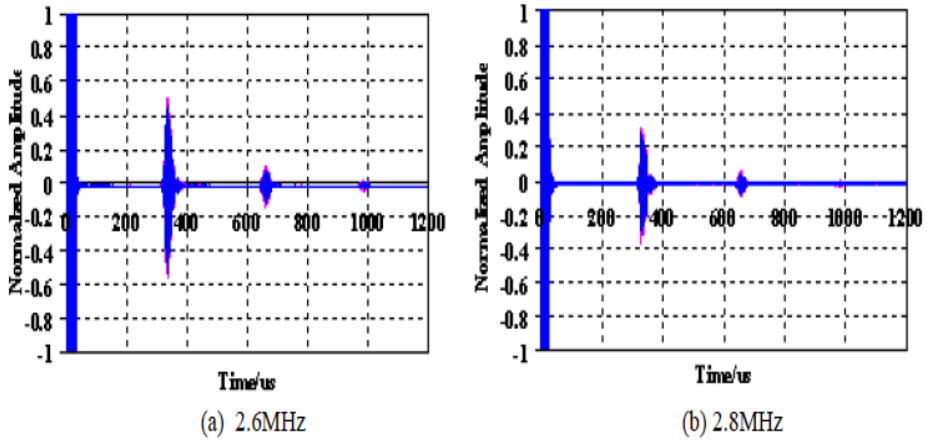

Fig.2.4: Waveforms typical of those obtained above 2MHz. There is almost no contrast between the delaminated specimen and the completely bonded specimen. Grey for no de lamination and black for 1/3 de lamination.(He et al., 2006)

It was concluded that ultrasonic guided wave pulse-echo technique can be applied to inspect large lengths of embedded rods.

Cawley (2007) studied the application of ultrasonic guided waves for the long range inspection of large structures such as airframes. The problem of overlapping of reflections from different features in complex structures was highlighted. An increase in feature density made it impossible to analyze an individual reflection or, an extra reflection from a defect. This problem was resolved by subtracting the current response from a baseline measurement taken when the state of structure was known and this made it possible to monitor the changes in the response of the structure. However, this method required a high degree of signal stability with time in the

absence of damage, or a scheme that could correct benign changes such as temperature variations. One such scheme, 'temperature compensation' was implemented and considerable results were obtained. It was emphasized that some other benign changes such as moisture uptake in adhesives are also a matter of concern and a great deal of research is required to realise a reliable health monitoring system for complex structures.

Ervin et al. (2008) investigated guided wave modes in both low and high frequency ranges capable of monitoring corrosion in reinforced concrete. The fundamental longitudinal modes L(0,1) and L(0,9) were chosen for experimental testing at low and high frequency respectively. L(0,1) mode was chosen because it shows negligible signal loss due to material absorption. It was used to access interfacial damage between steel and mortar. L(0,9) mode was selected because it is the fastest and lowest attenuating mode in the system. Experiments were conducted to examine the effect of reinforcing ribs, water and mortar on low and high frequency guided waves. Ultrasonic testing was carried out in a through transmission mode on rebar in air, rebar immersed in water, rebar embedded in mortar, corroded rebar in air and reinforced mortar specimens undergoing accelerated corrosion(**Fig.2.5**).

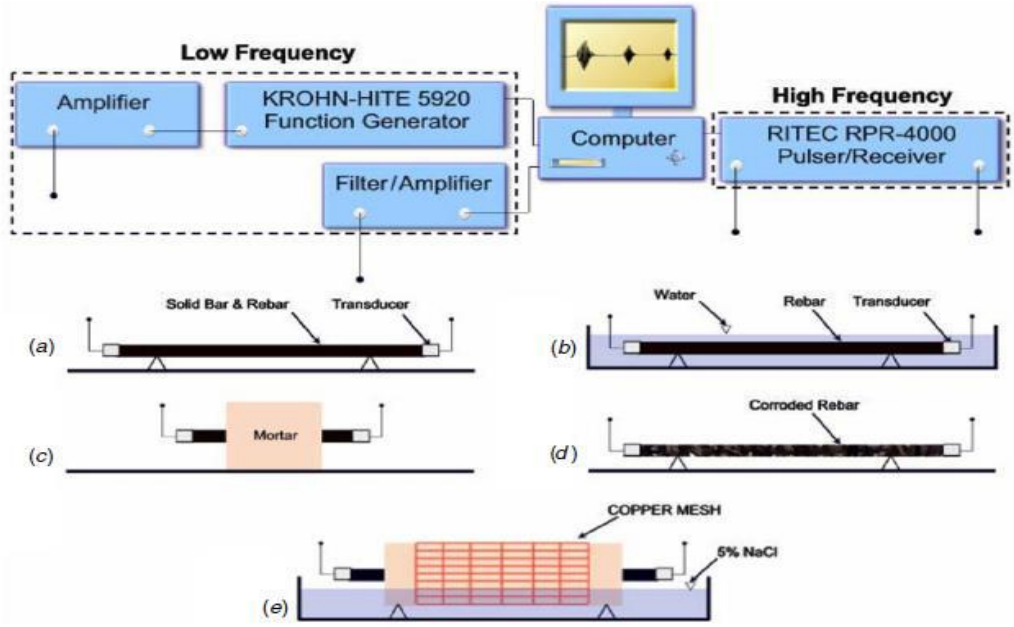

Fig.2.5: Through-transmission testing for low- and high-frequency longitudinal wave testing on (a) a solid bar and rebar in air, (b) rebar immersed in water, (c) rebar embedded in mortar, (d) corroded rebar in air and (e) reinforced mortar specimens undergoing accelerated uniform corrosion.(Ervin et al., 2008)

Testing showed that reinforcing ribs has an attenuative effect on guided wave propagation only in certain frequency ranges. Testing confirmed that L(0,1) mode has some sensitivity to water over the frequency range tested, with attenuation increasing with frequency. It was observed that the lowest frequencies of L(0,9) mode show sensitivity to water while the higher frequencies show diminished sensitivity. For the bars embedded in mortar, testing showed that the low frequency mode was highly attenuated; resulting in monitoring of relatively short distances (e.g.1m). The attenuation shown by L(0,9) mode was much smaller than L(0,1) mode. For rebar specimens extracted from accelerated corrosion tests, testing showed that L(0,1) was not substantially affected in the lowest range. However, interesting results were seen for L(0,9) mode. It was observed that there was no frequency content between frequency domain peaks when the corrosion damage frequency was low. As the corrosion level increased, the frequency content between frequency domain peaks, referred to as 'web' frequencies started to increase. The attenuation curves for rebar in air, water and mortar are shown in F**ig.2.6**.

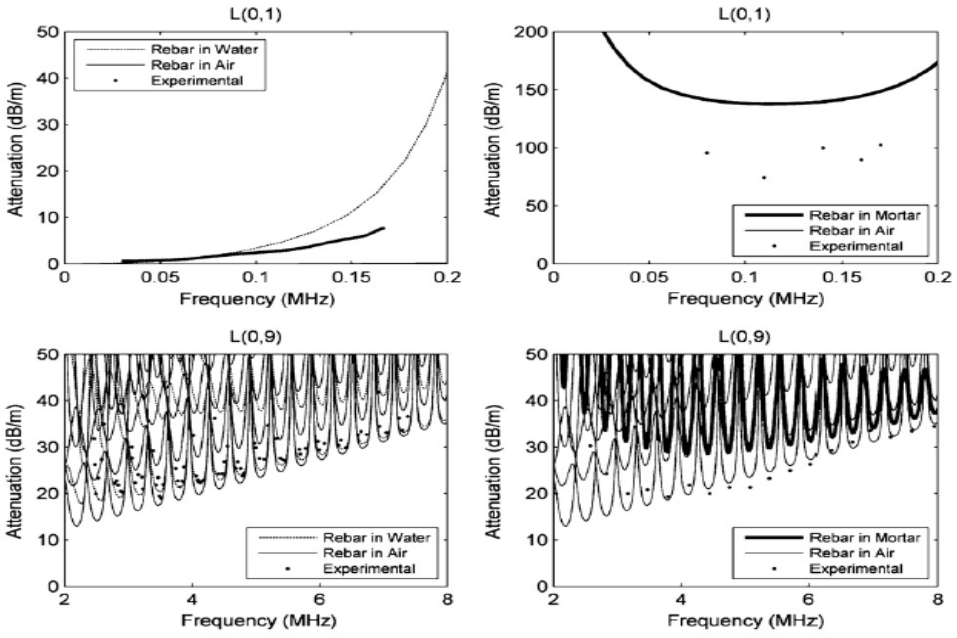

Fig.2.6: Theoretical attenuation curves with experimental attenuation measurements for rebar in air, immersion in water and embedment in mortar at low and high frequencies (Ervin et al., 2008)

For rebar specimens undergoing accelerated corrosion, testing showed that L(0,1) was highly attenuated such that it was not detected until after corrosion had initiated and corrosion product accumulation caused mortar cracking (**Fig. 2.7**).

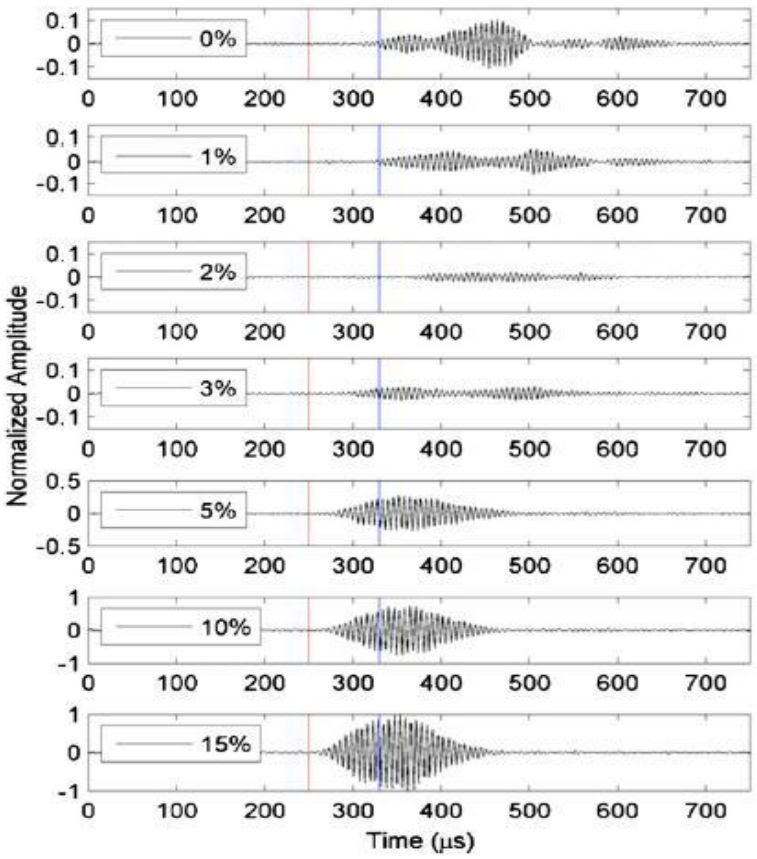

Fig.2.7: Time domains at different levels of mass loss for low-frequency monitoring of accelerated corrosion. Left and right vertical lines are the arrival times for the L(0, 1) and F(1, 1) modes, respectively. The input signal was a 164 kHz 15-cycle pulse, with a band pass of 159 kHz and 169 kHz. (Ervin et al., 2008)

Once detected, L(0,1) mode was sensitive to the combined effect of bond deterioration and mortar stiffness reduction. The results indicate that the signal strength of L(0,1) mode was increasing as the mass loss was advancing(**Fig.2.7**)

L(0,9) mode was relatively insensitive to the surrounding interface conditions at high frequencies. This allowed the monitoring of steel cross sectional area and bar topography, from the onset of corrosion to severe pitting (**Fig.2.8**).

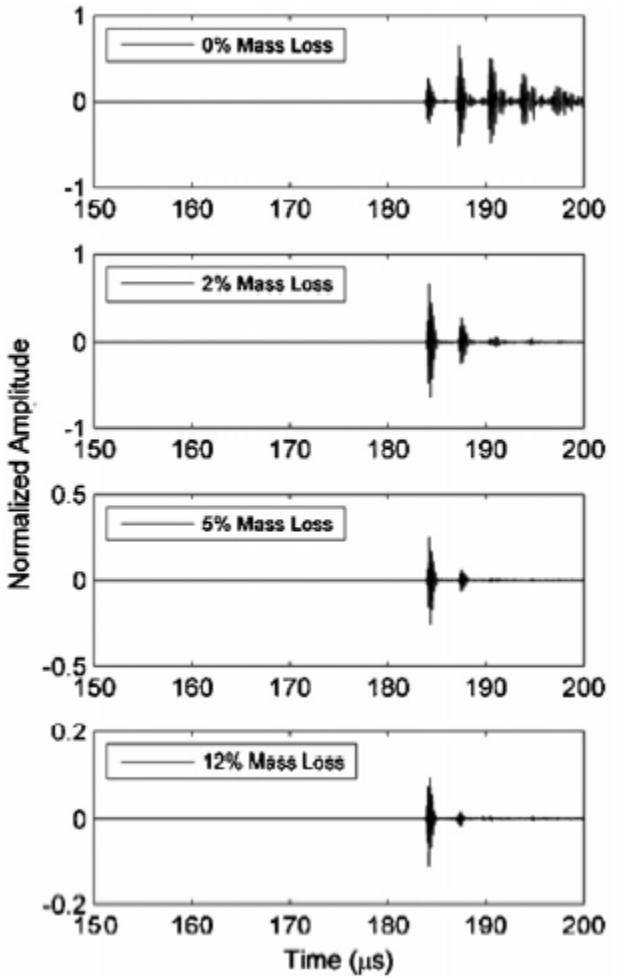

Fig.2.8: Time domain response at different levels of mass loss for high-frequency monitoring of accelerated corrosion. The input signal was a 5.08 MHz single cycle pulse, with a bandpass of 2 MHz and 10 MHz.(Ervin et al., 2008)

Mahmoud et al. (2010) investigated the use of ultrasonic waves for non-destructive structural health monitoring of CFRP bonded concrete specimens subjected to water immersion ageing at controlled temperatures of 25-60 degree Celsius. The feasibility of using non-destructive ultrasonic technique as an alternative to destructive technique was analyzed. Narrow-band transducers with center frequency of 110 kHz were used to generate and receive surface waves at the external face of CFRP. The signals received by the transducer were amplified, digitized and processed to extract the parameters: average power ($Pavg$), maximum amplitude ($Pmax$) and maximum power- frequency ratio ((P/F) max) in both time and frequency domains. The variations in these parameters due to water- immersion ageing at different temperatures were monitored over 12 weeks. Results indicated a decrease in the measured ultrasonic parameters due to ageing over time. A simultaneous

destructive study was carried out on mode-11 fracture loading of CFRP concrete samples subjected to some ageing conditions and temperature and a parameter, fracture energy was obtained. A correlation analysis was performed at each ageing temperature, between the non-destructive parameters ($Pavg$, $Pmax$) and destructive parameter, as shown in **Fig.2.9**.

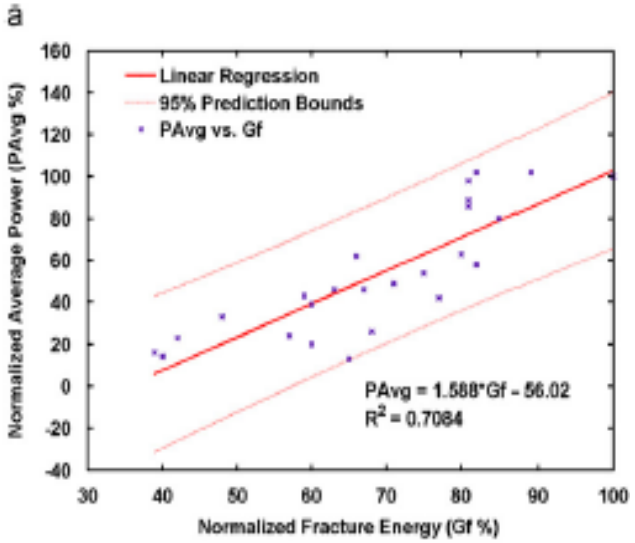

Fig 2.9 (a): Linear regression of non-destructive ultrasonic parameters vs. fracture energy results of CFRP–concrete samples subjected to accelerated aging temperatures: (a) average power (Pavg) vs. Fracture energy(GF).(Mahmoud et al., 2010)

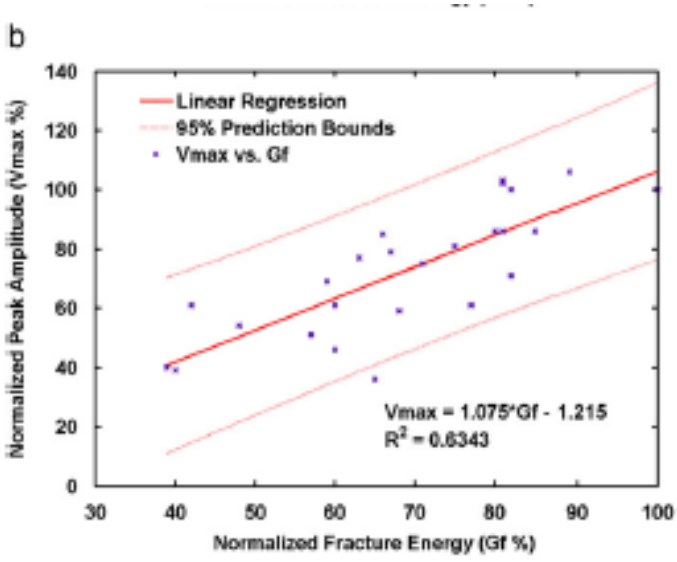

Fig 2.9(b): peak amplitude (V_{max}) vs. Fracture energy(GF) (Mahmoud et al., 2010)

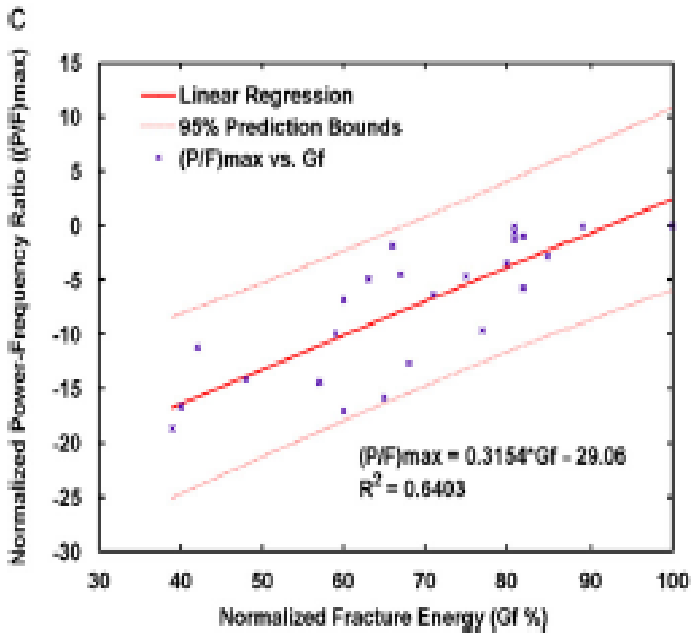

Fig 2.9 (c): Maximum power–frequency ratio of PSD ((P/F) max) vs fracture energy ( ). Linear equations and 95% prediction bounds are shown. (Mahmoud et al., 2010)

The results indicate a good correlation between the ultrasonic parameters and fracture energy at all temperatures. It was concluded that non-destructive ultrasonic technique can be used for the structural health monitoring of CFRP protected concrete structures.

Raisutis et al. (2010) analyzed the possibility of using non-destructive ultrasonic guided waves for inspection of small diameter CFRP rods used in gliders. The models such as 3D numerical solutions, finite difference and finite element were used to investigate the propagation of ultrasonic guided waves in defective CFRP rods with multiple de laminations. The experiments conducted demonstrate that ultrasonic guided waves can be applied for testing of defective CFRP rods. The immersion technique based on the excitation of longitudinal guided wave mode L(0,1) to monitor the amplitude of leaky waves over the rod, was proposed. The de lamination type defects were indicated by a reduction in amplitude or complete disappearance of leaky waves over a defected zone. It was shown that the propagation of L(0,1) guided waves was not hampered by the de lamination type defects. L(0,1) mode was just converted into other modes that did not generate leaky waves. Thus, a possibility of detecting a series of defects in CFRP rods was seen. The future scope for non-contact generation

of longitudinal L(0,1) guided wave mode by a more advanced ultrasonic technique was emphasized for online testing of CFRP rods.

Sharma and Mukherjee (2010) discussed the use of longitudinal guided ultrasonic waves to monitor notch and debond defects in steel bars in concrete simulating pitting and de lamination phenomenon caused by corrosion. The low and high frequency ultrasonic pulse echo and pulse transmission technique was used for early detection of damages in steel in RC beams. The exact location and magnitude of damage was indicated by efficient combination of the two ultrasonic monitoring techniques. Ultrasonic guided wave monitoring utilizing specific core and surface seeking modes was applied to identify corrosion mechanism in a bar embedded in concrete. In general, huge pitting and non-uniform area loss was highlighted by severe signal attenuation marks chloride corrosion, which was well unravelled by core seeking mode. It began with de lamination shown by signal rise with surface seeking mode. It was concluded that through judicious selection of ultrasonic modes, the complete corrosion mechanism in RC structures can be successfully identified.

Sharma and Mukherjee (2011) investigated the type of corrosion mechanism in chloride and oxide environments in RC beams. Ultrasonic guided waves with specific core and surface seeking modes were used for monitoring rebar corrosion in beams. It was observed that in case of Chloride corrosion in beams, when core-seeking mode was propagated, the signal was highly attenuated, thus indicating pitting and non-uniform area loss. When surface seeking mode was propagated, there was an initial rise in the signal strength and then a fall, thus indicating delamination followed by local loss of material. In case of Oxide corrosion in beams, it was observed that when core-seeking mode was propagated, there was a slow fall in signal strength, indicating the absence of pitting. When the surface-seeking mode was propagated, there was an initial drop in the signal due to the pressure build up by the formation of corrosion products, indicating a slow corrosion rate and localized corrosion and eventually, a gradual rise in signal strength was observed, indicating slow bond deterioration. The ultrasonic voltage trends of the received signal in both chloride and oxide corrosion specimens using surface-seeking and core-seeking mode are shown in **Fig. 2.10 (a) and 2.10 (b)** respectively.

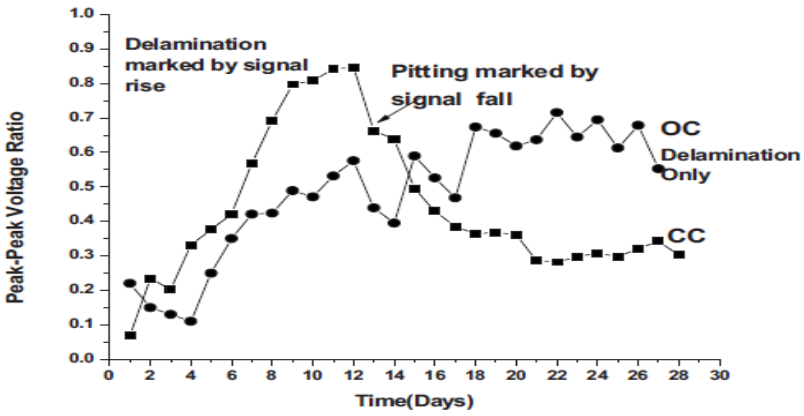

Fig.2.10 (a): Peak-peak voltage ratio with surface-seeking mode

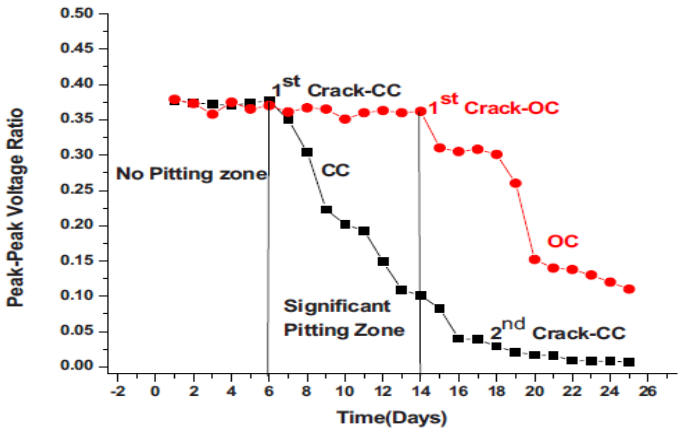

Fig.2.10(b): Peak-peak voltage ratio with core-seeking mode.

Thus, the mechanism and rate of rebar corrosion was successfully monitored in chloride and oxide environments through appropriate selection of modes. Simultaneous destructive tests were also carried out on RC beams, and it was found, that non-destructive Ultrasonic technique correlate well with the destructive technique.

Sharma and Mukherjee (2013) reported non-destructive evaluation of reinforcing bars that are corroding in the presence and absence of chlorides utilizing ultrasonic guided waves. Ultrasonic guided wave monitoring utilizing specific core and surface seeking modes to identify the type, rate, and mechanism of corrosion in a reinforcing bar in concrete subjected to different exposure conditions was discussed. The experimental investigation involved monitoring of RC beams undergoing accelerated impressed current corrosion. In general, huge pitting and non-uniform area loss was highlighted by severe signal attenuation marks chloride corrosion,

which was well picked up by core seeking mode. It began with de lamination shown by signal rise with surface seeking mode. In oxide corrosion, the rate of corrosion was slow, localized, and marked by slow bond deterioration as depicted by signal strength rise in surface seeking mode. Pitting was insignificant in core seeking mode in OC. Thus, it was observed that through a judicious selection of ultrasonic modes, different types of corrosion in RC structures can be successfully identified. Bars at different stages of corrosion were ultrasonically monitored in both oxide and chloride environments to explore the ability of ultrasonics to predict the level of deterioration of the bars. It was done successfully by correlating ultrasonic voltage ratio with destructive parameters of mass loss, tensile strength and bond strength in the two common corrosion environments. It was concluded that, although the use of guided waves is effective in identifying the presence of corrosion in rebars in widely varying environments, the method needs access to the ends of rebars. At site, bars that are most susceptible to corrosion need to be exposed at the ends to perform the test. Also the signal-to-noise ratio should be above the ground noise level.

2.2 USE OF ACOUSTIC EMISSION FOR CORROSION MONITORING

Yoon et al. (2000) studied damage in corroded Reinforced concrete using the Acoustic emission. He conducted a series of normal strength concrete beams tests using four-point flexural loading. The beams were 100 mm wide, 150 mm deep and 1150 mm long. Several different types of beams were tested to simulate different sources of damage and the list of beams tested is shown in **Fig.2.11**.

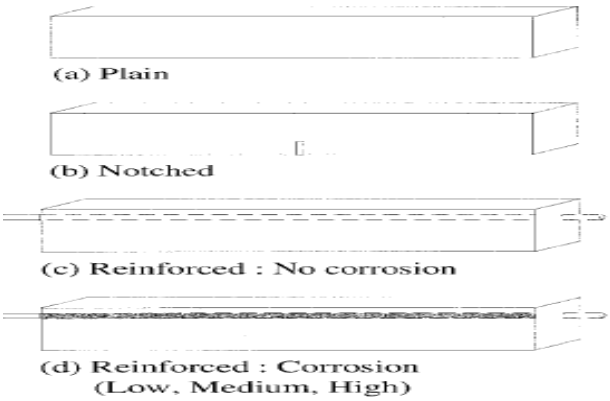

Fig.2.11: Types of concrete beam specimens (Yoon et al., 2000)

Three plain unreinforced beams and three notched plain unreinforced beams were used to obtain the initial response of distributed micro crack development and localized crack propagation, respectively. The reinforced specimens allow the determination of the characteristic AE response of a reinforced concrete element from several sources such as Micro cracking, Localized crack Propagation, Flexural cracking, Shear cracking and De bonding. In addition, three reinforced beams were corroded to three levels of distress using anodic current that was applied after 28 days of standard moist curing. The typical Load-displacement envelope for the plain and notched beams is shown in **Fig.2.12 (a).** The response of the non corroded and highly corroded beams is shown in **Fig.2.12 (b)**. The response of the unreinforced beams is divided into two regions to describe the presence of distributed micro cracking throughout the beam in region A and localized crack development in the region B. The response of the reinforced beam was divided into four regions: Region A represents the distributed microcraking; Region B describes the beginning of first crack localization in the constant moment region; Region C describes the continued development of micro cracking; and the Region D appears to correspond to the development of either a shear crack in the beam or bond-spitting cracking along the reinforcing bar.

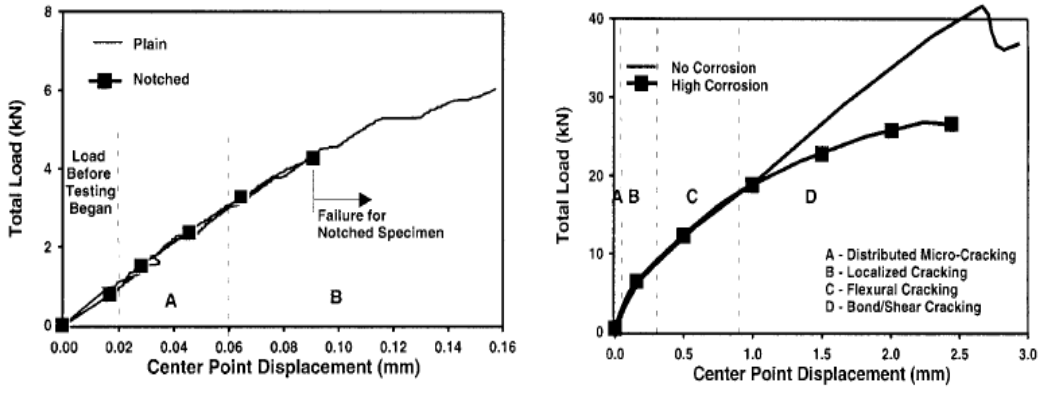

(a) (b)

Fig.2.12: Load Displacement envelope for a) Unreinforced beams b) Reinforced beams (Yoon et. al., 2000)

Fig. 2.13 and 2.14 shows the occurrence of AE events as a result of cyclic loading for different unreinforced and reinforced specimen. The load cycle shown as a fine line is also plotted in each figure. On the whole, in each load cycle the AE activity decreased as the load was held constantly or unloaded.

From **Fig.2.13 and 2.14**, it can be seen that there were fewer AE events during the whole test in the plain and the notched concrete specimens than the reinforced concrete specimens. Also it has been observed that secondary peaks of AE events develop in the unloading response after approximately four cycles (**Fig 2.14a-d**). this phenomenon does not appear in the unreinforced specimen (**Fig 2.13, a-b**).In early stages of loading, there is a large difference between the no. of AE events as shown in (**Fig 2.13, a-b**).a large no. of AE events were generated in the un corroded specimens whereas fewer AE events were observed in the corroded specimen; in the reinforced beams the higher the degree of corrosion, the lower the AE activity. Thus, the majority of micro cracking and longitudinal cracking along the reinforced beam has already dissipated by damage process due to corrosion (**LI et. al., 1998**).

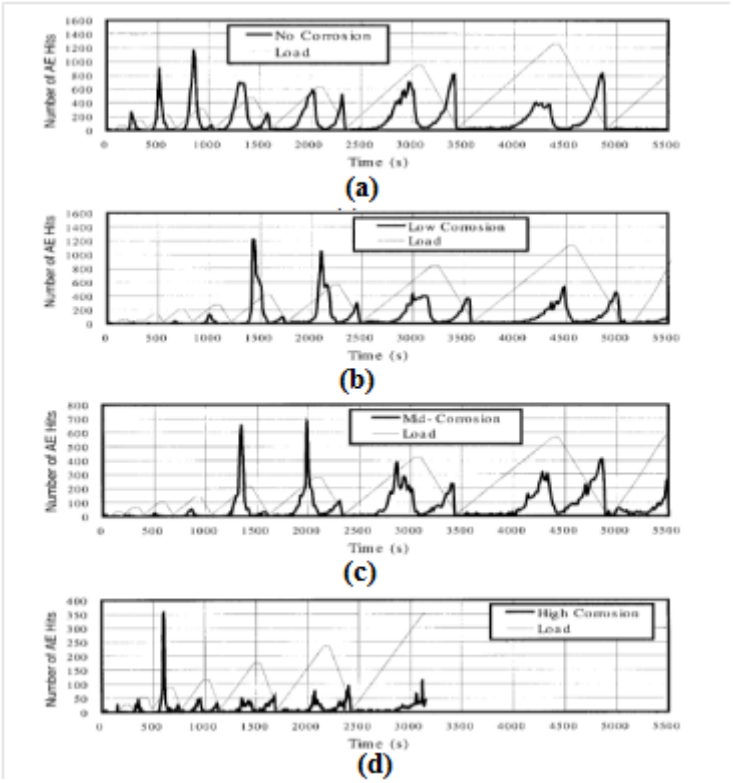

Fig.2.13: AE hits versus cyclic loading for reinforced beams (corroded and uncorroded beams) (Yoon et al., 2000)

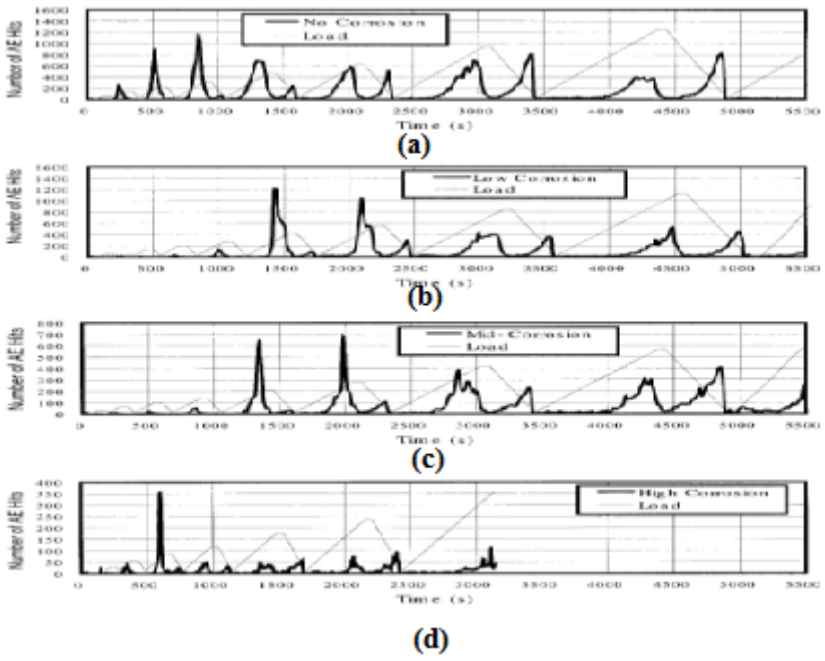

Fig.2.14: AE hits for cyclic loading for unreinforced beams (plain and notched) (Yoon et al., 2000)

The cross-plot is an effective technique to analyze the features of an entire AE signal at a glance for the purpose of distinguishing signal characteristics. **Fig.2.14** shows the results of a cross-plot of amplitude and duration of AE signals for unreinforced beams (plain and notched). The black diamond's indicate AE events from the notched specimen, whereas open circles indicate AE events from the un-notched concrete specimen. Signals correspond to Stage A and part of Stage B. These loading stages are characterized by distributed micro cracking and formation of localized cracks, respectively.

Tomoda et al. (2003) studied corrosion monitoring in reinforced concrete by acoustic emission. In the accelerated corrosion test, two types of mixture were employed. The water-to-cement ratios (W/C) were 45 % and 55%. In the crack-expansion test, W/C of concrete was 50%.

In the accelerated corrosion test, reinforced concrete slabs of dimensions 10 cm x 25 cm x 40 cm were made. In the crack-expansion test, a concrete plate of dimensions 10 cm x 25 cm x 25 cm was made. In order to simulate radial pressure due to corrosion product, expansive agent of dolomite paste was poured into a hole of 30 mm diameter. Three specimens were prepared for each W/C ratio, and the chloride contents were measured after accelerated corrosion. For W/C = 45%, core samples

were taken at 4 days, 10 days, and 12 days elapsed, while for W/C = 55% at 4 days, 8 days, and 10 days elapsed. These periods are determined from a comparison between AE activities. and half-cell potentials. High AE activities are observed at two stages of 3 days and 7 days elapsed. For non-destructive evaluation of corrosion, the half-cell potential measurement is normally carried out. From the potentials measured at the surface, the probability of corrosion is estimated as more than 90% when the potentials are lower than –350 mV.

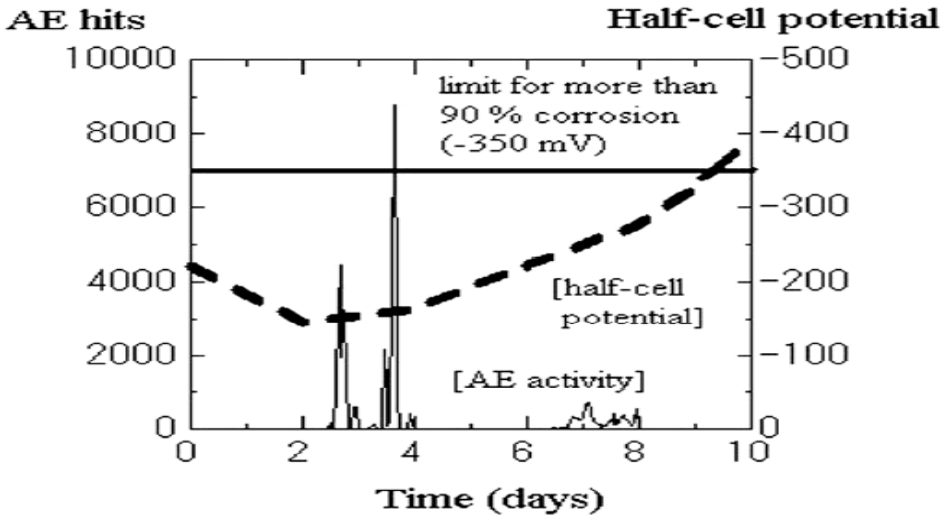

Fig.2.15: AE activity and half-cell potential vs. time during accelerated corrosion (W/C=55%) (Tomoda et al.,2003)

As seen in **Fig.2.15,** the potentials start to decrease, around at the first AE activity (finished at 4 days). Then the potential reaches lower than –350 mV after 10 days, following the second AE activity (finished at 8 days). Consequently, the test of one specimen for W/C = 55% was finished at 4 days, and the other was completed at 8 days. The third specimen was conducted up to 10 days. Results in **Fig.2.16** reveal that AE activities could provide earlier warning than the half-cell potential measurement.

Distribution of chloride contents in depth was determined, and results are given in **Fig. 2.16**. At the location of concrete cover, chloride ions per m3 becomes higher than 1.2 kg after 12 days in a sample with W/C = 45%. In contrast, it reaches over 1.2 kg after only 8 days for W/C = 55%. This is because the permeability increases with an increase in W/C ratio in concrete. According to the Standard Specification (JSCE, 2001), the lower and upper bounds for triggering corrosion are prescribed as 0.3 kg/m3 and 1.2 kg/m3, respectively.

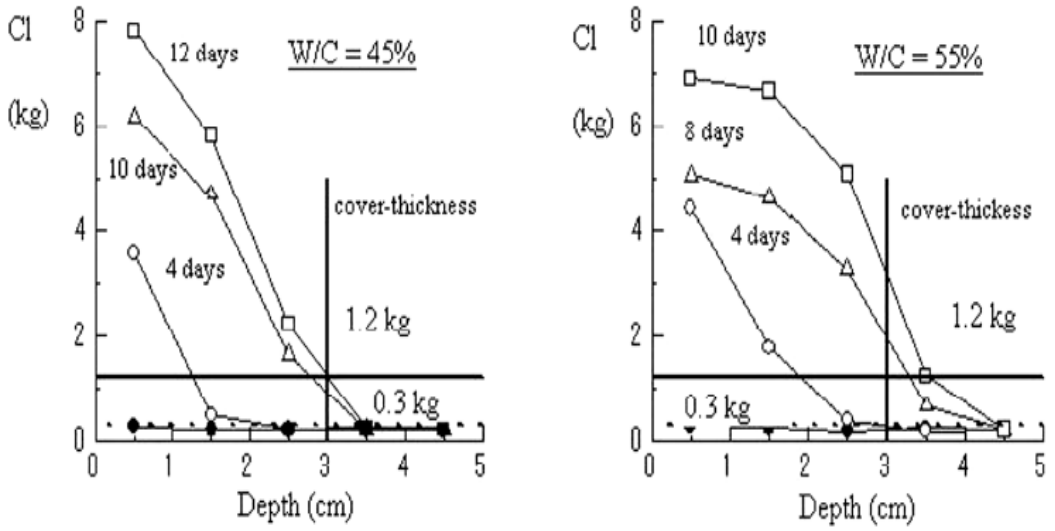

Fig.2.16: Distribution of chloride ions in depth (Tomoda et al.,2003)

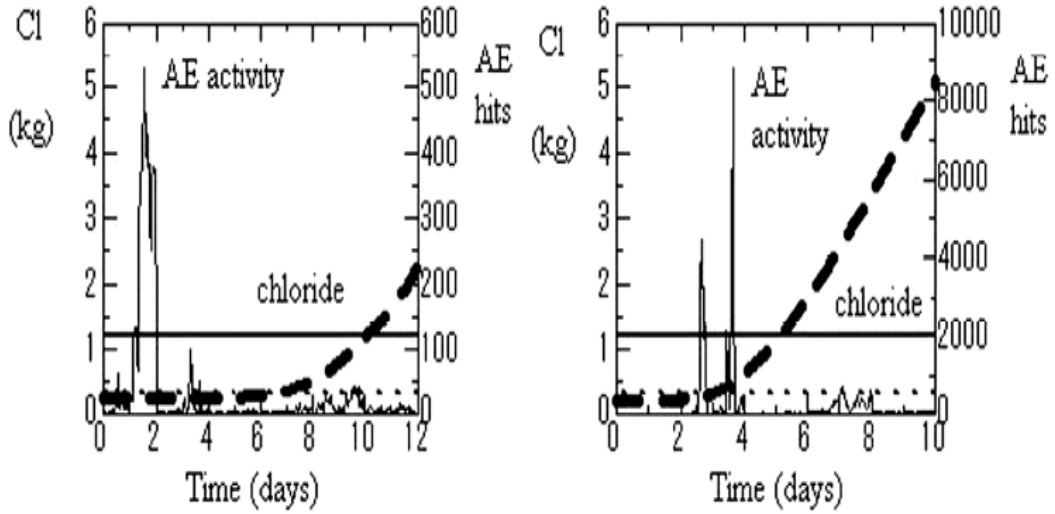

Fig.2.17: Comparison between AE activities and chloride contents (Tomoda et al., 2003)

Consequently, the amount of chloride contents, C(t), was computed at cover-thickness based on Fick's law

$$C(t) = Co\ (1 - erf\ (x/2[Dt]1/2)) \quad \text{.....(4.1)}$$

where, Co is the surface concentration, D is diffusion coefficient, t is time and erf is Gauss's error function. Results are compared with AE activities in **Fig.2.17**. Here, chloride contents in concrete were determined first from potentiometric titration. The surface concentration and the diffusion coefficient were estimated by the regression analysis, by fitting the distribution using fick's law equation. Obtained values of the

surface concentration, Co, and the diffusion coefficient, D, are 10.02 kg/m^3 and 6.05 x 10-8 cm^2/sec, respectively. Right after the chloride contents become higher than the lower bound (0.3 kg), the first high AE activity is observed in both cases of W/C = 45% and 55%. At the stage where the chloride content exceeds the upper bound (1.2 kg), another high AE activity is observed. These results demonstrate that high AE activities of the two stages are observed in the accelerated corrosion test. One is the stage where the chloride content reaches 0.3 kg/m^3, and the other is the stage where the chloride level becomes higher than 1.2 kg/m^3 in concrete.

These are in remarkable agreement with the deterioration process due to salt attack, which is prescribed in the Standard Specification. According to the process shown in **Fig.2.18**, there exist the first stage for the initiation of corrosion from the incubation to the development period, and the second for the nucleation of cracking from the development period to the accelerated corrosion.

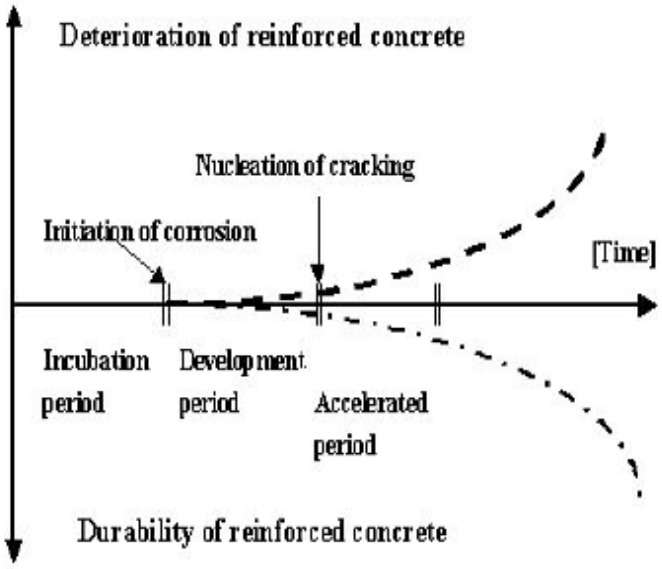

Fig.2.18: Deterioration process due to salt attack. (Tomoda et al., 2003)

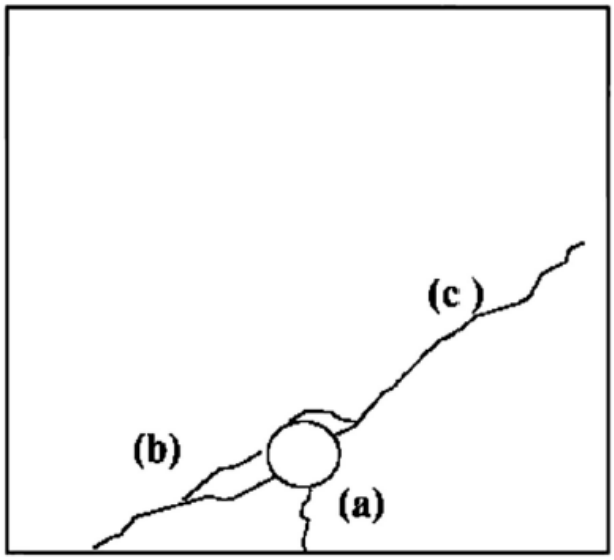

Fig.2.19: Crack pattern observed after the test (Tomoda et al., 2003)

Nucleation of typical corrosion cracks was simulated by employing expansive agent. A hole of 30 mm diameter to represent the rebar location was made at 3 cm depth from the side, corresponding to 3 cm cover-thickness. After casting expansive agent into the hole, surface cracks were observed after two days. During extension of these cracks, AE events were detected by six AE sensors .After the test, SiGMA analysis was conducted. Three main cracks observed are shown in **Fig.2.19**, which are labelled as crack traces (a), (b), and (c). In reference to the cross-section of a reinforced concrete member this model simulates, crack trace (a) corresponds to a surface crack, which is normally observed as corrosion cracking. Crack trace (b) is commonly observed as a spalling crack due to corrosion. An internal crack (crack trace (c)) is generally not taken into account, because this is inaccessible to usual visual inspection. AE events analyzed by SiGMA procedure were first located, and then were classified as three clusters responsible for crack traces (a), (b) and (c) from **Fig.2.20**. All the results of SiGMA analysis are plotted in **Fig.2.21**. AE events analyzed are marked with arrow or cross symbols. The arrow symbol represents a tensile crack, and the arrow direction indicates the crack opening direction. Shear cracks are denoted by cross symbols, and their two orientations correspond to the crack motion vector and the crack normal vector, respectively.

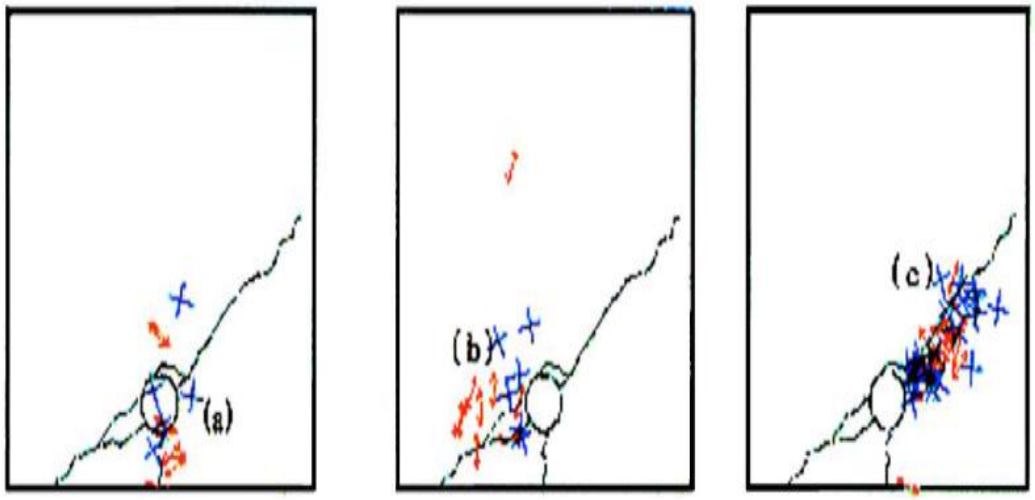

Fig.2.20: Results of SiGMA analysis classified in three clusters (Tomoda et al.,2003)

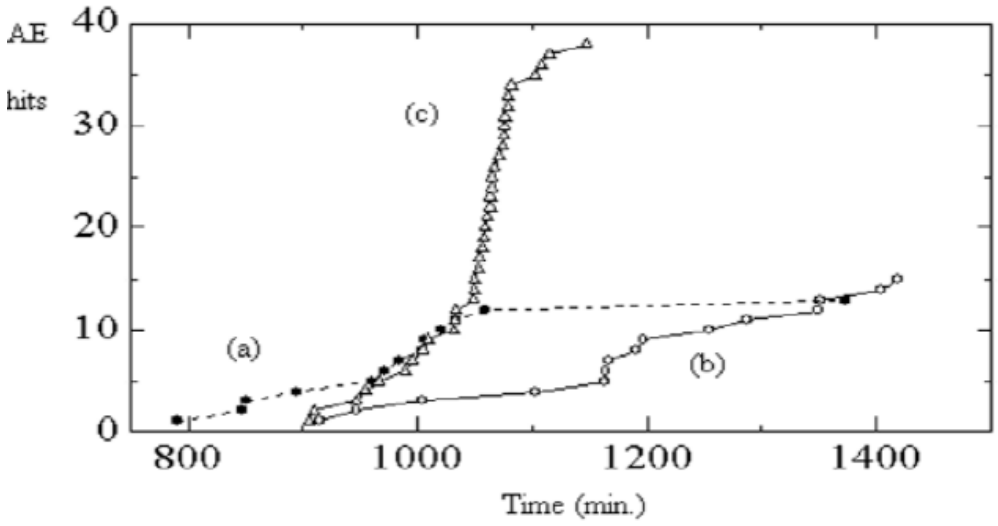

Fig.2.21: AE activities during nucleation (Tomoda et al., 2003)

Concerning crack trace (a), tensile cracks running vertically to the surface are mostly visible from outside. In contrast, shear cracks are not explicitly associated with the extension of surface-breaking cracks. For crack trace (b), tensile cracks are primarily observed at the locations far from the reinforcement or close to the stress-free surface, while shear cracks are mostly observed near the reinforcement. In crack trace (c), tensile and shear cracks are fully mixed up. Results obtained are summarized, as follow:

- In the accelerated corrosion tests, AE occurrence is monitored continuously. Investigating ingress of chloride ions, a relationship with chloride concentration and AE activity is obtained. Right after the chloride contents become higher than 0.3 kg/m^3, a high AE activity period is observed. Subsequently, at the stage where the chloride contents become higher than 1.2 kg/m^3, another high AE activity period is observed.
- Two stages of high AE activities are observed in the accelerated corrosion test, which remarkably correspond to the two stages in the deterioration process due to salt attack. These are the initiation of corrosion from the incubation period to the development and the nucleation of cracking from the development period to the accelerated. This suggests that these two stages are possibly identified by in situ AE monitoring.
- The corrosion probability by the half-cell potential reaches over 90% after the appearance of these two stages. It confirms that AE monitoring could provide earlier warning of corrosion than the half-cell potential measurement.
- Applying SiGMA procedure, nucleation mechanisms of a surface crack, a spalling crack, and an internal crack due to the expansion of corrosion product are identified. The surface breaking crack is nucleated dominantly by tensile cracks. For the spalling crack, both the tensile and the shear cracks are generated. Tensile cracking is dominant near a stress-free surface, but the main mechanism of the internal crack is of shear-crack motion.
- In the case of visual inspection, the detection of the surface and spalling cracks is the main target. Monitoring the nucleation of tensile cracks by applying SiGMA procedure, it is possible to estimate and predict the extension of these two type s of cracking. It is noted that the internal crack could be generated following the surface crack, and the main mechanism of the internal crack is of shear.

Ohtsu et al., (2007) studied the corrosion process in Reinforced concrete identified by Acoustic emission. RC slabs tested were of dimensions 300mm × 300mm ×100mm. Reinforcing steel bars of 13 mm diameter are embedded with 15 mm cover thickness for longitudinal arrangement. An accelerated corrosion test and cyclic wet -dry test were conducted. Half cell potentials at the surface of the specimen

were measured by portable corrosion-meter. In the accelerated corrosion test, the measurement was conducted twice a day, right after discontinuing the current. Chloride concentrations were measured at several stages .At first; the initial concentration was measured by using a standard cylinder sample after 28-day moisture curing. A relationship between the AE activity and the half-cell potentials measured are shown in the **Fig.2.22.**

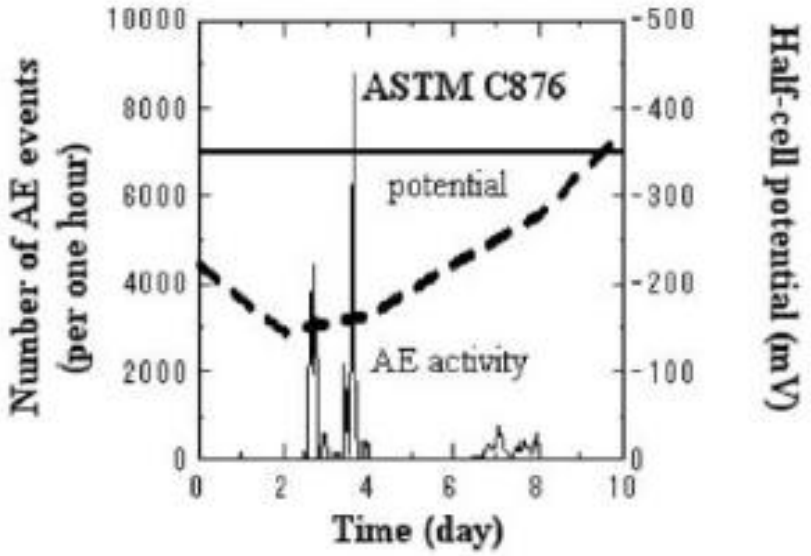

Fig 2.22: AE activities and Half-cell potential in accelerated corrosion (Ohtsu et al., 2007)

The no. of AE events is plotted as a total of two channels counted for one hour. Two periods of high AE activities are clearly observed at around 3 days elapsed and 7 days elapsed. It is noted that half cell potentials start to decrease after the first activity, but are still higher than -350mV around the second activity. Because the half cell potential lower than -350mV is prescribed as more than 90% probability of corrosion. Results suggest that the corrosion in the rebar is detected by AE activity more confidently than the half cell potential.

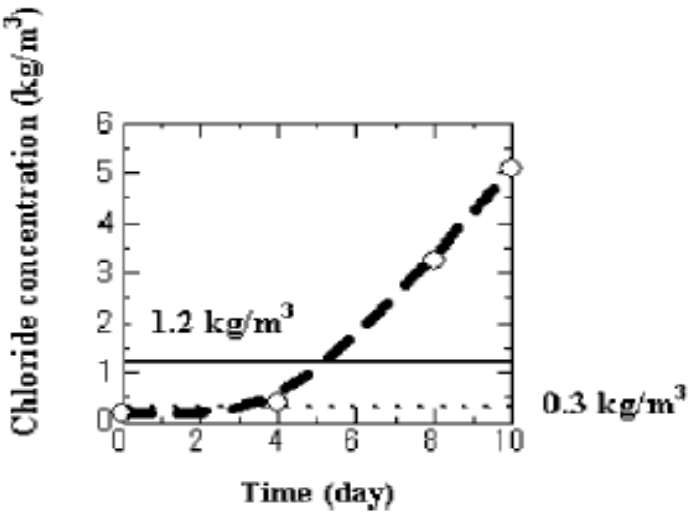

Fig.2.23: Ingress of chloride ions during accelerated corrosion test (Ohtsu et al., 2007)

Total chloride concentrations were determined in depths, and the chloride concentrations at cover thickness were analytically estimated. **Fig.2.23** shows the ingress of chloride ions during the accelerated corrosion test. A broken curve shows the estimated values analytically and open circles indicate the measured values in the test agreement between the estimated and the measured values are reasonable. Two threshold values are denoted, one is the lower-bound threshold for the onset of corrosion (0.3 kg/m^3 in concrete volume) and the other is the threshold value for performance based design. Acc. to the code [standard specifications for concrete structures- version of construction [(JSCE 2002)], concrete with chloride content over 1.2 kg/m^3 in concrete volume is not accepted for construction to prevent the corrosion. Comparing with the **Fig.2.22**, it is observed that chloride concentration becomes higher than 0.3 kg/m^3 after the first AE activity , and it reaches over 1.2 kg/m^3 following the second AE activity.

For AE activities in cyclic Test, the no. of AE events and the half cell potentials during the cyclic test are shown in the **Fig. 2.24**. The no. of AE events for one hour is again plotted. AE events are periodically observed along with the cycles of wet and dry. The first high AE activity is observed at 40 days elapsed, while the second activity is not obvious. According to half cell potentials, the values start to decrease at around 100 days elapsed.

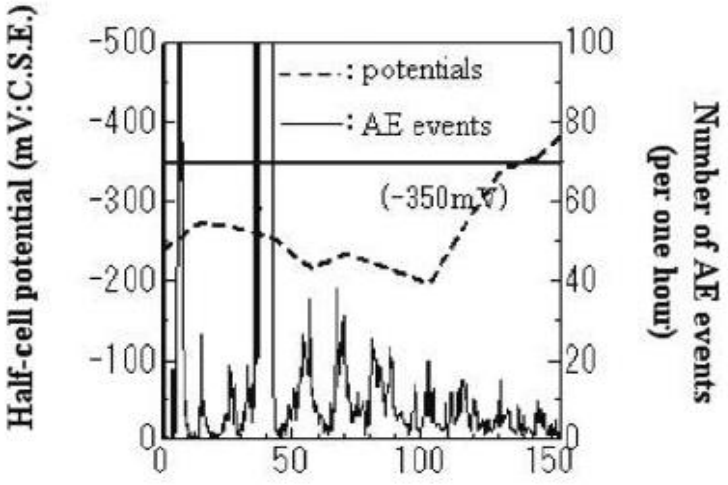

Fig.2.24: AE Activities and Half cell potentials in cyclic wet-dry test (Ohtsu et al., 2007)

In order to identify the second AE activity, the RA values and the average frequency were determined analytically. Corresponding to first period as denoted by an arrow symbol, the RA values becomes large and the average frequency is low.

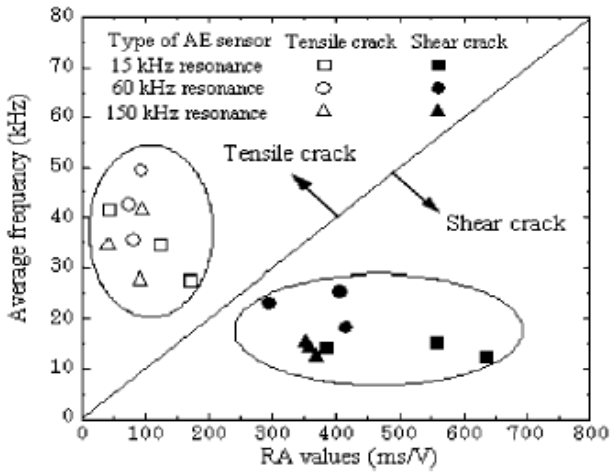

Fig.2.25: Classification of cracks by AE indices (Ohtsu et al., 2007)

Acc. to **Fig.2.25**, AE sources are classified as shear cracks. Toward 100 days elapsed, the increase in the RA value is observed. Thus, the second period is reasonably identified around at 100 days elapsed, where the RA values are low and the average frequencies are high. From **Fig.2.25**, tensile cracks are to be nucleated at the period. The b-value was determined for each wet-dry cycle as the average value.

The b-value becomes large at the 1st period and then the b-values keep fairly low. This result implies generation of small shear cracks at the first period. He concluded,

- That during the 1st period of high AE activities, the RA values become high, the average frequencies are low and the b-value is large. This implies that small shear cracks are actively generated as AE sources. Approaching to the 2nd period, the RA values become low, the average frequencies are getting higher and the b-values are small. The fact reasonably suggests that fairly large tensile cracks are generated due to expansion of corrosive product.
- Compared with AE results, it is found that the onset of corrosion starts, when the chloride concentration exceeds the lower -bound threshold.
- Removing rebars from the specimen, it is confirmed that rebars could corrode after chloride concentration reaches over the specified threshold, and AE activities after 100 days result from concrete cracking due to expansion of corrosive products in rebars.

Ohtsu et. al. (2010) studied the Acoustic emission Techniques for rebar corrosion in Reinforced corrosion. A reinforced concrete specimen tested was of dimensions 1000 mm × 570 mm ×100 mm. Two deformed steel-bars (rebars) of 13 mm nominal diameter were embedded with 20 mm cover -thickness. Configuration of the specimen is illustrated in **Fig.2.26**.

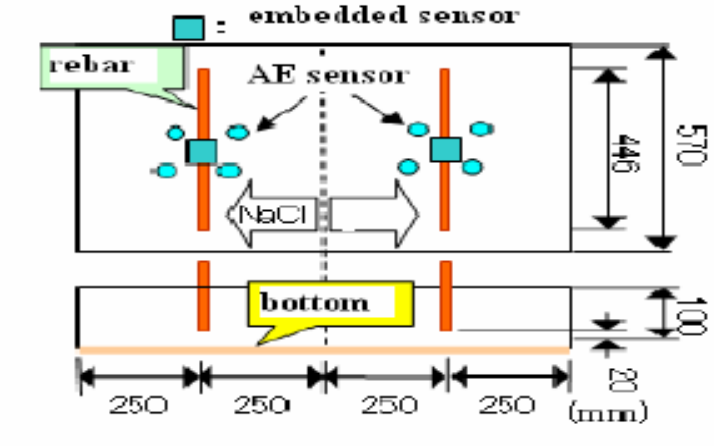

Fig.2.26: Sketch of reinforced concrete slab tested (Ohtsu et al., 2010)

A cyclically dry-wet test was conducted. Half cell potential at the surface of the specimen was measured by a portable corrosion meter. Chloride concentrations were measured at several periods. Total number of AE hits and the half -cell potentials during the test are shown in **Fig.2.27**. In the figures, the total number of AE hits observed during the test is plotted by a solid curve. The 1st AE activity around at 14 days elapsed is clearly observed, while the 2nd activity is found at 60 day around in the NaCl portion.

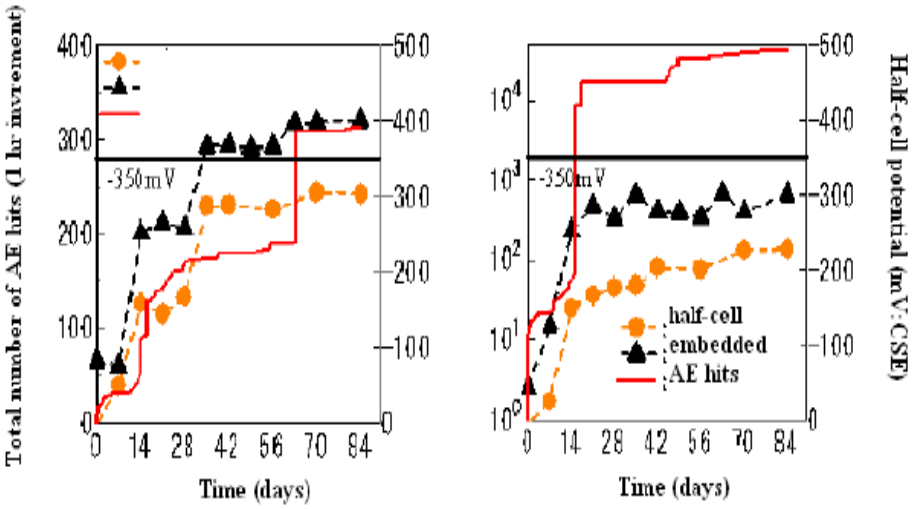

Fig.2.27: Total AE hits and half cell potentials in the NaCl portion (left) and water portion (right) (Ohtsu et al., 2010)

The curve of AE activity in the NaCl portion is in remarkable agreement with the typical corrosion loss of the phenomenological model. The AE activity could be generated by concrete cracking due to expansion of corrosion products (Zongjin et. al, 1998). It suggests that AE activity can be observed in concrete specimen. Comparing AE activity with half-cell potentials, it is found that with the increase in the number of AE hits, the potentials shift to more negative values. Here, two kinds of potentials are plotted. One is the potentials measured at the surface and the other is those by the embedded sensor. The embedded sensor shows more negative potentials. Still, the decreasing trends are similar.

In the NaCl portion, at the 2nd period of high AE activity around 60 days elapsed, the potentials reach to more negative than -350 mV. In the water portion, the decreasing manner of the potentials is in reasonable agreement with that of AE activity. In this case, the 1st high AE activity is only observed, and the

potentials did not reach more negative than -350 mV. Relations between chloride concentrations at the cover thickness and AE activities are shown in **Fig.2.28**.

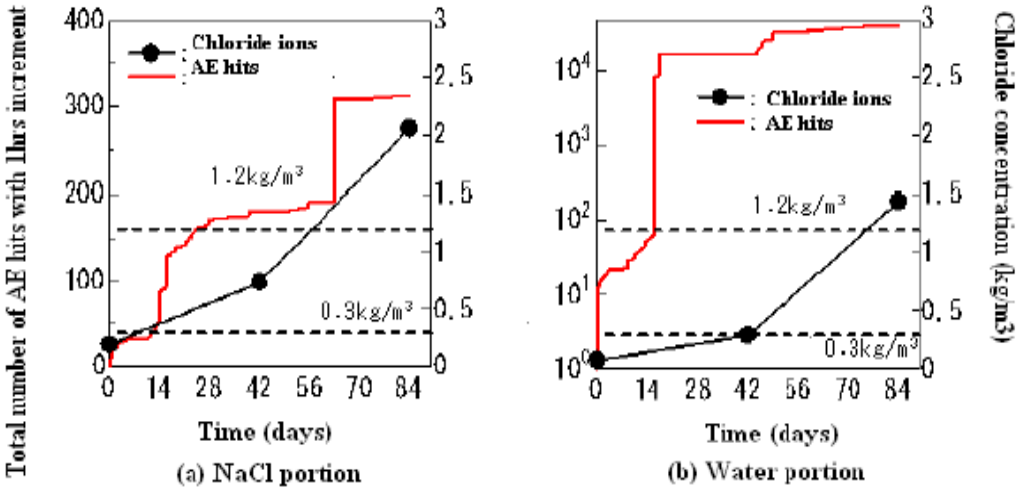

Fig.2.28: Total number of AE hits and chloride concentration (Ohtsu et al., 2010)

It is found that chloride concentration becomes higher than 0.3 kg/m^3 around at the 1st high AE activity, and it reaches higher than 1.2 kg/m^3, resulting in the 2nd high AE activity in the NaCl portion. In the water portion, the 1st high AE activity is observed prior to the stage, where chloride concentration becomes over 0.3 kg/m^3. Comparing AE activities in **Figures 2.27 and 2.28** with the typical curve of corrosion loss for steel in sea water immersion (**Mlchers and Li, 2006**), it could be summarized that two high AE activities reasonably correspond to two periods of the onset of corrosion and the nucleation of cracking. Corresponding to high AE activities twice, two active periods of AE events are observed in the NaCl portion. In contrast, only activity at the 2nd period is emphasized in the water portion. By employing the flaw location procedure, AE events were located. Then, it was found AE events located at the 1st period in the NaCl portion were only found around locations of AE sensors. So, AE wave-forms were examined. AE events detected at the 1st period were of so small amplitudes that AE sources could be mistakenly located at the location of the nearest sensor, where AE waveform was detected of the biggest amplitude. Consequently, AE source locations at the 2nd period of high AE activity are shown in **Fig.2.29**. It is realized that AE sources are reasonably located around rebar locations. This implies that corrosion activity due to concrete cracking, which is generated by

expansion of corrosion products in rebar, is readily detected and located by AE technique.

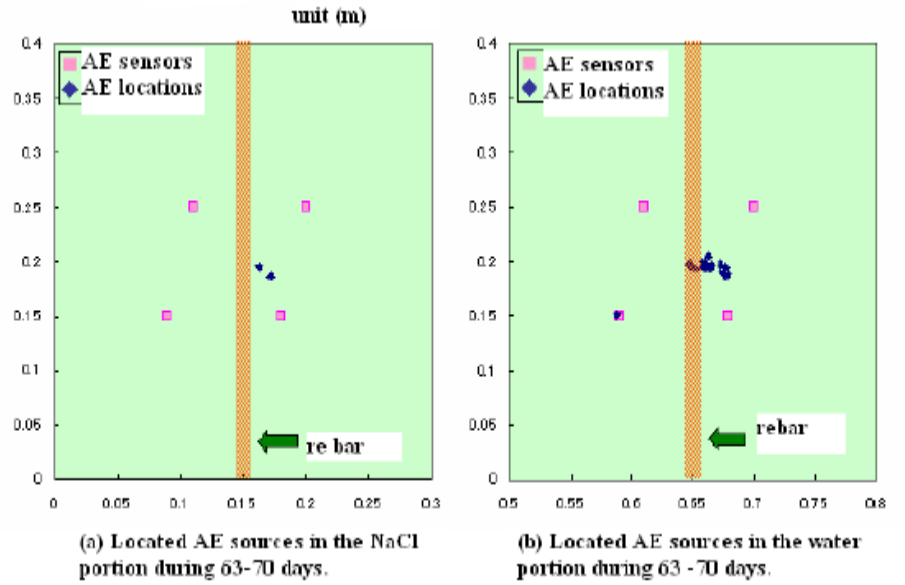

(a) Located AE sources in the NaCl portion during 63-70 days.

(b) Located AE sources in the water portion during 63 - 70 days.

Fig.2.29: AE sources located at the 2nd high AE activities in the test (Ohtsu et al., 2010)

Kawasaki et al. (2013) studied the corrosion mechanisms in Reinforced concrete by acoustic emission. In the paper, AE activities under a cyclic wet and dry test are investigated and these results are investigated by an electron probe microscope (EPMA). In order to investigate the Kinematical information of AE sources and nucleation of micro-cracks inside concrete, AE sources due to rebar corrosion in reinforced concrete are identified by SiGMA analysis (Simplified Green's functions for Moment tensor Analysis). In addition, characteristics of AE signals are investigated by using AE parameter analysis and Ib-value analysis.

Three beams of dimensions 100mm X 75mm X 400 mm were made. A deformed rebar of 13 mm diameter is embedded with 20 mm cover -thickness. The process of corrosion due to salt attack was simulated by a cyclic dry and wet test. AE measurement was continuously conducted using an AE measuring system. Six sensors of 150 kHz were attached to the surface of the beam. The frequency range of the measurement was 10 kHz to 2MHz every week; the AE measurements were temporarily stopped to conduct a half cell potential measurement. After AE measurement, the other two beams were cut and SEM (scanning Electron Micrograph) observation was conducted to investigate the microstructures around the rebar.

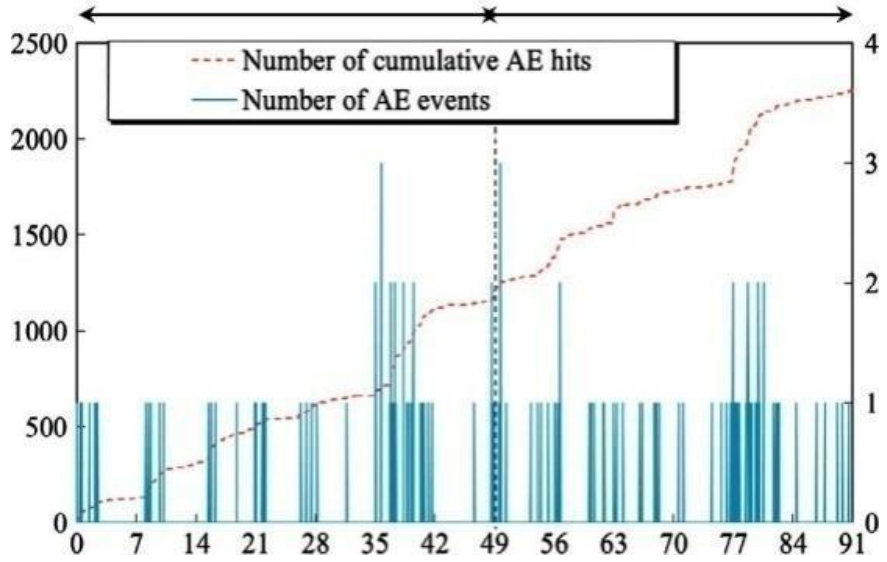

Fig.2.30: Number of cumulative AE hits and AE events (Kawasaki et al., 2013)

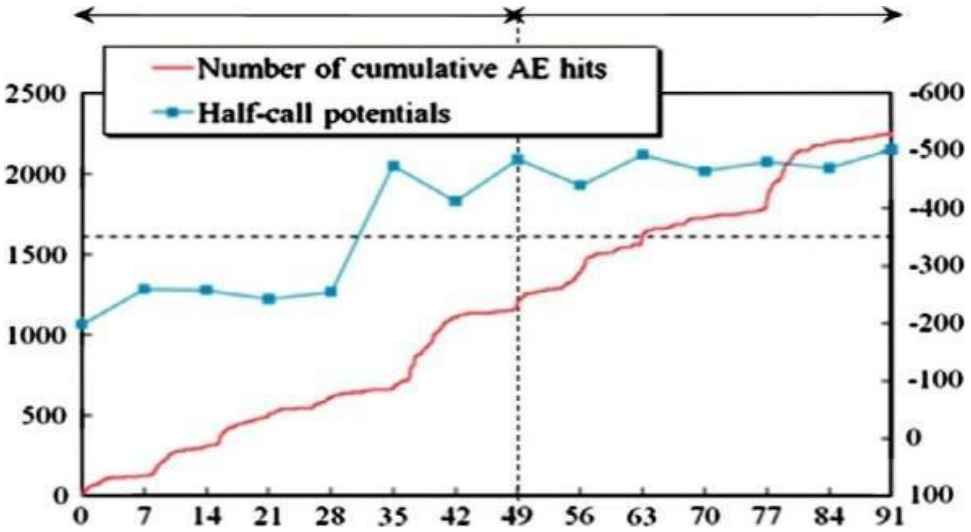

Fig.2.31: Number of cumulative AE hits and half cell potentials (Kawasaki et al., 2013)

Cumulative AE hits and AE events for every 1 hour of all 6 channels are shown in **Fig.2.30**. One AE event consists of 6 signals which were detected and analyzed by all 6 AE sensors. AE hits and AE events start to gradually increase during the first 42 days and the calm period of AE activity for a week is observed. The calm period is found after increase of the AE hits and AE events from 35 days to 42 days. In addition, the second increase of AE events was observed at 49 days. Therefore, the calm stage that was observed from 42 days to 49 days corresponds to Phase 2 in **Fig.2.32**. Following the calm phase, AE hits and AE events increase continually. The

curve of cumulative AE hits is in good agreement with the curve of corrosion loss. Thus, it leads to the fact that the onset of corrosion occurred during the first 42 days and the corrosion-induced cracks due to expansion of corrosion products could occur from 49 days to 91 days. Based on these findings, the corrosion process is divided into Stage 1 and Stage 2 as shown in **Fig.2.31**. Here, Stage 1 corresponds to Phase 1 and Phase 2, Stage 2 corresponds to Phase 3 and Phase 4.

Cumulative AE hits are compared with half-cell potentials in **Fig.2.31**. The half-cell potentials start to decrease after 28 days. Then, the potentials keep negative and less than -350 mV in Stage 2. Thus, the increase in AE activity could be associated with the de-crease trend of the half-cell potentials. After Stage 1, corresponding to continuous increase in AE activity, corrosion-induced cracks in concrete is to be nucleated due to expansion of corrosion products in rebar. The corrosion could be started from the start. However, the half -cell potentials cannot detect the small corrosion. On the other hand, AE can detect very tiny corrosion phenomenon. That's why AE activities detected from the beginning in **Fig.2.33**.

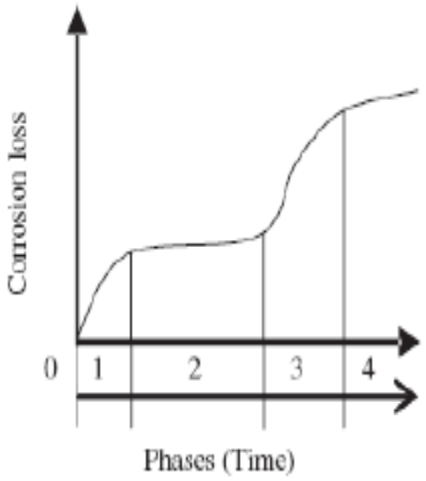

Fig 2.32: Evaluation of corrosion loss in steel under seawater immersion (Melchers and Li, 2006)

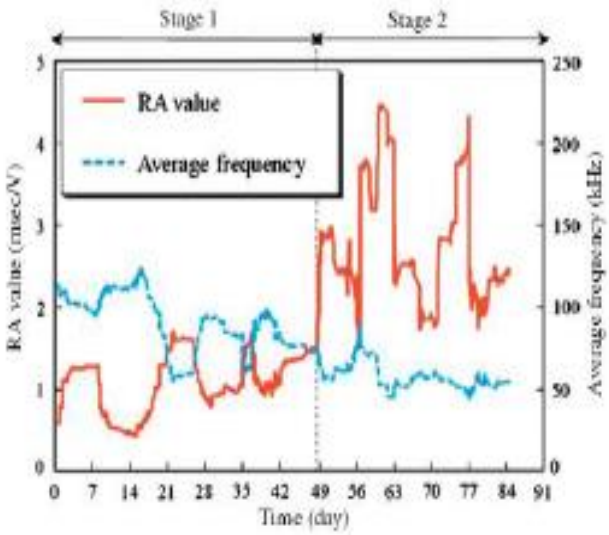

Fig.2.33: Variations of RA value and averaged frequency (Kawasaki et. al, 2013)

Variations of the RA values and the average frequency are given in **Fig.2.33**. Although the trend of variation is not clear at Stage 1, the RA values start to increase at Stage 2. From 14 days to 21 days elapsed at Stage 1, an abrupt increase in the RA value and the decrease in the average frequency are observed. This suggests that generation of other than tensile cracks due to the onset of corrosion in rebar. Interestingly the decrease of the half -cell potentials follows this generation. At Stage 2, the increase in the RA values and the decrease in the average frequency are further observed, suggesting nucleation of corrosion-induced cracks in concrete.

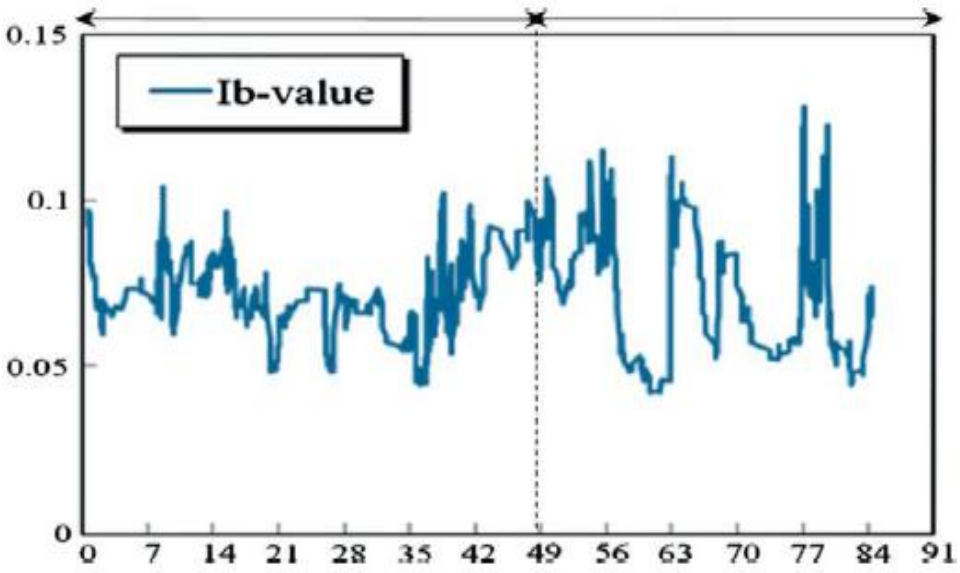

Fig.2.34: Variations of RA value and averaged Frequency (Kawasaki et. al, 2013)

Variation of the Ib-values is given in **Fig.2.34**. The large drops observed between 21 days and 35 days, before the first dramatically increase of AE activities. This might be implied that modest micro-cracks are generated as the onset of corrosion at the surface of the rebar. Due to high AE activity at Stage 2, the Ib-values decrease. Since results of Ib-values at 56 and 84 days elapsed are comparatively lower than those of the Stage 1, large-scale cracks are considered to be actively generated as corrosion-induced cracks in concrete. Furthermore, fluctuations of Ib-values in Stage 2 are even bigger than those of Stage 1. These results imply that cracks were repeatedly generated as the onset of corrosion and the corrosion-induce cracks in concrete.

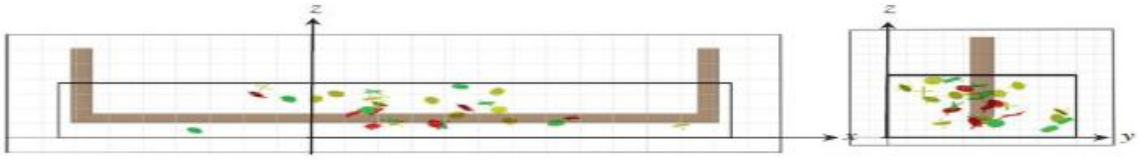

Fig.2.35: Results of SiGMA analysis during the first 49 days (Kawasaki et al., 2013)

Fig.2.36: Results of SiGMA analysis from 49 days to 90 days (Kawasaki et al., 2013)

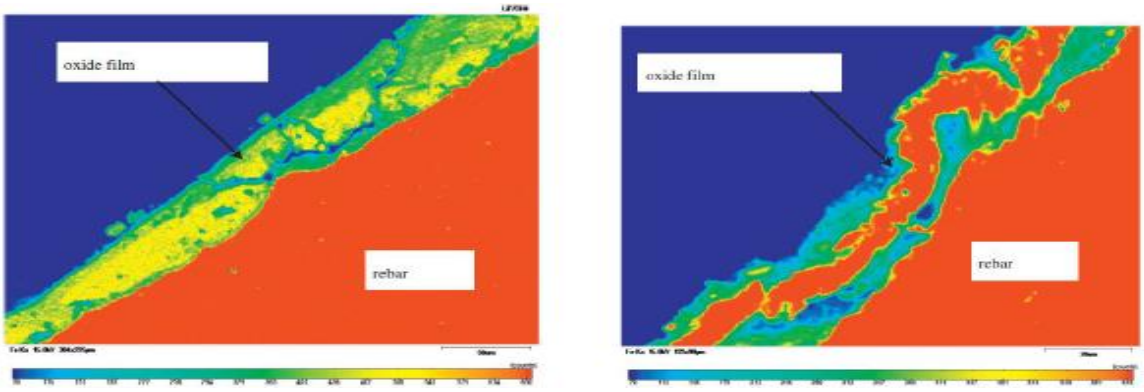

Fig.2.37: Mapping image of Fe of rebar on EPMA at 49 days (stage 1) and 90 days (stage 2) (Kawasaki et al., 2013)

Two Stages in the corrosion process are confirmed, in relation to the onset of corrosion in rebar and the nucleation of corrosion-induced cracks in concrete. At the onset of corrosion, the decrease of the RA value and the increase of the average

frequency are observed. At the same time, the decrease of the Ib-value is confirmed. It implies that the onset of corrosion could be identified by AE parameter analysis. Particular AE activity is found at Stage 2, corresponding to Phase 3 and Phase 4 in the phenomenological model. Due to corrosion-induced cracks, many of AE hits are observed. At Stage 2, the in-crease of the RA value and the decrease of the aver-age frequency are observed. Then, the fluctuations of Ib-values in the Stage 2 are even bigger than those of Stage 1. This implies that Ib-value is effective to detect both the onset of corrosion and the corrosion-induced crack. At Stage 1, AE events were located in the specimen while no cracks were observed by the stereo-microscope. It implies that AE phenomena occurred due to corrosion initiation as the shear and the mixed-mode cracks. At Stage 2, micro-cracks were observed at the cross-section by the stereo-microscope. The locations of the AE sources by the SiGMA analysis (shown in **Fig.2.35** and **Fig.2.36**) are agreement with those of the corrosion-induced cracks in concrete, and AE sources are mostly of tensile cracks.

2.3 CLOSING REMARKS

This chapter presents the literature review on the use of ultrasonic guided wave technique and acoustic emission technique for monitoring the corrosion process in RC structures. Both these techniques were found to be very efficient in the corrosion monitoring of the structures. In this study, both these techniques are used for monitoring the RC beam specimen subjected to accelerated induced corrosion.

CHAPER 3

EXPERIMENTAL PROGRAM AND METHODOLOGY

3.1 GENERAL

The objective of this study is to investigate the suitability of ultrasonic guided waves and acoustic emission technique to be able to monitor the behaviour of RC beam specimens subjected to accelerated corrosion by impressed current method. The specimen were continuously monitored by the acoustic emission technique where as the ultrasonic monitoring was done after every 24 hours. Finally, the results from both these monitoring technique were compared.

3.2 TEST PROGRAM

The test program involved:

- Determination of basic properties of constituent materials namely cement, fine aggregates, coarse aggregates and steel bars as per relevant Indian standard Specifications. Steel bars were also monitored by guided waves to check their quality.
- Casting of RC beams of dimensions150mm X 150mm X 700 mm with a 1000mm steel rod of 25 mm diameter embedded in it such that 700 mm of steel rod is inside the concrete cover using M20 grade concrete.
- Acoustic emission sensors, 2 in number are mounted on the front face and 2 sensors are placed on the bottom face of the R.C beam specimen for the purpose of corrosion monitoring.
- Subjecting the specimens to accelerated corrosion at a constant voltage of 20V to ensure that corrosion is taking place.
- Corrosion is continued for a period of 30 days.
- Ultrasonic monitoring of the specimens after every 24 hours till the signals vanishes.
- Continuous acoustic emission monitoring is done for complete 30 days of corrosion.

Fig.3.1 shows the complete test procedure in the form of flow chart.

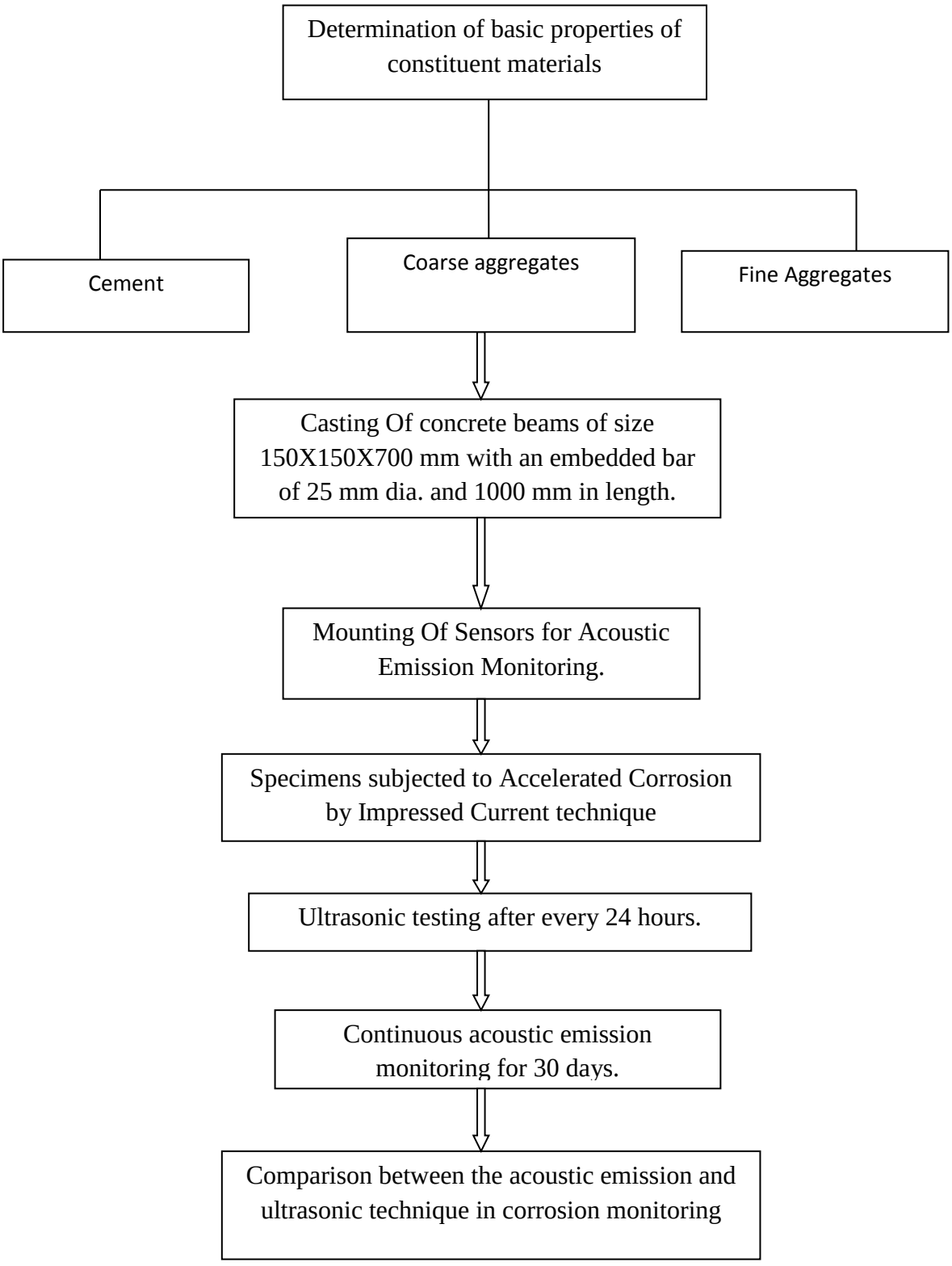

Fig.3.1: Test program in the form of flow chart

3.3 MATERIALS USED

RC beams were casted in a mould of size 150mm X150mm X700mm with a provision for embedding steel in it. The specifications and properties of various materials used for casting are as under:

- **Cement**: Ordinary Portland cement of 43 grade (O.P.C 43) was investigated. The cement was of uniform colour i.e. grey with a light greenish shade and was free from any hard lumps. Summary of various test conducted on cement is given in **Table 3.1**. All these tests were carried out in accordance with the procedure laid down in IS: 8112-1989.
- **Fine aggregates**: The fine aggregates used for the experimental work was locally procured and conformed to grading zone III. Sieve analysis was carried out in the laboratory as per IS 383-1870. Fine aggregates were first sieved through 4.75mm sieve to remove aggregates greater than 4.75 mm in size and were then washed to remove the dust. The physical properties and sieve analysis of fine aggregates are shown in the **Table 3.2** and **Table 3.3** respectively.

Table 3.1: Physical properties of cement

S.No	Characteristics	Values Obtained	Standard Values
1	Normal consistency	33%	_
2	Initial setting time	48 min	Not less than 30 min
3	Final setting time	240 min	Not more than 600 min
4	Fineness	4.8 %	_
5	Specific gravity	3.09	_
6	Compressive strength		

S.No	Days	Values obtained experimentally
1	3	24.8
2	7	37.5
3	28	46.8

Table 3.2: Physical properties of fine aggregates

S. No	Characteristics	Value
1	Specific gravity	2.59
2	Bulk density	1.33 g/cc
3	Fineness modulus	2.63
4	Water absorption	0.89
5	Grading zone (based on percentage passing 600 micron)	Zone III

Table 3.3: Sieve analysis of fine aggregates

S.No.	IS-Sieve (mm)	Wt. Retained (gm)	%age Retained	%age Passing	Cumulative % retained
1	4.75	14.5	1.45	98.55	1.45
2	2.36	37	3.70	94.85	5.15
3	1.18	246.5	24.65	70.20	29.80
4	600 µ	205.5	20.55	49.65	50.35
5	300 µ	287.5	28.75	20.90	79.10
6	150 µ	177	17.70	3.20	96.80
7	Pan	32	3.20		
	Total	**1000.00**		**SUM**	**262.65**
				FM =	*2.62*

- **Coarse aggregates**: Crushed stone aggregates of size 20mm were used throughout the experimental study. The aggregates were washed to remove the dust and dirt and were dried to surface dry condition. The aggregates were tested as per IS 383-1970. The results of various tests conducted on coarse aggregates are given in **Table 3.4** and **Table 3.5** shows the sieve analysis results.

Table 3.4: Physical properties of coarse aggregates

S. No.	Characteristics	Value
1	Type	Crushed
2	Specific gravity	2.69
3	Water absorption	0.5557 %
4	Fineness Modulus	6.95

Table 3.5: Sieve Analysis of Coarse aggregates

S. No.	Sieve size	Weight retained(gm)	Percentage retained	Percent Passing	Cumulative percentage retained
1	80	0.00	0.00	100.00	0.00
2	40	0.00	0.00	100.00	0.00
3	20	68.5	2.28	97.72	2.28
4	10	2776.5	92.55	5.17	94.83
5	4.75	113.5	3.78	1.38	98.62
6	Pan	0.00	0.00	0.00	
	Total	**3000.00**		**SUM**	**195.73 + 500 =**
				FM =	*6.95*

FM of 20 mm coarse aggregates= (195.73+500)/100=6.95

- **Water**: Fresh and clean tap water was used for casting the beams in the present study. The water was free from organic matter, silt, oil, sugar, acidic material as per Indian standard.
- **Steel Reinforcement**: Mild steel bars of one metre length and 25 mm diameter were used as reinforcement. 700 mm was embedded in concrete and 300 mm was exposed to the environment, in order to make electrical connections and conduct pull-out tests later on. Table 4.6 shows the properties of the reinforcing bars used for the casting of RC beams.

Table 3.6: Properties of reinforcing bars used for casting specimens

Type and size of the bar	Ultimate Tensile stress (MPa)	Yield stress (MPa)	Young's modulus (GPa)	Percentage Elongation
Mild steel, 25 mm	410	240	200	23

3.4 Preparation of Test specimens

3.4.1 Preparation and preconditioning of steel bars

Steel bars are cut to the desired length of 1000 mm. Each bar is then wire brushed to remove any surface scale. These are then cleaned by soaking them in analytical reagent hexane and allowed to dry in the air. Before embedding these bars in the concrete, these beams were also monitored ultrasonically to check their quality.

3.4.2 Casting of RC beams

Concrete mix is prepared using 43 grade O.P.C, fine aggregates (Medium sized river sand) and crushed stone coarse aggregates with a nominal size of 20mm. The mix is designed as per the Indian standard guidelines. Mixed design was calculated as 1:1.5:3. The water cement ratio is 0.5 and compressive strength of concrete after 28 days is 29 MPa.

In the present program, the RC beams were cast in mould of 150mm X 150mmX 700 mm with 700 mm of steel bar embedded in concrete cover and 300 mm of length exposed to the surrounding environment. First of all, interior of the beam mould was oiled, so that beams could easily be removed from the mould after 24 hours. Initial weight of the bars is measured. When the bars had been placed in position, concrete mix was poured and vibrations were given so that the mix gets compacted. The vibration is done until the moulding is completely filled and there are no gaps left. The beams were then removed from the mould after 24 hours. After de moulding, the beams were cured for 28 days using an open tank. The concrete surface of the beams was then cleaned up and all dirt and loose materials were removed. It was then cured for a period of 28 days prior to its corrosion monitoring.

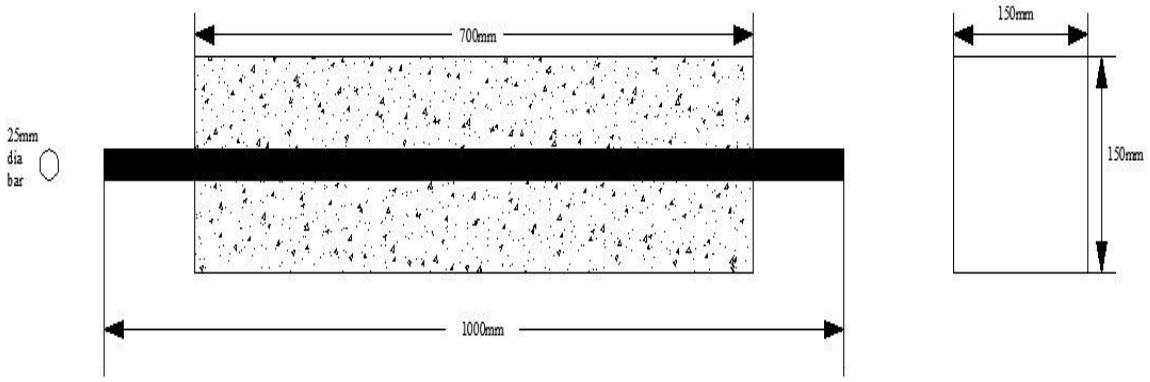

Fig.3.2: Test specimen with embedded bar.

3.4.3 Inducing Corrosion in concrete

The corrosion is a very slow process and in order to carry out our study we accelerated the corrosion process. In other words, we can say that beam was artificially corroded. The objective of inducing corrosion to the reinforcing bar is to simulate the corrosion damaged concrete. The commonly used methods of inducing corrosion in RC specimens can be recalled as Salt spray (**Gadve et al., 2008**), Chloride diffusion (**Masoud and Soudki, 2006**) and impressed current method. Previous studies have shown that the test specimens kept in a salt spray chamber for more than 100 days did not show any visible signs of corrosion. This method was not found suitable

considering the time constraint. This method was not considered because it did not simulate the present condition of interest.

Alternate immersion into NaCl solution and drying of the specimens also induces corrosion. However, the quickest method of inducing corrosion is by impressing anodic current. In this method, NaCl solution is supplied to the specimens and a direct current is passed making the reinforcement bar as an anode and another metal nobler than it in electrochemical series as cathode.

Fig.3.3: Test specimen with arrangement for induced corrosion

In this investigation, the specimens are kept fully saturated by continuously dripping with 3.5% NaCl solution as shown in **Fig.3.3**. Mats are placed over the tops to provide even distribution of NaCl solution. The rebar is used as anode. A stainless steel (SS) mesh is rolled around 300 mm length of specimen and tied together with metal ties in order to assure electrical continuity and is used as cathode (**Fig.3.3**). The reinforcement extended 150 mm on both sides past the concrete to allow easy access for making electrical connections to the steel. The constant voltage of 20 V is impressed in order to accelerate corrosion. The power supply (SciTech) used is shown in the **Fig.3.4**.

Fig.3.4: SciTech power supply

Stainless steel mesh used in the present study could supply 1000mA DC at 64V. The rebar is connected to the positive terminal of the external DC source and negative terminal is connected to the SS mesh. It is more common to maintain a constant voltage between the cathode and the anode (**Masoud and Soudki, 2006 Gadve et al., 2008**;).

3.4.4. Corrosion Testing

It is an established fact that corrosion takes place only when the chloride concentration at the rebar value reaches the critical value. The ultrasonic waves were used to identify the extent to which corrosion has occurred or to identify the mechanism of corrosion in the R.C beam by measuring the ultrasonic signals while the bar is subjected to accelerated induced corrosion A constant voltage of 20 V was maintained between the cathode and anode by the power supply. Acoustic Emission monitoring was also done continuously for 30 days and finally both the techniques were compared in their efficiency of monitoring the propagation of corrosion in the R.C beam.

3.5 ULTRASONIC GUIDED WAVE INVESTIGATION

3.5.1 Specimen and set up details

For ultrasonic guided wave investigation, pulse-echo (PE) testing method is adopted. In the pulse-echo method, a piezoelectric transducer with its

longitudinal axis located perpendicular to and mounted on or near the surface of the test material is used to transmit and receive ultrasonic energy. The set-up for ultrasonic guided wave investigation is shown in **Fig.3.5.** The ultrasonic waves are reflected by the opposite face of the material or by discontinuities, layers, voids, or inclusions in the material, and received by the same transducer where the reflected energy is converted into an electrical signal. The digital to analog converter (DAC) digitizes the input and received pulse and is displayed on the display. The signals received are in form of voltage-time (V-t) graphs. The ultrasonic test set-up in this study uses DPR-300 pulse receiver system (**Fig.3.7**) and Karl Deutsch contact transducers (**Fig.3.8**). Actual set up used in the study is also shown in **Fig.3.6.**

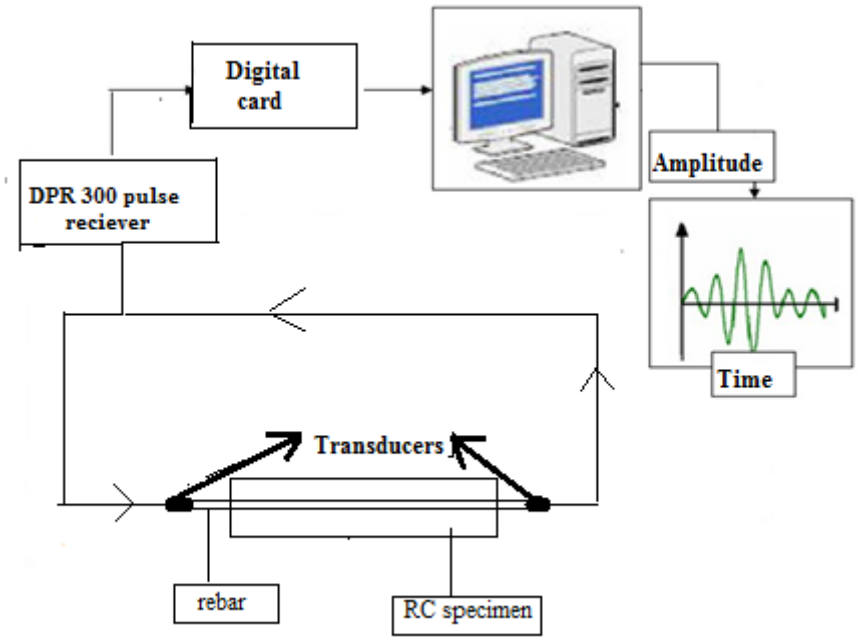

Fig.3.5: Schematic representation of Ultrasonic monitoring.

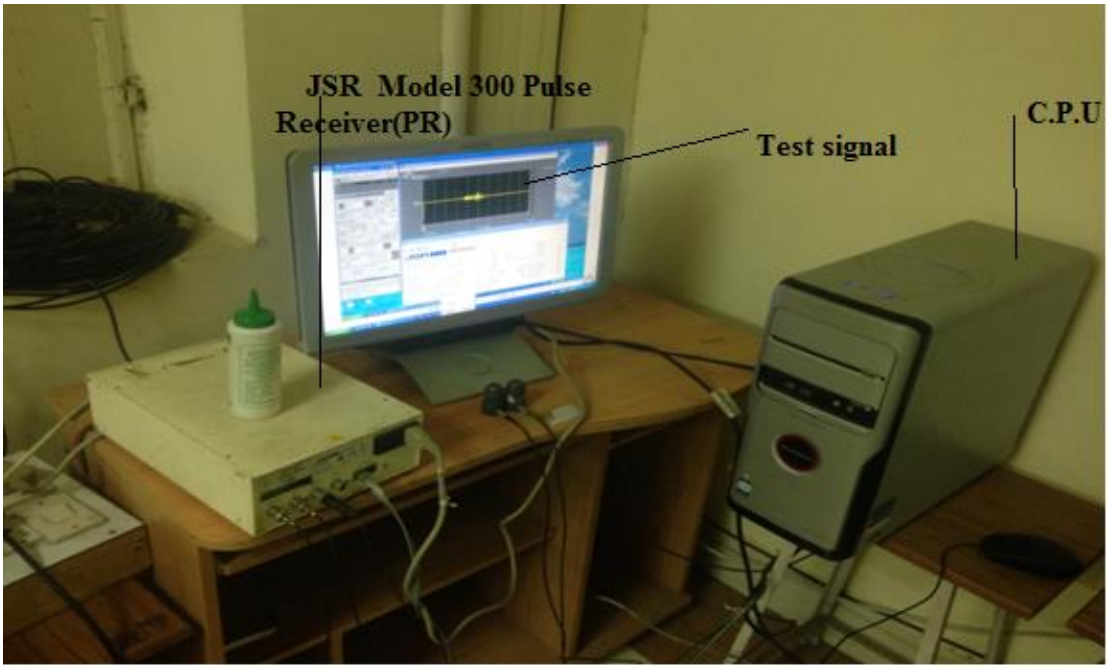

Fig.3.6: Actual Ultrasonic set up used for corrosion monitoring

Fig.3.7: Pulse receiver used.

Fig.3.8: Karl Deutsch contact transducer used in the study.

3.5.2 Selection of excitation mode and frequency

The selection of a suitable test mode and frequency is done after analyzing the dispersion curves using the software DISPERSE. Modes that have lowest signal attenuation and at the same time are easily distinguishable are selected. Generally, modes at low attenuation are used to maximize the inspection range and at the same time to minimize the effects of dispersion and also minimize the interference of other modes in the received signal. Dispersion curves for a mild steel bar of 25mm diameter in infinite expansion of concrete are shown in **Fig.3.9(a), Fig.3.9(b), Fig.3.9(c)**.(**Sharma and Mukherjee 2010,2011,2013)**

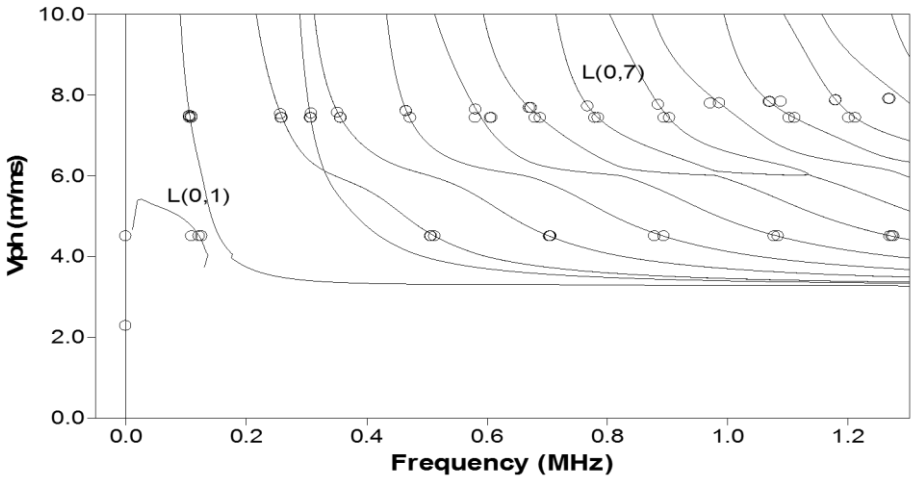

Fig.3.9 (a): Phase velocity Vs Frequency

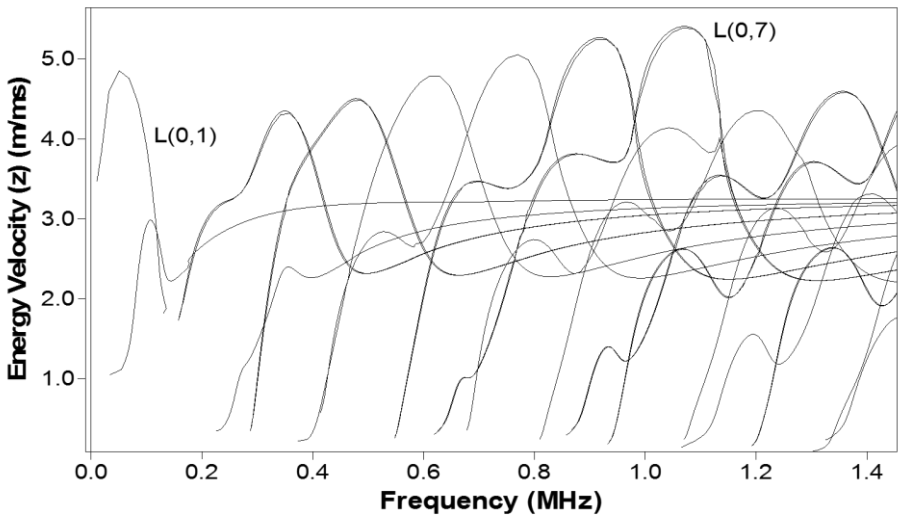

Fig.3.9 (b): Energy Velocity Vs Frequency

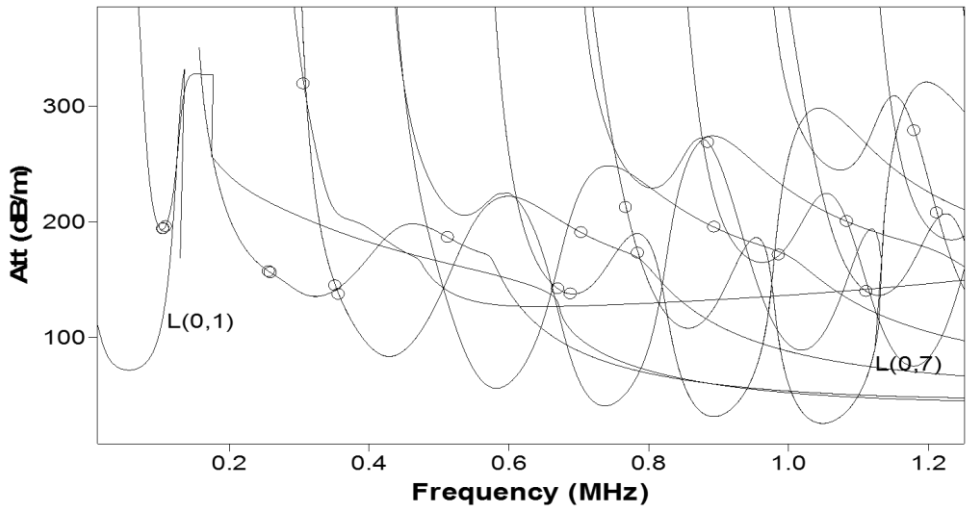

Fig.3.9(c): Attenuation Vs Frequency

Fig. 3.9: Dispersion curves for 25mm dia. bar (Sharma & Mukherjee, 2010,2011,2013)

When there is an interface such as a crack, void or flaw in the wave path, part of the energy is reflected back from the interface and received by the same transmitting transducer. The reflected energy is converted into an electrical signal which is processed in a computer and digitized for display. From the display, the time of flight between the excitation and reflected pulse is measured. Knowing the velocity of the wave, the location of the defect can be calculated as follows:

$$D = Vt \quad \text{.....(3.1)}$$

Where,

D = Distance of defect from transducer end,

V = Velocity of wave

t = Time of Flight.

Now in this case the distance travelled by the wave would be equal to double the length of the bar that would be 1200 mm and the speed of wave would be the speed of wave varies from 5 km/s to 6 km/s. Therefore the time at which the peak has to be noticed would be between 200μs and 250 μs.

The selection of frequencies for testing was done using the software DISPERSE. They were also validated by experimentally confirming the signal fidelity. The modes that are easily distinguishable and have lowest signal attenuation were selected. For bars embedded in concrete, which is a layered waveguide system, leakage plays an important role**.** Frequency regions with lowest attenuating modes are the ones with displacements profiles centered in the middle of the bar to minimize leakage but at a low enough frequency to avoid substantial absorption. Dispersion curves have already been shown in **Fig. 3.9(a)**, **Fig.3.9 (b)**, **Fig.3.9(c)**. Hence, fundamental mode, L(0,1) mode at 100 KHz starting at zero frequency with low attenuation was selected(**Fig.3.9(a)**). Another important mode L(0,7) at 1 MHz forms a low leakage mode corresponding to maximum energy velocity and minimum attenuation(**Fig.3.9(c)).(Sharma & Mukherjee,2010,2011,2013).**

Another important feature for the selection of modes was mode shape that determines the radial distribution of displacement and density (**Fig.3.10**). It is a known fact that oxygen corrosion and chloride corrosion have different effects on the bar. Oxygen corrosion mainly affects the surface of the bar and chloride concentration leads to the pitting inside the bar. Thus the mode that has significant surface component would be sensitive to oxide corrosion. Hence, it is evident that L(0,1) is such mode, and hence, it is named as Surface Seeking Mode(**Fig.3.10a**). The chloride corrosion, on the other hand, would manifest itself in a mode that progresses mainly through the core of the bar and has negligible surface component (**Fig.3.10b**). **(Sharma & Mukherjee, 2010, 2011, 2013).**

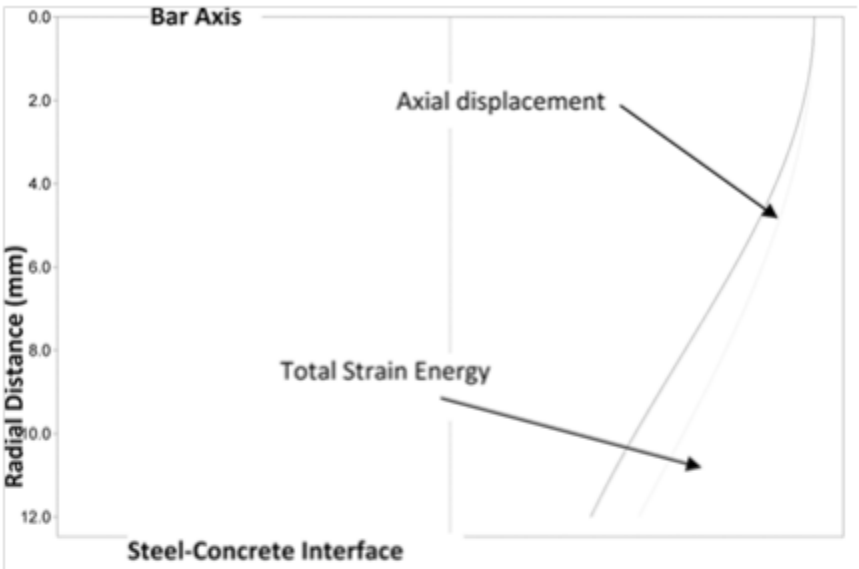

3.10(a): Surface seeking mode L(0,1) at 0.1 MHz

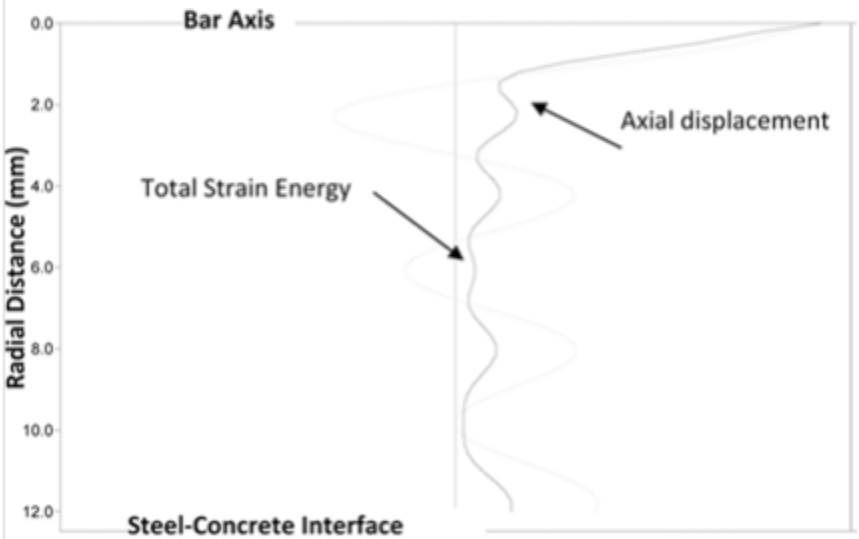

3.10(b): Core Seeking Mode L(0,7) at 1 MHz

Fig.3.10: Mode Shapes (Sharma & Mukherjee 2010, 2011, 2013)

3.6 ACOUSTIC EMISSION MONITORING

The phenomenon of acoustic emission is defined as the propagation of elastic waves due to release of localized internal energy, such as micro-fracture in elastic material. Structural deformation processes such as plastic deformation, crack expansion and other kinds of material degradation are the

sources of the AE activity. Detection, amplification, filtering and analysing the signal are some of the important issues in AE technology. AE monitoring system typically consists of sensors, preamplifiers and AE acquisition and analysis system.

In our study the corrosion process was accelerated by the impressed current technique. The research aims to identify the onset of corrosion by means of AE in RC specimens. The schematic representation of AE set up is as shown in the **Fig.3.11**:

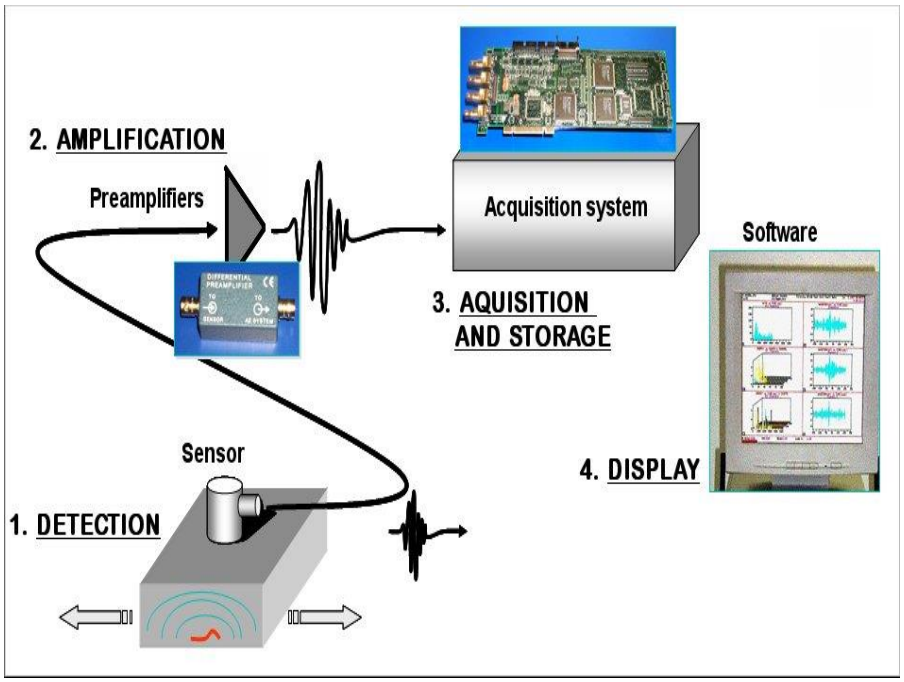

Fig.3.11: Schematic representation of the AE monitoring

AE data acquisition system used for experimentation was Micro II digital AE system provided by PAC (Physical Acoustics Corporation) **MISTRAS GROUP** which is shown in the **Fig.3.12**.

Fig.3.12: Data acquisition set up used for the study

Sensors are placed on the surface of the structure to record acoustic emission signals. Sensors are available in wide range of shapes and sizes as shown in the **Fig.3.13**.

Fig.3.13: Acoustic Emission Sensors generally used

Acoustic Emission sensors which were used for monitoring the corrosion in the present study are shown in the **Fig.3.14**.

Fig.3.14: R3α Sensors for AE Acquisition used in the study.

The specifications of the sensors used in the present study are shown in the **Table 3.7**.

Table3.7: Specifications of the sensors

Operating frequency range	35-100 KHz.
Resonant frequency	150 KHz
Physical Dimensions	19mm dia.× 22.4mm height
Weight	31 grams
Case Materials	Stainless Steel

The preamplifiers used in the study are shown in the **Fig.3.15**

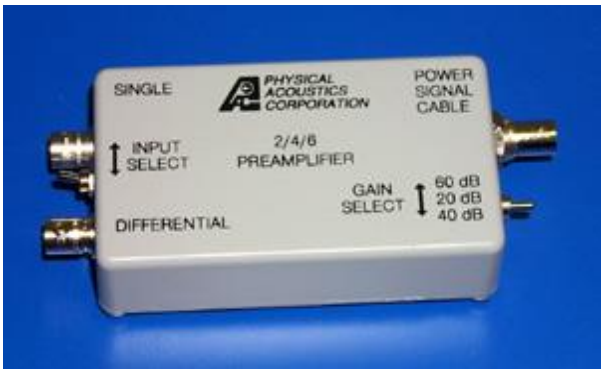

Fig.3.15: Pre-amplifier used in the study.

Good coupling of the sensors to the test specimen is necessary for the effective transmission of AE signals. Sensors are attached on the surfaces

using magnetic holders, glues, even rubber bands and tapes. A layer of couplant such as vacuum grease, ultrasonic gel, and oil is applied between the two surfaces. Operating frequency range is important during sensor selection. The common frequency range for AE testing in civil infrastructure is 100-300 kHz.

Experiment was carried out on a RC beam specimen of 150mm X150mmX700mm along with a bar of 1000mm long and 25mm diameter embedded in concrete such that 150mm length is exposed to the environments from both sides. The acquisition system has 8 channels and is expandable up to 32 channels. However, we used four R3α sensors (resonant at 150 KHz) and preamplifiers with a gain set at 40 db and frequency range of 20-1200 KHz.

Two sensors were mounted on the front face of the RC beam specimen and two sensors were mounted on the bottom face of the beam specimen. The position of the sensors is shown in the **Fig.3.16** and **Fig.3.17**.

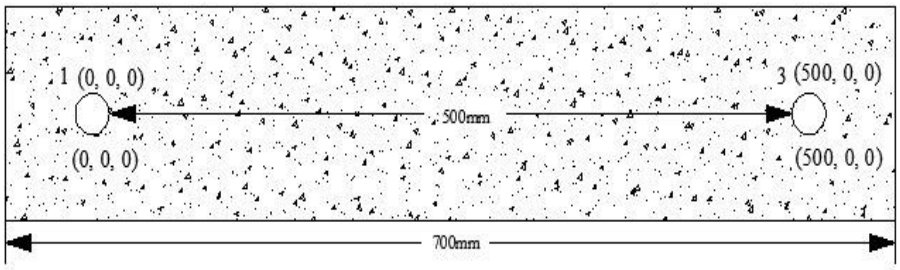

Fig.3.16: Location of sensors on the front face of the beam

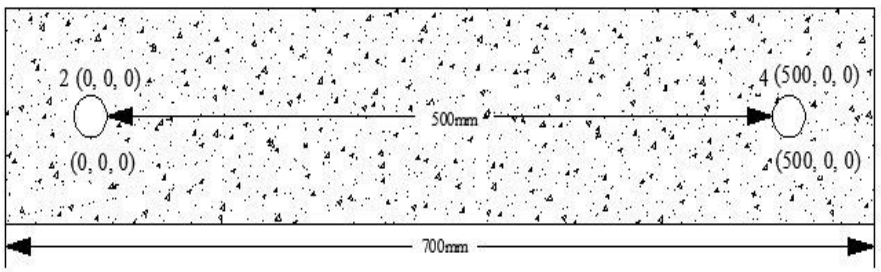

Fig.3.17: Location of sensors on the bottom face of the beam

The sensors mounted on the test specimen are shown in the **Fig. 3.18**:

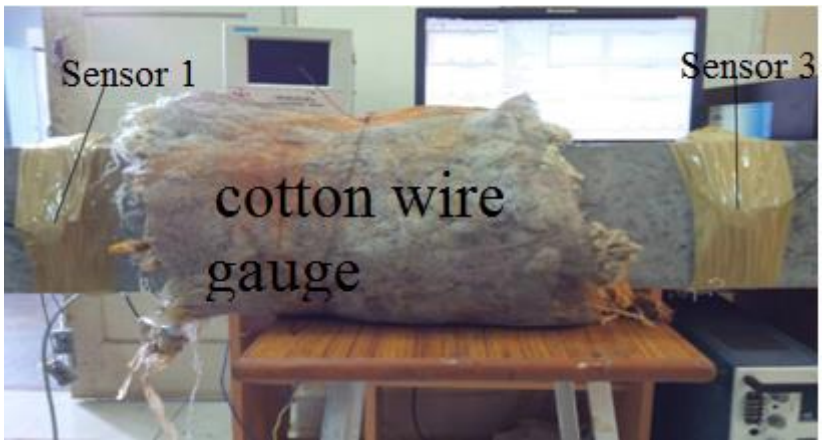

Fig.3.18: Actual sensors mounted on the beam.

A band pass filter of 20-400 KHz was set in the software control of the data acquisition system. A threshold value was set at 45 db for experimental purpose. The experimental set up used in the study is shown in the **Fig.3.19**.

Fig.3.19: Experimental set up used in the study.

Hence, it is clear from the above figure that any acoustic activity occurring in the specimen is detected by the sensors. These signals are amplified by the pre-amplifiers before entering the data acquisition system.

The data acquisition set (Micro II Digital AE system) which processes the data and finally displays the data on the monitor screen.

AE signals were generated by breaking 0.5mm pencil leads at selected locations on the plate and in each position pencil lead break tests were done thrice. (**Fig.3.20**)

Fig.3.20: Pencil lead break apparatus (Kafle, 2012)

Fig.3.21: pencil break test done in the study.

The AE signals were generated by breaking 0.5mm pencil leads on the selected locations on the surface of the RC beam specimen and in each position pencil lead break test were done twice. This was done to make sure that sensors are mounted properly on the RC beam specimen and they are able to detect the reflections though their amplitude would be smaller than the crack related signal.

The AE process involves the use of sensors to detect released strain energy from the growing cracks. Hence, this technique has been widely used in the field of civil engineering for health monitoring.

3.7 CLOSING REMARKS

In this chapter monitoring of corrosion in RC beam specimen using ultrasonic guided waves technique and acoustic emission technique is discussed in detail. Monitoring for corrosion gives a bright picture of various changes in the structural behaviour of the structure due to corrosion. Thus, it can be established that proper monitoring of the structure to determine the extent of corrosion can help us in determining the appropriate measures required to be taken in initial stages of degradation due to corrosion before it reaches to an alarming level.

CHAPTER 4

RESULTS AND DISCUSSION

4.1 GENERAL

In this chapter, the final results from ultrasonic monitoring technique as well as the acoustic emission monitoring technique for corrosion are presented and discussed. Along with that, a comparison of both the ultrasonic monitoring and acoustic emission monitoring has been done in order to find out the efficacy of a typical monitoring method during various stages of corrosion.

4.2 ULTRASONIC GUIDED WAVE MONITORING

Ultrasonic guided wave monitoring can be done using pulse-echo method and pulse-transmission method. However, in this experimental work, pulse-through method has been used to monitor various stages of corrosion in R.C beam specimen. For that purpose two modes i.e. core seeking mode and surface seeking mode has been used to catch various corrosion phenomenon i.e. de lamination and pitting. It has been already established that the surface seeking mode is very much able to detect the de lamination of rebar with the concrete cover (**Sharma and Mukherjee, 2011, 2013**). And the core seeking mode detects the pitting that occurs in the rebar due to corrosion (**Sharma and Mukherjee, 2011, 2013**). Hence, both the techniques are useful in identifying the corrosion pattern occurring in the rebar. Results from both the techniques are presented in the following sections.

4.2.1 Surface seeking mode L(0,1) at) 0.1 MHz

The variation in received signal using L(0,1) at 0.1 MHz is discussed in this section. The signatures are shown for 5^{th} day, 10^{th} day, 15^{th} day, 20^{th} day, 25^{th} day and finally 30^{th} day to understand in detail the trend of the corrosion variation and in the end the peak to peak amplitude variation per day is also shown.

The signature for first day using surface seeking mode is shown in the **Fig.4.1** i.e. the healthy reading.

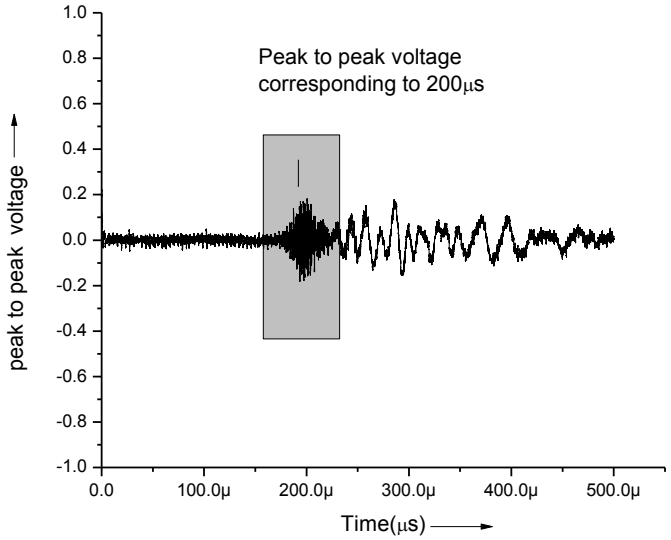

Fig.4.1: Healthy reading using surface seeking mode.

The signature for the 5th day is shown in **Fig.4.2**

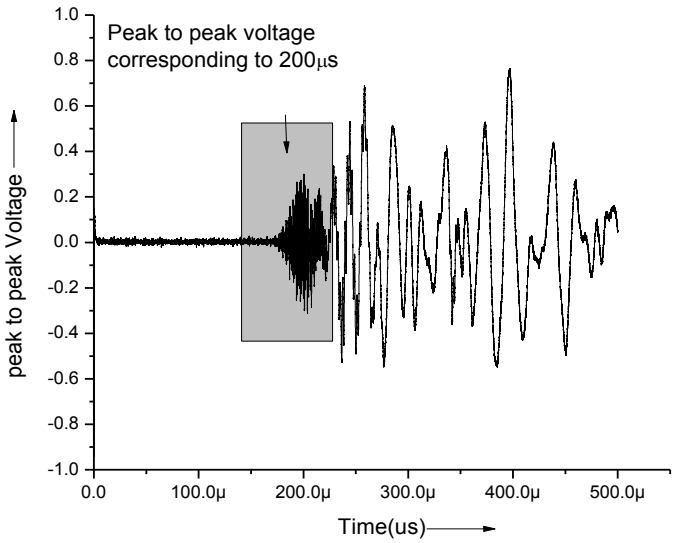

Fig.4.2: 5th day peak to peak voltage.

Here , from the above two graphs, we can see that there is an increase in the peak to peak voltage due to delamination of the bar from the surrounding concrete as a result of corrosion. It is due to debonding of the bar from the surrounding concrete causing less leakage of signal into concrete and hence the rise of the received signal.

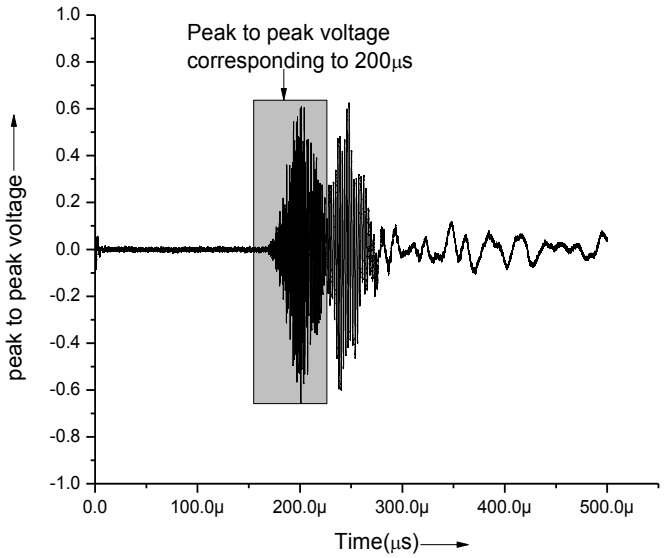

Fig.4.3: 10th day peak to peak voltage.

On the 10th day signal it is observed that the peak voltage reaches its peak value and then starts dropping further due to pitting of the bar now after the delamination in first 10 days. From 10th -30th day signal continues to drop indicating pitting has started and continues after initial delamination.

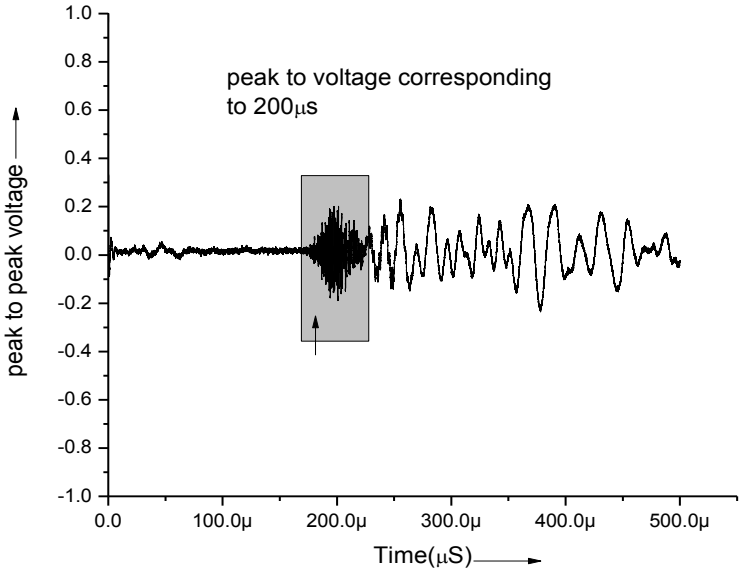

Fig.4.4: 15th day Peak to peak voltage

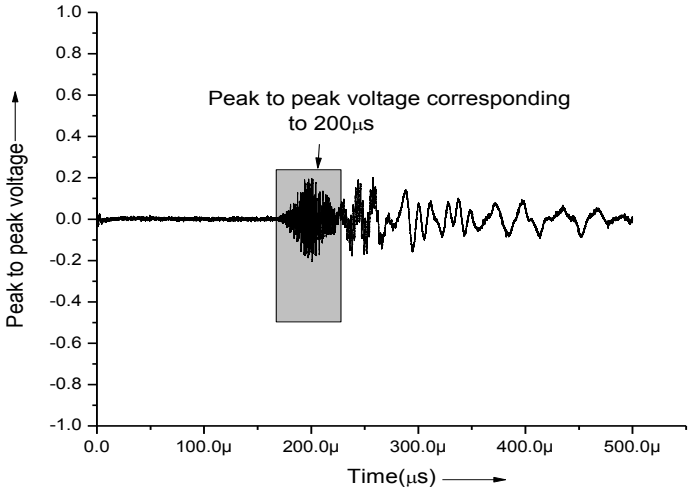

Fig.4.5: 20th day peak to peak voltage

Clearly, magnitude has started to drop since the pitting is increasing in the rebar with increasing exposure to corrosion as pitting causes loss in cross-section of the bar increasing reflections and wave scattering resulting in signal drop.

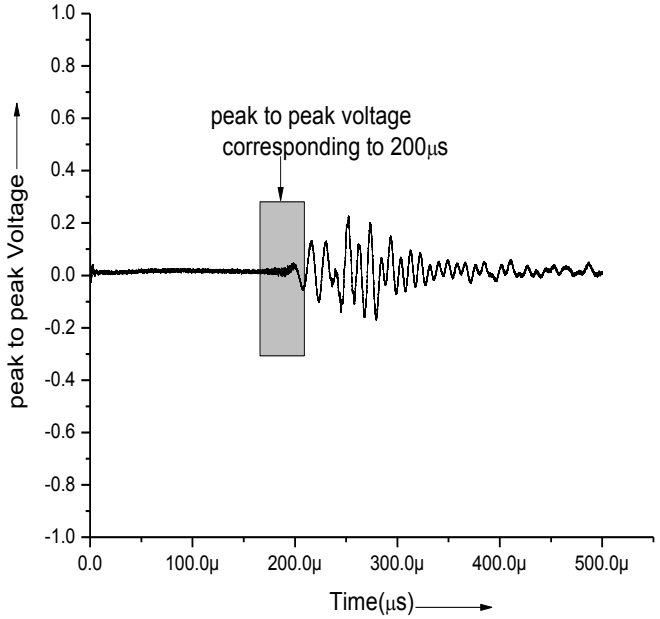

Fig.4.6: 25th day peak to peak voltage.

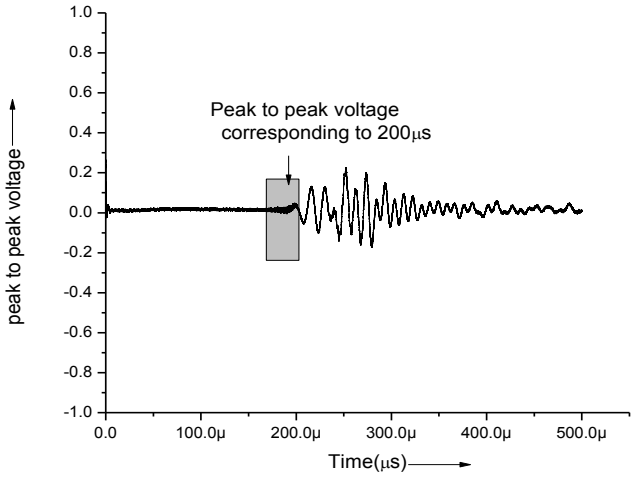

Fig.4.7: 30th day peak to peak voltage

It can be clearly seen from the last signature i.e. 30th day signature that the peak to peak voltage has become almost zero. However to understand this corrosion process in detail we need daily variation in the peak to peak voltage. **Fig.4.8** shows the trends of received signal using surface seeking mode. Initially for 1-10 days there is rise in the signal amplitude pointing towards the delamination of the bar from the surrounding concrete. Further from 11-30 days signals drop indicating signal loss due to pitting.

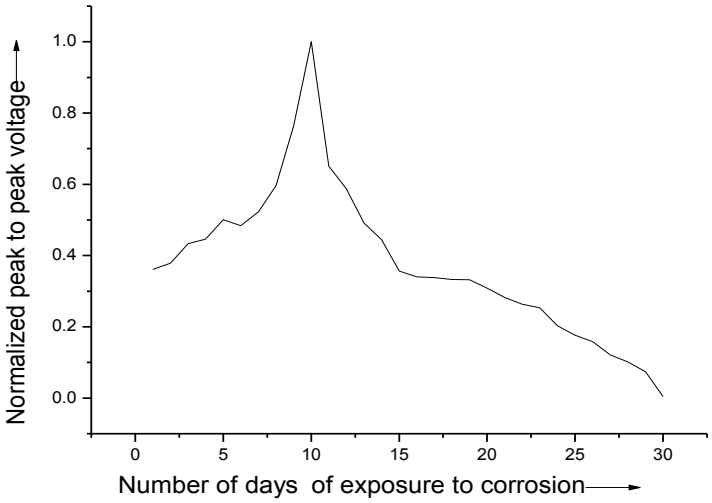

Fig.4.8: Normalized peak to peak voltage vs. Number of days of exposure to corrosion for surface seeking mode L(0,1).

The variation can also be shown in the form of the bar chart

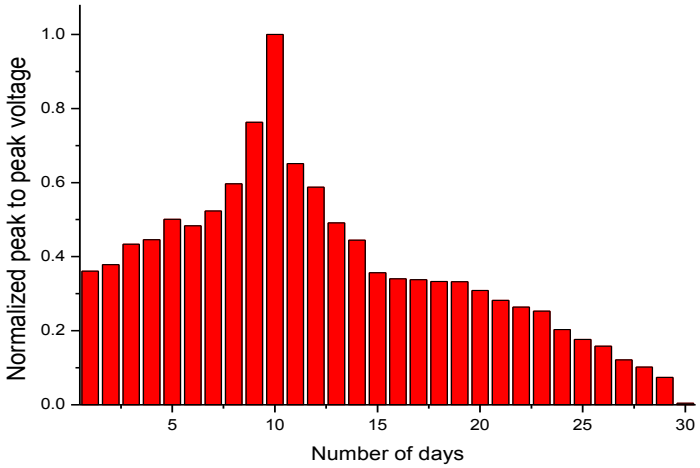

Fig.4.9: Normalized peak to peak voltage vs. Days.

From the **Fig.4.9**, it can be clearly seen that the peak to peak voltage signal changes minutely for few days after the initiation of corrosion in RC beam specimen. But after 5 days of accelerated corrosion in RC beam specimen there is a significant rise in the signal strength up to 10 days. In short we can summarise that the period in which the signal strength reaches maximum signifies the de lamination of the rebar from the concrete cover. After 10 days it can be seen that there is a steep fall in the signal strength which corresponds to the initiation of pitting corrosion in the rebar.

4.2.2 Core seeking mode L(0,7) at 1MHz.

The variation in received signal using L(0,7) at 1 MHz is discussed in this section.The signatures are shown for the healthy specimen, 5^{th} day, 10^{th} day, 15^{th} day, 20^{th} day, 25^{th} day and finally 30^{th} day to understand in detail the trend of the corrosion variation.

The signature for the healthy specimen is shown in the **Fig.4.10**.

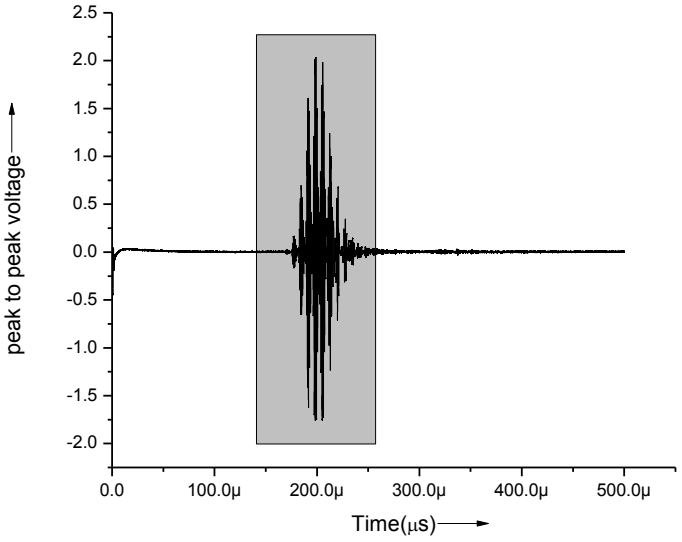

Fig.4.10: Healthy reading for core seeking mode

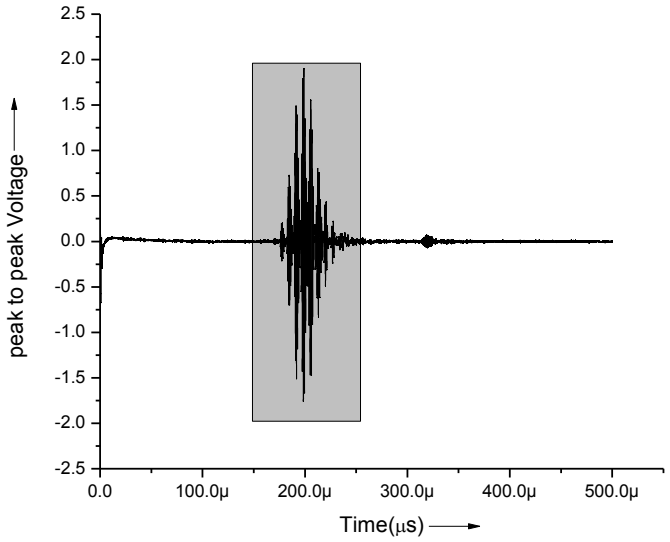

Fig.4.11: 5th day peak to peak voltage

From the signature until 5 days, it is observed that there is not much variation in the signal strength since delamination predominates during the first 10 days as observed with surface seeking mode. Core seeking mode which is sensitive to core change does not change much in first five days.

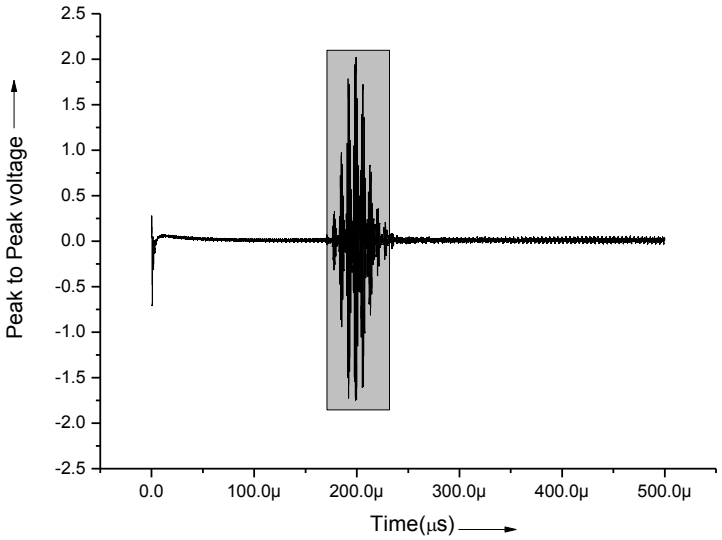

Fig.4.12: 8th day peak to peak voltage

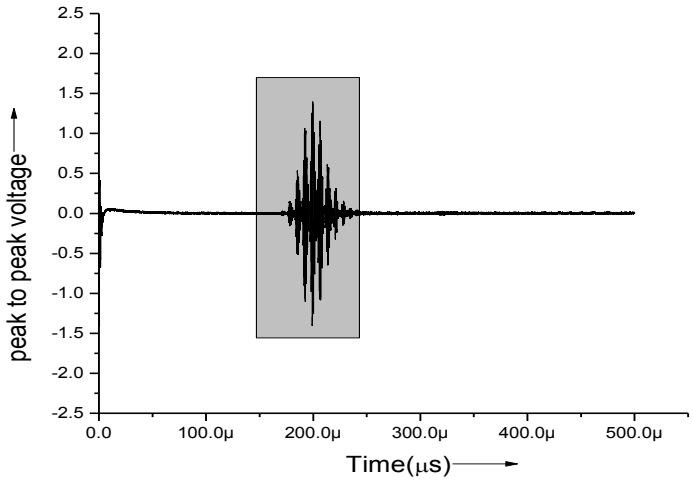

Fig.4.13: 10th day peak to peak voltage.

From 5th day onward there is a visible trend in fall in signal. It clearly depicts that pitting corrosion has started and from here on peak to peal voltage will certainly fall as the corrosion progresses because of signal attenuation due to signal scattering and mode reflections.

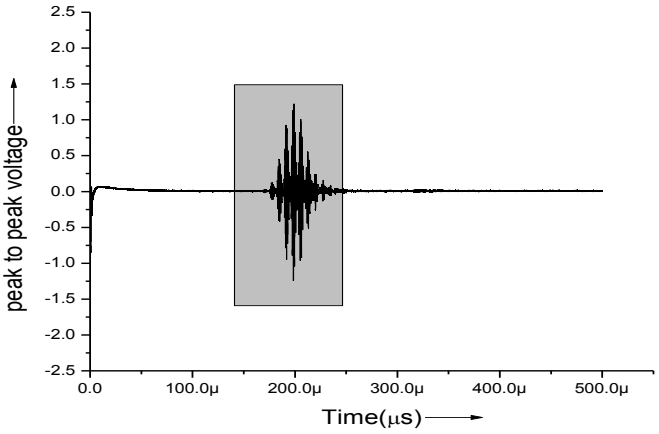

Fig.4.14: 15th day peak to peak voltage

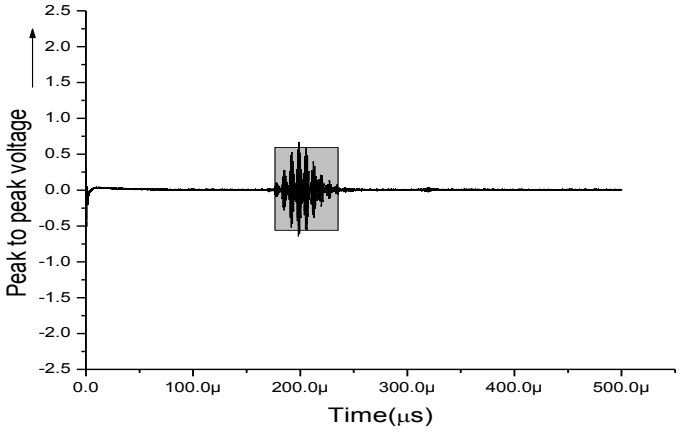

Fig.4.15: 20th day peak to peak voltage

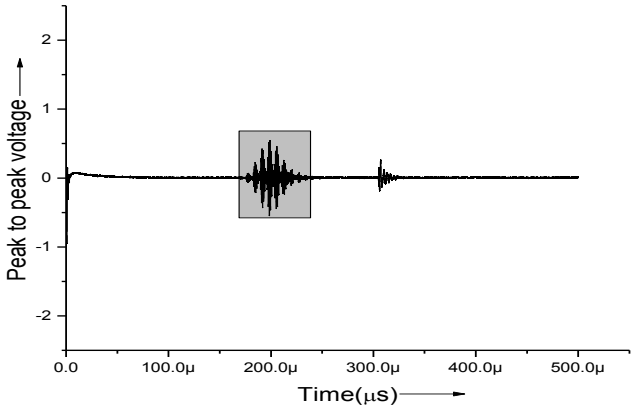

Fig.4.16: 25th day peak to peak voltage

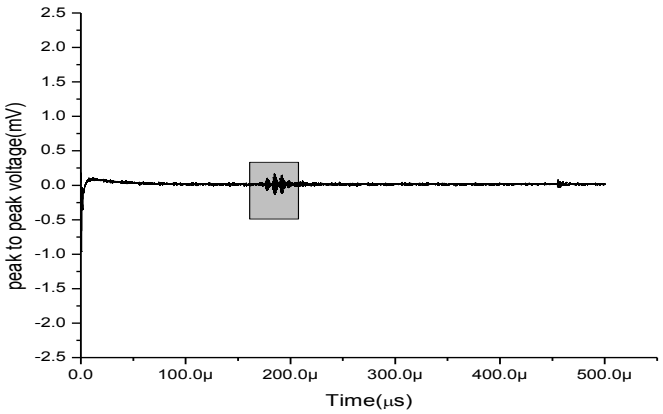

Fig.4.17: 30th day peak to peak voltage

It can be clearly seen from the last signature i.e. 30th day signature that the peak to peak voltage has become almost zero. However to understand this corrosion process in detail daily variation in the peak to peak voltage of the signal is plotted. This process is well explained by the normalized plot. (**Fig.4.18**)

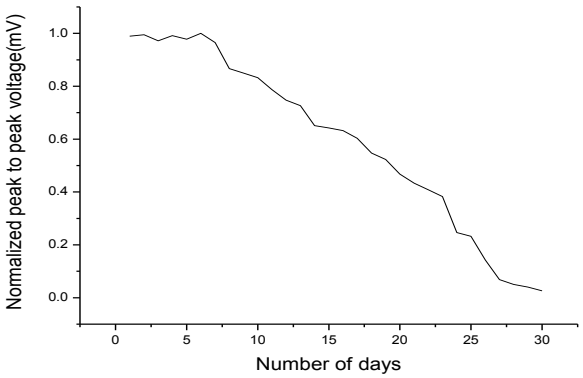

Fig.4.18: Normalized peak to peak voltage vs. No. of days for core seeking mode L(0,7)

From the **Fig.4.18**, it can be clearly seen that the peak to peak voltage signal remains constant for around 5 days of accelerated corrosion. And after 5 days of corrosion the peak to peak voltage signal drops quickly and reaches a very low value until 30 days. This signifies that core seeking mode is able to detect pitting and non-uniform area loss due to accelerated corrosion after seven days. The results can also be shown in the form of the bar chart.

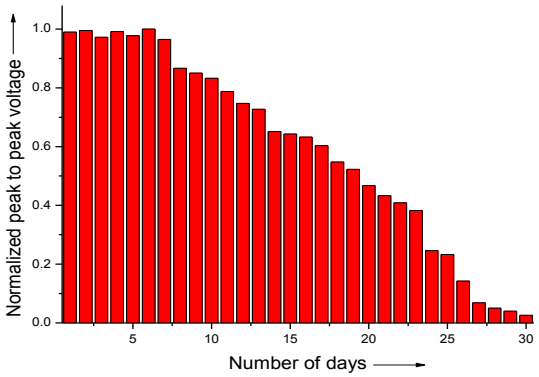

Fig.4.19: Normalized peak to peak voltage vs. No of days

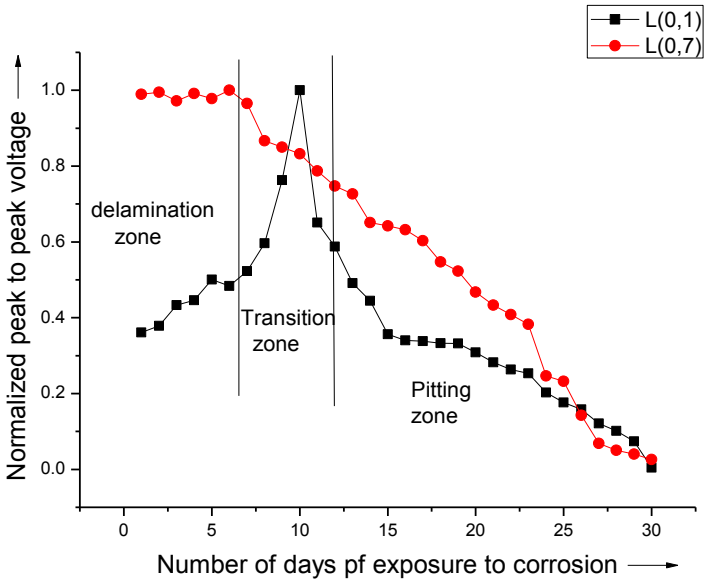

Fig.4.20: Combined trend of peak to peak voltage for surface seeking mode L(0,1) and core seeking mode L(0,7)

From the combined trend using core and surface seeking mode (**Fig.4.20**), it is observed that there are 3 zones in corrosion mechanism of rebar in concrete (**Sharma & mukherjee, 2011, 2013**).

- During first five days L(0,1) signal rises whereas there is not much variation in L(0,7) signal. This indicates predominant surface changes but inappreciable core changes. This zone is referred to as "Delamination zone".

- During six to twelve days L(0,1) continued to rise whereas L(0,7) fell significantly. This shows that now corrosion makes inroads deeper in the bar and is not restricted to the surface only. Therefore, both the modes of corrosion are present. Therefore, this zone is referred to as "Transition Zone".
- After 12^{th} day both L(0,1) and L(0,7) signal fall continuously showing the same trend. During this stage, pitting is predominant. Hence, this zone is referred to as the "pitting zone".

Further corrosion is also monitored and mechanism is also understood using acoustic emission technique.

4.3 ACOUSTIC EMISSION TESTING TECHNIQUE AND RESULTS

As seen in the previous sections Ultrasonic guided wave monitoring technique are very good for picking up the later age corrosion after 5 days. But at this stage sufficient deterioration has taken place which does not take give an idea of initiation of corrosion. **Fig 4.21**and **Fig.4.22** show the trend of signal strength for the first five days of accelerated corrosion from surface seeking mode and core seeking mode respectively.

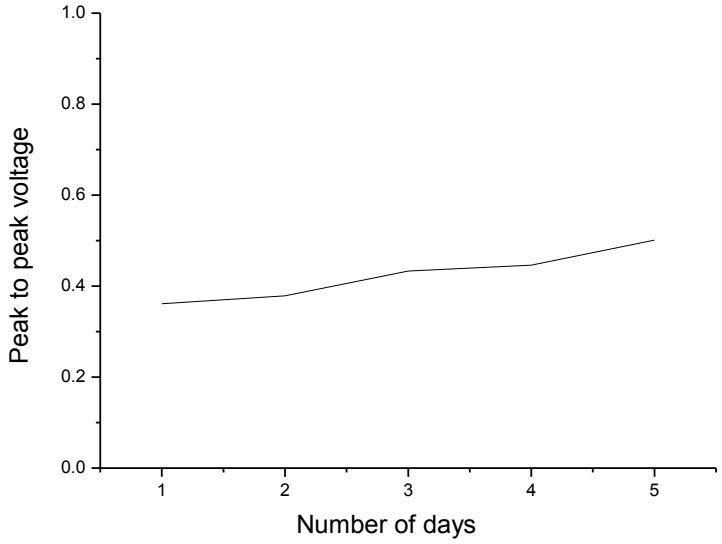

Fig.4.21: Peak to peak voltage for five days in surface seeking mode.

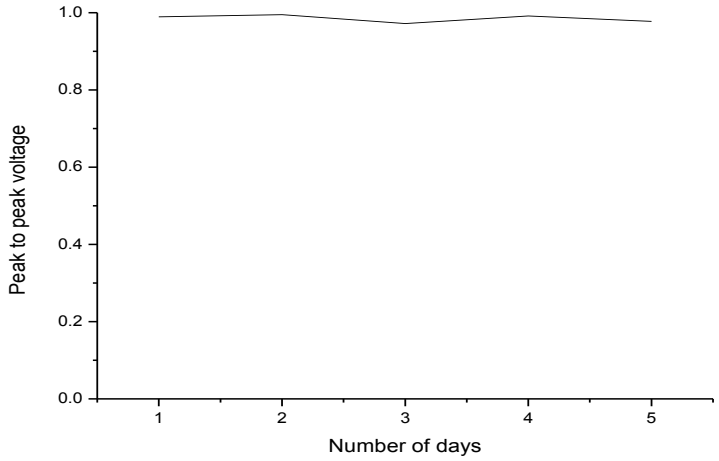

Fig.4.22: Peak to peak voltage for five days in core seeking mode.

It can be seen in the **Fig.4.21** and **Fig.4.22** that there is no significant variation in the signal strength and hence it can be established that there is complete uncertainty in the detection of the propagation of corrosion using ultrasonic guided wave monitoring. In other words, Ultrasonic guided waves monitoring fails to predict the initiation of the corrosion. Most importantly this technique needs the accessibility of the rebar. Also since in guided wave the monitoring is done through rebar, effect of corrosion initially and at later stages is not monitored on concrete and its effect on concrete which is important for structural engineers is not investigated. **Fig 4.23** shows the condition of the RC beam specimen subjected to 5 days of accelerated induced corrosion.

Fig.4.23: The condition of RC specimen after 5 days of exposure to accelerated induced corrosion.

In the **Fig.4.23** it can be clearly seen that sufficient deterioration has already taken place. Hence, there is an urgent need to assist with a technique which can give an early sign/ indication of damage due to corrosion or a technique which is able to detect the initiation of corrosion. Hence to overcome the limitation of ultrasonic guided wave monitoring technique Acoustic Emission Technique is used in the present study and its efficacy is found out. **Fig 4.24** and **Fig.4.25** show the results obtained from acoustic emission technique in form of hits and events for the first five days.

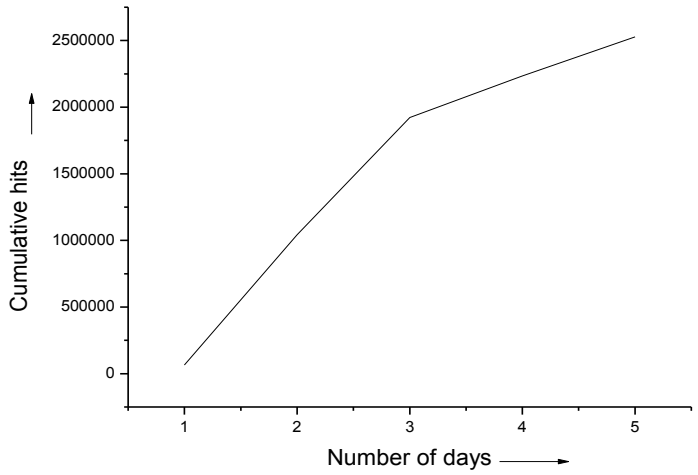

Fig.4.24: Number of cumulative hits for first five days

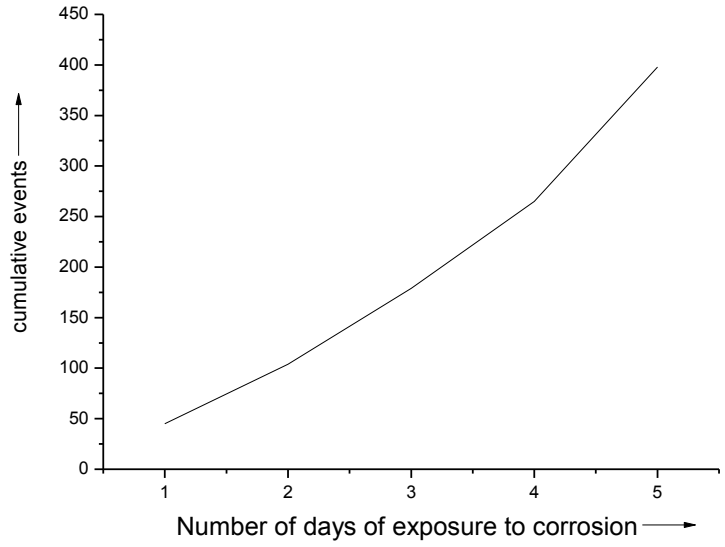

Fig.4.25: Number of cumulative events for first five days

Fig.4.24 and **Fig4.25** show the cumulative hits and cumulative events for first five days due to accelerated corrosion in RC beam specimen. The numbers of hits as well as events start increasing immediately after accelerated corrosion has started in the RC beam specimen. Therefore, it can be established that acoustic emission monitoring is able to detect the initiation of corrosion unlike ultrasonic guided wave monitoring which do not show any significant variation in the peak to peak voltage for the first five days. Also, this method does not require the accessibility of the rebar. Sensors can be directly attached on the surface of the specimen. Hence, it gives the complete information about the effect of corrosion in surrounding concrete and not only in the rebar as in ultrasonic guided waves technique.

The acoustic emission technique starts the detection of corrosion immediately after the initiation of accelerated corrosion. The acoustic activity in the concrete after 10 hours is shown in **Fig.4.26.** On all respective sensors 1-4, it indicates that initial corrosion events start occurring immediately and corrosion events/activity is very sharp around sensor 1, then in sensor 4 and later on in sensor 2 and sensor 3.

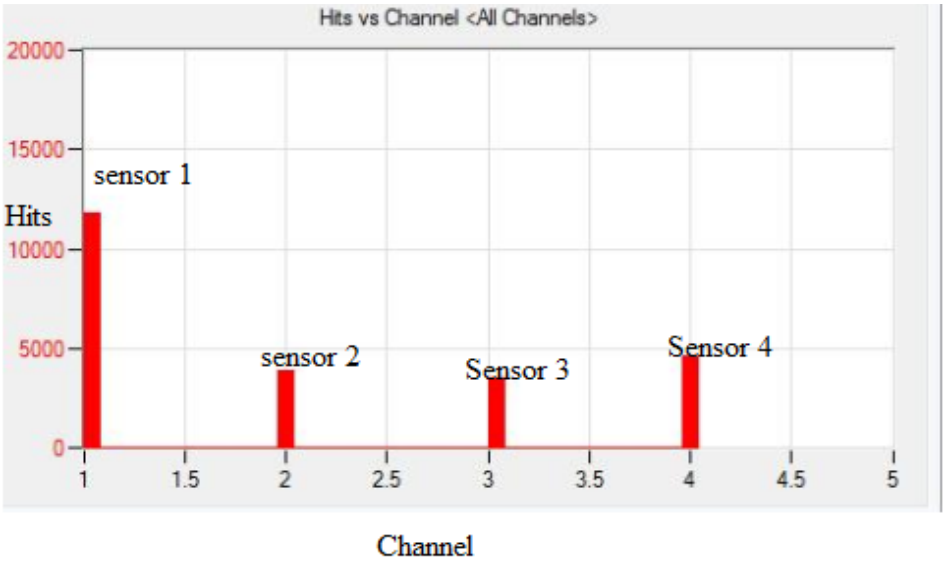

Fig.4.26: AE hits as detected by the sensor after 10 hours

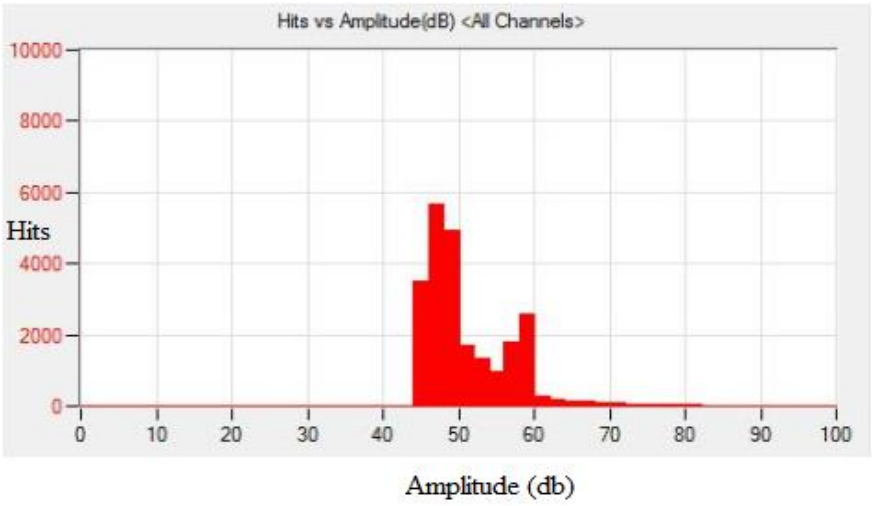

Fig.4.27: Amplitudes of hits detected by the sensor after 10 hours.

Fig.4.27 also clearly suggests that sensors attached to the concrete surface have already detected the acoustic activity occurring in the RC specimen subjected to the accelerated corrosion in the form of hits of different amplitudes. Amplitude of most of the hits lied in the range 45-50db.

.Hence, both **Fig4.26** and **Fig 4.27** clearly explain that Acoustic Emission Technique can detect the corrosion process immediately.

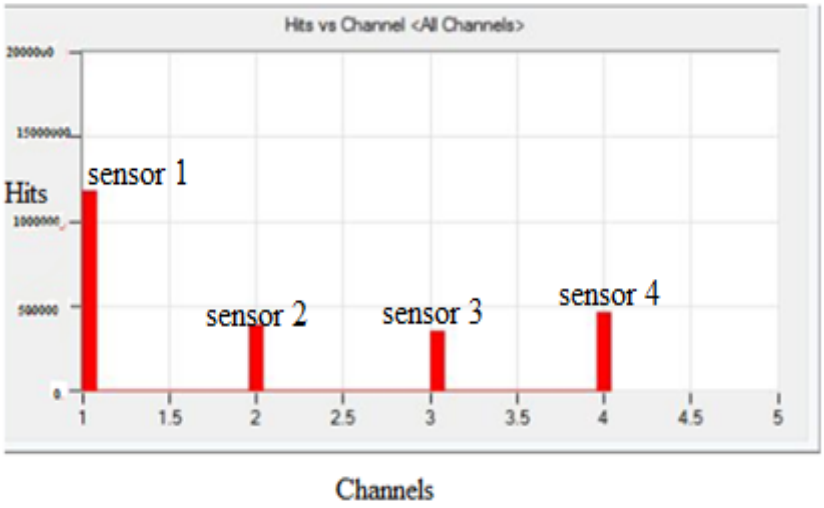

Fig.4.28: Hits detected by sensors after 10 days of accelerated corrosion

In **Fig.4.28** it can be seen that number of hits detected by each sensors have increased as the corrosion in the beam increases in 10 days. The trend of corrosion actually remains same as in 10 hours. Maximun activity is observed in sensor 1 and then in

sensor 4 since the crack propagation started from the position where sensor 1 and sensor 4 are mounted.

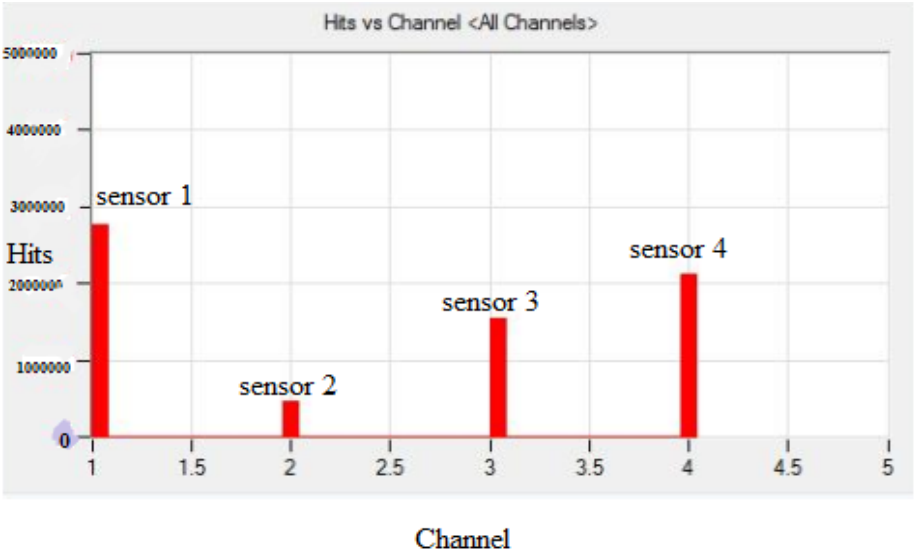

Fig.4.29: Hits detected by sensor after 20 days of corrosion.

In 20 days trends (**Fig.4.29**), it is observed that the hits have increased as the corrosion occurs in the RC beam specimen subjected to the accelerated corrosion. But now sensor activity is increasing in sensor 4 as well as sensor 3. It indicates the development of cracks around sensor 3 and sensor 4. This is because cracks have now developed throughout the RC beam specimen

This was also confirmed by the physical inspection of the beam **Fig.4.30.** The cracks developed on the front face of the beam are shown in the **Fig. 4.30**.

Fig.4.30: Condition of specimen after exposure to 20 days of accelerated corrosion

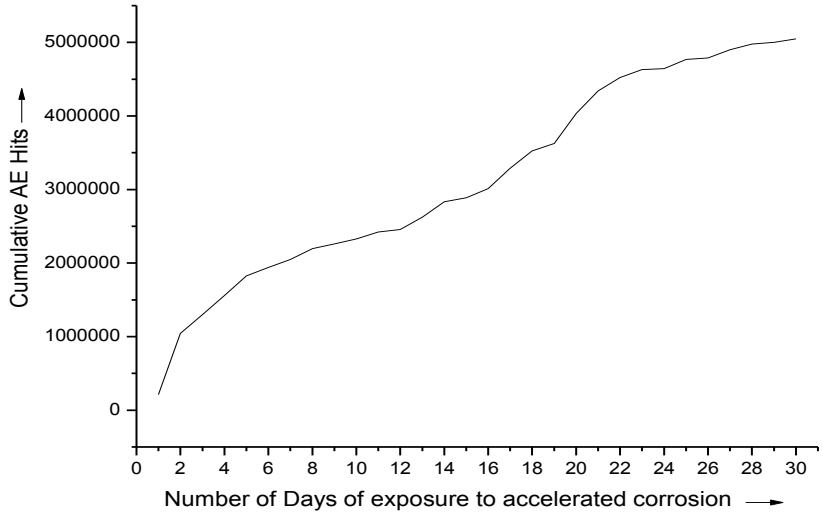

Fig.4.31: Cumulative AE Hits after 30 days of accelerated corrosion

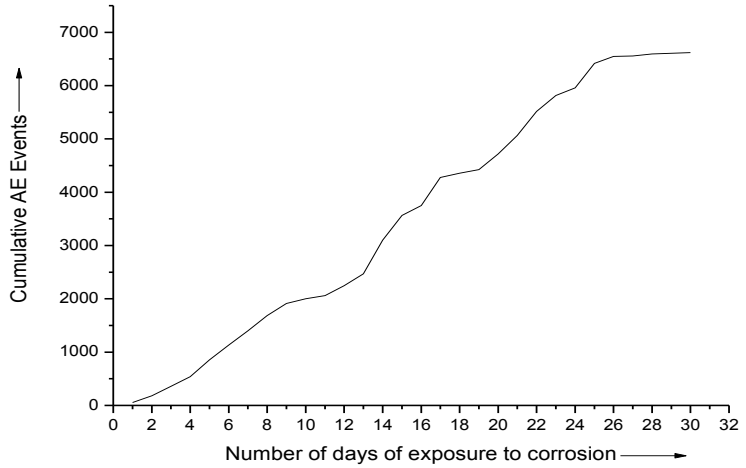

Fig.4.32: Cumulative AE events after 30 days of accelerated corrosion.

Fig.4.31 and **Fig.4.32** clearly shows that cumulative AE hits increase rapidly in the initial 1-20 day which is due to the energy released during the delamination of the steel bar from the surrounding concrete causing cracks in the surrounding concrete. But after 20 days the rate of increase of AE hits and AE events is slow because majority of cracks have occurred and lesser amount of acoustic energy is released in the form of further crack development.

Hence, it can be concluded that Acoustic Emission is very effective in picking up the initial effect of corrosion on concrete in RC beams and can indicate the

development of the crack within some hours in the form of AE hits and events. It picks up corrosion initiation as well as progression wonderfully in comparison to the other techniques.

Ultrasonic guided wave technique, as discussed earlier, is very effective in picking up the later age corrosion after some days. Acoustic Emission has an advantage over ultrasonic guided wave technique in picking and pointing towards crack deformation and location in concrete rather than in steel as in ultrasonic guided wave technique. Therefore, the combination of Ultrasonic guided Wave monitoring and Acoustic Emission Technique can be used very effectively for monitoring the active corrosion phenomenon in RC structures.

AE not only indicate about the crack development but it also tells us about the exact location of the AE events in the form of following graphs.**Fig4.33** and **Fig.4.34** show the location of crack as well as the amplitude of the released acoustic energy for the first day which can be related to cracks development initiation but also the location of events vis-a-vis position of sensor.

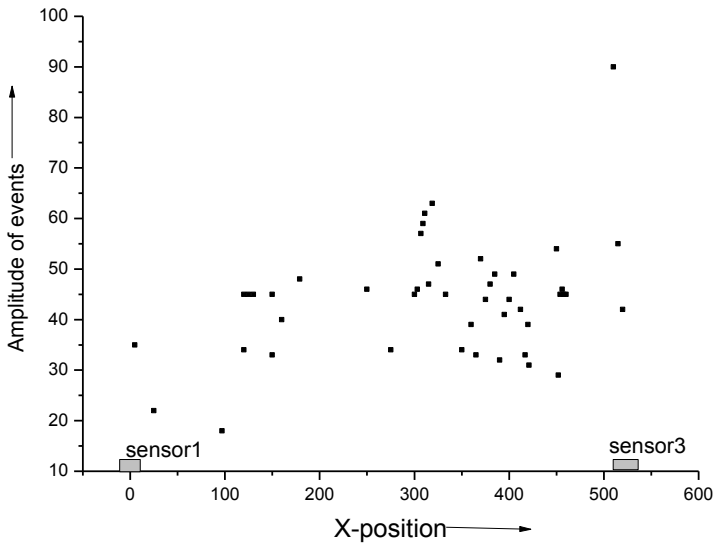

Fig.4.33: Amplitude of events vs. X-position for the first day (Group 1)

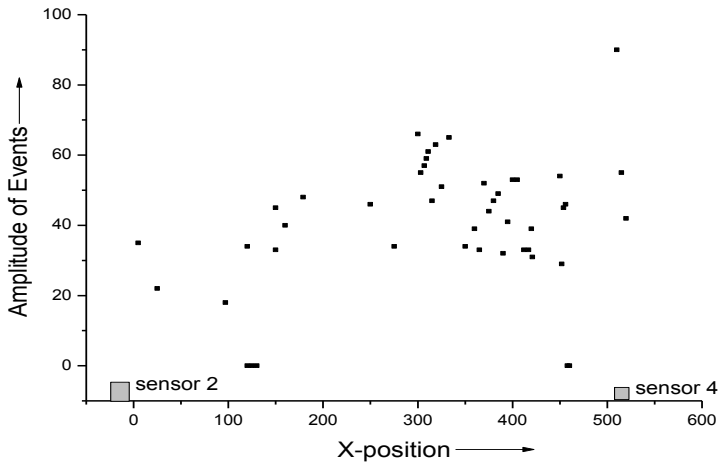

Fig.4.34: Amplitude vs. X-position for the first day (Group 2)

Fig.4.33 and **Fig.4.34** clearly show the location of cracks as detected by group 1 and group 2 of sensors. Group 1 consists of two sensors (sensor 1 and sensor 3) whereas group 2 consists of remaining two sensors (sensors 2 and sensors 4). It can be clearly seen that the amplitude of cracks in the middle of the beam is relatively higher because wide cracks are developed in the middle portion of the beam.

Fig.4.35 shows the location of the crack and the amplitude of the released acoustic energy for all the four sensors during all 30 days of accelerated corrosion.

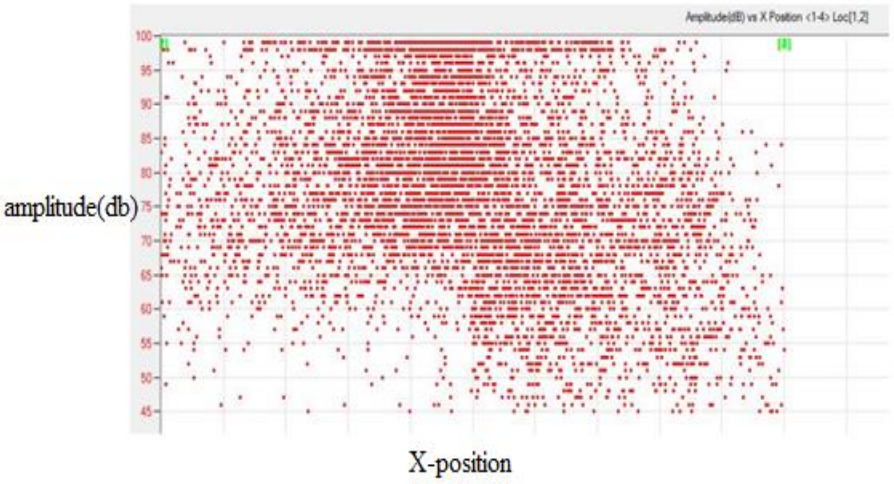

Fig.4.35: Amplitude vs. X-position for all the four sensors

The **Fig.4.34** clearly shows that the crack are developed throughout the length of the beam but the magnitude of the amplitude of cracks was relatively higher in the middle portion of the beam which depicts that the large sized cracks are developed in this portion as compared to the other parts. Also the cracks are more concentrated in the middle portion. This was confirmed visually (**Fig.4.36**), which shows the development of major cracks from the middle of the beam. The confirmation using AE in **Fig.4.35** and **Fig.4.36** shows that AE is a good technique to relate the corrosion process.

Fig.4.36: Cracks developed in specimen after 30 days of accelerated corrosion.

4.4 CLOSING REMARKS

This chapter presented the results of the corrosion monitoring of RC structures using both Ultrasonic guided wave technique as well as acoustic Emission technique. In ultrasonic guided wave technique, both the surface seeking mode and core seeking modes were discussed in detail and efficiency of both these techniques in the corrosion monitoring process was discussed. Thereafter, it was established that ultrasonic guided wave technique is very effective in picking up the later age corrosion. Also, but sufficient corrosion has already taken place till that stage. Acoustic emission technique, however, was found to be very effective in determining the early stage corrosion. Hence, the limitation of the ultrasonic guided wave technique was overcome by the acoustic emission technique. Hence, the combination

of both ultrasonic guided wave technique and acoustic emission technique can be effectively used for the corrosion monitoring process.

CHAPTER 5

CONCLUSIONS AND FUTURE SCOPE OF WORK

5.1 CONCLUSIONS

Following conclusions can be obtained from ultrasonic guided wave monitoring and acoustic emission monitoring of RC beam specimen subjected to accelerated corrosion using impressed current technique done in this research work.

- Ultrasonic guided wave technique and acoustic emission technique have proven to be very effective in monitoring the corrosion in RC structures.
- In ultrasonic guided wave monitoring the surface seeking mode and the core seeking mode are very much able to explain the mechanism of RC beam specimen subjected to accelerated corrosion by signal measurement on embedded bar in concrete. Both the modes also help in examining the delamination as well as pitting effect of corrosion on RC beams.
- In acoustic emission monitoring, the increase in number of cumulative hits and number of cumulative events are very much able to explain the propagation of cracking due to corrosion in RC beam specimen. As the corrosion exposure increases, number of AE hits and events rises considerably.
- AE sensors if placed appropriately also indicate the exact location of AE events and hence crack in the beam.
- Rate of growth of AE events on the display screen indicates the map of crack growth in the specimen which is very useful.
- From the results of both the ultrasonic guided wave monitoring and acoustic emission monitoring, it can be established that the acoustic emission technique is very effective in detecting the propagation of corrosion during the initial stages. Whereas, the ultrasonic guided wave monitoring proves to be very effective in detecting the propagation of corrosion in the later stages.
- In order to have an appropriate idea of corrosion in RC structures it would be very effective to use both the acoustic emission technique as well as the ultrasonic guided wave technique.

- It has also been concluded that acoustic emission technique has an edge over ultrasonic guided wave technique for an access to the steel rebar embedded in the concrete is required in case of ultrasonic guided wave technique whereas acoustic emission sensors can be directly mounted on the concrete surface and relate to corrosion effect on concrete.
- But a disadvantage acoustic emission technique as compared to ultrasonic guided wave technique is that it is very cumbersome to analyse the huge volume of AE data obtained from acoustic emission technique unlike the data obtained from ultrasonic guided wave monitoring.

5.2 FUTURE SCOPE OF WORK

The present study emphasized on the two non-destructive techniques (ultrasonic guided waves technique and Acoustic Emission Technique) for the monitoring of corrosion in RC beams. Combination of Acoustic Emission Technique and Ultrasonic Guided Wave Technique has proven to be very effective in the corrosion monitoring process as far as this study is concerned.

Lot of work in the area needs to be done before the acoustic emission technique as well ultrasonic guided wave technique can be adopted as corrosion monitoring technique.

- More number of samples justifying the technique especially acoustic emission technique needs to be investigated and studied before Acoustic Emission Technique is established for corrosion monitoring in RC structures.
- Effect of placement/ attachment of sensors on the beam on the AE signals need to be assessed.
- Mechanism of fracture needs to be studied numerically and related to fracture parameters vis-a-vis corrosion.

REFRENCES

Ahmed, S.,(2003). " Reinforcement corrosion in concrete structures, its monitoring and service life predictions- a review". Cement and concrete composites 25. Pg 459-471.

Beard,M.D., Lowe,M.J.S., and Cawlay,P.,(2003). "Ultrasonic Guided Waves for Inspection of Grouted Tendons and Bolts", Journal Of Materials In Civil Engineering , ASCE.

Behnia,A., Chai, H.K., and Shiotam, T.O,(2014). "Advanced structural health monitoring of concrete structures with the aid of acoustic emission". Construction and building materials vol(65), pg 282-302.

Cawley,P.,(2007). "Practical Guided wave inspection and applications to structural health monitoring". 5th Australasian Congress on Applied Mechanics, Brisbane, Australia.

Elbatanouny , H.K, Larorhe,A., Mazzoleni,P., Ziehl, P.H, and Matta, F.,(2012). " Acoustic Emission and cyclic load test criteria development for prestressed girders". Structural faults and repair, Edinburgh, Scotland, U.K.

Ervin,B.L., and Reis,H., (2008). " Longitudional guided waves for monitoring corrosion in reinforced mortar". Measurment science and technology. 19 pp, IOP science.

Fowler,T.J., Blessing,J., Conlisk,P., and Swanson, T., (1989). " The HUNPAC Procedure, Journal of acoustic emission,8(3):1-8.

Gadve,S., Mukherjee,A. and Malahotra, S.N.,(2008). A thesis on " active protection of FRP wrapped reinforced concrete structures against corrosion". Indian Institute of Technology, Mumbai.

He, C., Velsor, J.K.V., Lee,C.M., and Rose,J.L.,(2006). "Health Monitoring of Rock Bolts Using Ultrasonic Guided Waves".Review of Quantitative Nondestructive Evaluaion Vol 25, American Institute of Physics.

Kawasaki, Y., Tomado , Y. And Ohtsu, M.,(2010). " AE monitoring of corrosion process in cyclic wet-dry test". Construction and building material 24,pp.2353-2357.

Lee, C., Bonacci, J., Thomas, M., Khajenpour, S., and Hearn, N., (2000)."Accelerated Corrosion and Repair of Reinforced Concrete Columns Using CFRP Sheets." Journal of Civil.

Li(2006). "Corrosion Monitoring of Rebar by Compression Sensitivity of CFRC". Journal of Experimental Mechanics. College of Science, Wuhan University of Technology, Wuhan 430070, China.

Mahmoud, A. M., Ammara, Hussein. H., Mukdadi, Osama. M., Ray, Indrajit., Imani, Fatemeh. S., Chen, An., Davalos, Julio. F.,(2010). ―Non-destructive ultrasonic evaluation of CFRP–concrete specimens subjected to accelerated aging conditions‖ NDT & E International, 43, 635–641.

Masoud, S., and Soudki, K., (2006). "Evaluation of corrosion activity in FRP repaired RC beams." Cement & Concrete Composites, Vol.(28), pp.969–977.

Na, W.B., Kundu,T., and Ehsani,M.R.,(2002). "A Comparison of Steel / Concrete and Glass Fibre Reinforced Polymer / Concrete Interface Testing by Guided Waves", Materials Evaluation.

Ohtsu, M., and Tomado,Y., (2007). "Damage evaluation and corrosion detection in concrete by acoustic emission". Proceedings of 6th international conference on fracture mechanics of concrete and concrete structures, vol 2, pp 981-989.

Ohtsu, M., Uchida, M., Okamoto, T., and Yuyama, S. (2002). " Damage assessment of reinforced concrete beams qualified by acoustic emission". ACI Structural Journal
99 (4), 411–417.

Ohtsu, M., and Tomoda, Y. 2008. Phenomenological Model of Corrosion Process in Reinforced Concrete Identified by Acoustic Emission. ACI Materials Journal,

105(2), 194-199.

Ono, K.,(2010). “Application of acoustic emission for structure diagnosis”. Konfrencia, Naukowa, 317-334.

Pavlakovic,B.N., Lowe,M.J.S., and Cawley,P.,(2001). “High Frequency Low-Loss Ultrasonic Modes in Imbedded Bars”. Journal of Applied Mechanics, Vol. 68, ASME.

Renaldas, R., Kazys, R., Zukauskas, E., Mazeika, L., and Vladisauskas,A.,(2010). **“**Application of Ultrasonic Guided Waves for non-destructive testing of defective CFRP rods with multiple delaminations**”.**NDT&E International, Vol. 43, page 416–424.

Sethy, M.S., (2005).“Text Book of Concrete technology” S. Chand and Company Ltd, New Delhi.

Sharma, S., (2010). “ Monitoring of damage in reinforcement in concrete”. Phd thesis, department of civil engineering, Thapar University, Patiala.

Sharma. S. and Mukherjee, A., (2010). **“**Longitudinal Guided Waves for Monitoring Chloride Corrosion in Reinforcing Bars in Concrete”.Structural Health Monitoring, Vol. 9, page 555.

Sharma, S. And Mukherjee,A.,(2011). “Monitoring corrosion in oxide and chloride environment using ultrasonic guided waves”. Journal of materials in civil engineering 23(2): 207-211.

Sharma, S., and Mukherjee, A.(2013). “ Non-destructive evaluation of corrosion in varying environment using guided waves”. Research in non-destructive evaluation 24(2):63-88.

Xu,J.(2008)., “ Non-destructive evaluation of prestressed concrete structures by means of acoustic emission monitoring. Dissertation, department of civil engineering, university of auburn, auburn, Alabama,308.

Yoon, D.J., Weiss,J.W. and Shad, P.S., (2000). “Assessing damage in corroded reinforced concrete using acoustic emission.